An Assessment of the Effect of X-ray Radiation on DNA Marker Profiles Obtained from Human Teeth

A Thesis Presented for the
Master of Arts
Degree
The University of Tennessee, Knoxville

Erin Lynn Knapp
August 2013

Acknowledgements

First, I would like to thank my advisor, Dr. Graciela Cabana, for her support, ideas, and editing prowess. I also am thankful for the help and support from my committee members, Dr. Benjamin Auerbach and Dr. Lee Jantz.

I would also like to thank everyone who attended the lab meetings at the Molecular Anthropology Lab over the last few semesters. You have all been great sounding boards. I also need to thank Dr. Michael Keene and my writing coach Ellen Rideout for helping me revise and revise again.

I thank the Forensic Anthropology Center and the William M. Bass Endowment for the funding, materials, and ability to perform this thesis research. I thank Dr. Randall Pearce, DDS for providing the tooth samples to the University of Tennessee Department of Anthropology. I also thank the Molecular Anthropology Labs and Molecular Biology Resource Facility for allowing me the use of the facilities to process and analyze my samples.

Many thanks to Joseph A. May and Veronica Brown for help analyzing my samples and learning how the fragment analyzer machine and software work. Thanks to Cathy Graves, R.T. at the UT Student Health Center for helping me X-ray my samples.

Finally, thanks to my friends and family for encouraging me in every way to pursue my graduate education.

Abstract

X-ray radiation is known to destroy cells and damage DNA, yet human remains from forensic anthropology cases are routinely exposed to X-ray radiation as part of the documentation and evidence collection process. If X-ray radiation significantly impacts the quality of DNA extracted from human remains in forensic cases, then the validity of a resulting genetic profile is called into question. To better understand how X-ray radiation affects DNA profiles, specifically profiles consisting of short tandem repeat (STR) markers, this study followed standard forensic X-ray and genetic profiling protocols to obtain DNA profiles on individual molar teeth, before and after they were exposed to a single X-ray dosage event.

The results of the study demonstrate that X-ray radiation did indeed affect DNA profiles, in two ways. First, the total number of DNA markers recovered pre-and post-X-ray radiation decreased significantly between the pre- (control) and post-(experimental) irradiation. Second, the overall amount of DNA per genetic marker recovered was significantly reduced, as measured by Relative Fluorescence Units (RFUs). Interestingly, contrary to expectations, the DNA markers recovered did not exhibit significant shortened fragments lengths post- irradiation, otherwise known as "allelic stutter." Thus, it seems that X-ray exposure tended to damage DNA marker variants to such an extent that DNA markers were completely unrecoverable post-irradiation, rather than simply damaged to a point of producing allelic stutter.

Importantly, X-ray radiation altered DNA marker profiles of individual cases before and after X-ray radiation. The post-radiation sample exhibited a significant amount of "allelic dropout," leading to a condition known as "false homozygosity," when one only DNA variant for a given locus is represented in a genetic profile instead of the two different variants that may actually be found in the sample. These results indicate further research is required to understand

the stochastic effects of X-ray irradiation on DNA, and suggest that forensic samples undergo DNA analysis prior to exposure to X-ray radiation.

Table of Contents

List of Tables

List of Figures

Introduction

This study examines the potential effect of X-ray radiation on a standard set of DNA markers used for forensic genetic profiling purposes.

Years of research have shown that X-rays damage deoxyribose nucleic acid (DNA) by severing DNA bases off DNA strands, as well as splicing DNA strands either partially or completely (Boon et al. 1984, Cadet et al. 2003, Dertinger 1969, Fuciarelli and Zimbrick 1995, Granier and Gambini 1990, Grosovsky et al. 1987, Hada and Sutherland 2006, Hutchinson 1966, Nikjoo et al. 1997, Nikjoo et al. 2001, Nikjoo et al. 2002, Ostling and Johanson 1984, Pizzarello 1982, Putkonen 2010, Semenenko and Stewart 2004, Siddiqi and Bothe 1987, Shafirovich and Geacintov 2010, Sutherland et al. 2002, Swarts et al. 1992, Ward 1981, Ward et al. 1994, Wolff, 1967). The chromosomal location of damage on a DNA strand is not predictable, but when damage does occur, it appears clustered (Nikjoo et al. 1997). During the life of an organism, X-ray-induced damage is mitigated by various repair functions. After death, most of these repair functions are no longer operational (Grosovsky et al. 1988). Therefore it has been generally assumed that any X-ray radiographs taken of deceased organisms will cause irreparable DNA damage.

Despite the fact that X-ray radiation is known to damage DNA, the extent to which it damages DNA in forensically relevant materials is not well understood. Yet, forensic remains are regularly X-rayed as part of case documentation and evidence recovery. Up to this point, only two published studies have addressed the question of whether it is possible to recover DNA from bone – a forensically relevant material – after X-ray radiation. The first, Gotherstrom et al. (1995), divided an unspecified bone element from *Sus scrufa* (domestic pig) into three sections,

keeping one third as a control section. Another third was irradiated at a "normal" (i.e., unspecified) dose of radiation typical of archaeological samples, and the other third at a much higher dose. DNA was extracted, copied via a process called "amplification" (described later), and visualized on an agarose gel. Based on the degree of brightness of DNA bands on the gels, they determined that the bone sample exposed to a low dosage of radiation produced less DNA than the control sample, and the sample exposed to the highest dosage produced little to no DNA. From this, they concluded that DNA extractions on bone should be performed prior to X-ray analysis.

The second published study, Grieshaber et al. (2008), exposed the distal phalanges of *Sus scrufa* to X-ray and Computed Tomography (CT; CT scanners produce computer generated three-dimensional images from a collection of X-ray images or slices). The researchers attempted to extract and copy (amplify) three differently sized fragments of 100, 200, and 300 base pairs (bp). They were unable to obtain any larger (400 bp) fragments, but were better able to obtain 200 bp fragments, albeit with some troubleshooting, and were often able to recover the smallest 100 bp fragments. Though they found that they were able to recover comparable amounts of DNA from all bones that were either X-ray or CT irradiated, but as with the previous study, DNA recovery was determined via a visual inspection of fluorescence levels of DNA bands on an agarose gel.

Unfortunately, the studies' research design were limited for this study's purposes; that is, they do not inform whether extracted DNA could be used to build a complete enough DNA profile for forensic identification purposes. Gotherstrom et al. (1995) and Grieshaber et al. (2008) utilized a relatively crude visualization technique to determine that DNA was recovered, such that they were unable to closely examine the degree of fragmentation, if any, caused by

exposure to X-ray. This is important because DNA fragmentation could ultimately hamper recovery of the sections of DNA necessary to forensically identify human remains using currently accepted methods.

A recent study looked at the effect of X-ray (as CT scans) on a substance containing already degraded DNA – preserved bird skins from museum collections (Paredes et al. 2012). The researchers exposed sections of skins to CT and found that the amount of fragmentation of DNA before and after scanning did not significantly change. More specifically, the preserved specimens already exhibited DNA degradation and they found that X-ray exposure did not significantly increase the amount of degradation already present. This study did not look at any specific markers, but broadly visualized the overall pattern of fragment sizes and amount of DNA in the sample. This was accomplished using a special DNA analysis "chip" that measures DNA fluorescence on an Agilent 2100 Bioanalyzer machine. This machine uses capillary electrophoresis to measure fluorescence much like the ABI PRISM ® 3100 genetic analyzer utilized in this study. Software was then used to infer DNA fragment size from fluorescence signal and fragment migration time. The researchers statistically compared this "DNA fragmentation profile," both pre- and post-scanning, with a paired *t*-test, in which they found no significant differences.

In sum, the Gotherstrom et al. (1995) and Grieshaber et al. (2006) studies suggest that DNA recovery is hampered by X-ray radiation. The Grieshaber et al. (2006) study additionally suggests that DNA, however damaged, is still recoverable from irradiated bone. It should be noted that these two studies used mitochondrial DNA (mtDNA) only, which is present in much higher copy numbers per cell than nuclear DNA. Most forensic studies, however, rely on nuclear DNA for genetic profiles. Last, the Paredes et al. (2012) study indicates that DNA recovered

from compromised materials that have been X-ray irradiated, such as preserved bird skins, is not overly fragmented, None of these studies were explicitly designed to show whether or not forensic identification markers could be fully recovered from X-rayed skeletal material.

In a forensic context, it is important to know if X-rays significantly impact the quality of DNA from human remains, in terms of the forensic markers used to identify human remains. If radiation produced by X-rays significantly changes the shape or length of the DNA fragments needed to identify human remains, then accurate DNA profiles cannot be compiled. A DNA "profile" can be used to identify individuals based on the DNA makeup (also referred to as DNA fingerprinting). DNA profiles are compiled using specific genetic markers. In this study, "core" DNA markers from the Combined DNA Index System (CODIS) constitute a DNA profile. CODIS is a state and federal DNA database consisting of DNA profiles using 13 specific markers. These markers are located in different regions of the human genome that are do not code for proteins, or "noncoding DNA." These DNA profiles are derived from biological samples such as blood, bone, teeth, or other tissues. These 13 "core" markers enable law enforcement agencies to create standardized profiles to compare evidence from crime scenes to samples of a known origin or to local and national DNA profile databases (Franklin County, New York [Accessed 3 May 2013]).

Once we understand whether or not forensically relevant DNA markers can be extracted from X-rayed material, we will be able to analyze cold case remains that already have been X-rayed for other types of analyses, such as looking for tool markings on the bones, and apply modern DNA identification methods. Or, if a current case has been sampled for DNA and then X-rayed, it will still be possible to perform subsequent DNA tests if deemed necessary.

The research presented in this thesis will explore the effects of ionizing damage, if any, caused by X-ray radiographs taken of modern human teeth. Research has shown that DNA extracted from teeth is protected by enamel and therefore less likely to be damaged than DNA extracted from other bones (Schwartz et al. 1991). DNA profiles were obtained from non-exposed and exposed teeth samples, and compared. The teeth used in this study likely contain DNA that is already degraded, given that the samples were stored in a water and alcohol mixture for an unknown amount of time, but not more than five years. Thus, this research compares the DNA profiles of the pre- and post-X-rayed samples without knowing the "true" DNA profiles of the samples. However, the pre- and post-exposure profiles can be compared to assess whether or not X-ray radiation affects the quality and reliability of the genetic profile obtained.

Chapter 1 begins with background information on DNA structure and degradation, followed by a discussion of DNA markers (especially the type used in this research) and low template DNA. The final sections of Chapter 1 will discuss X-ray and ionizing radiation, and how they damage DNA. It will also review forensic protocols related to the X-raying of human remains.

Chapter 2 will discuss the materials and methods used in this research. The contents of this chapter will enable the reader to replicate the results obtained in this thesis. Chapters 3 and 4 will outline the results and a discussion thereof. Summary tables of statistical analyses will be provided within the text where relevant, while additional data tables can be found in the appendix. Finally, Chapter 5 will provide a discussion of the conclusions drawn from this thesis research and future considerations and implications. A discussion of another type of DNA

marker, SNPs or Single Nucleotide Polymorphisms, and their potential use in human identification will conclude the chapter.

Chapter 1: Background

This chapter presents basic knowledge on the structure of DNA and DNA degradative patterns to provide background to this study's research design regarding the effects of X-ray radiation on DNA. The DNA markers being used in this study include the 13 "core" CODIS markers which consist of short tandem repeats or STRs. This type of DNA marker, though excellent for the purposes of individual identification, is somewhat more vulnerable to DNA damage than other types of DNA markers. Thus, the problems that may arise with this type of DNA marker when exposed to X-ray radiation, and the subsequent potential impact n DNA profiles constructed for forensic purposes, are discussed.

The DNA molecule is comprised of various parts that may be vulnerable to damage from X-ray radiation and decay. Depending on the shape and configuration of the DNA molecule it may be more or less protected from irradiative damage and decay. After an organism's death, DNA damage from decay and degradation occurs from various environmental factors in the absence of living repair mechanisms.

Certain DNA markers are important for forensic identification. Protocols and commercial kits have been developed to locate and make copies of, or "amplify" these DNA marker sequences accurately and reliably. In addition to X-ray radiation, natural processes such as hydrolysis and oxidation complicate these procedures by potentially damaging DNA marker fragments.

X-rays produce ionizing radiation that stochastically damages DNA, potentially shortening the required fragments to non-diagnostic lengths. Biological anthropologists have

developed published standards for the X-ray radiation of skeletal remains that are also applied in forensic contexts (i.e., Buikstra and Ubelaker 1994), but at the time of this writing there are no legally enforceable standards with regards to how, why, and when human remains may be X-rayed. Most forensic anthropology labs determine their own internal standards, which may or may not correspond with Buikstra and Ubelaker (1994). Therefore, it is important to investigate whether any damage caused by X-ray radiation affects DNA profiles.

DNA Structure

Deoxyribose nucleic acid (DNA) is comprised of three major parts: nitrogenous bases, deoxyribose sugars, and phosphates. The nitrogenous bases are of four types: adenine (A), guanine (G), thymine (T), and cytosine (C). A and G are purines with a double ring structure, and C and T are pyrimidines with a single ring structure. A sugar, phosphate, and nitrogenous base comprise a unit referred to as a "nucleotide". One end of each DNA strand terminates in a phosphate at the fifth carbon in the sugar ring (5' end) and the other terminates in a hydroxyl group at the third carbon in the sugar ring (3' end)—one strand is 5'-3' (downstream) oriented and the other is 3'-5' (upstream) oriented.

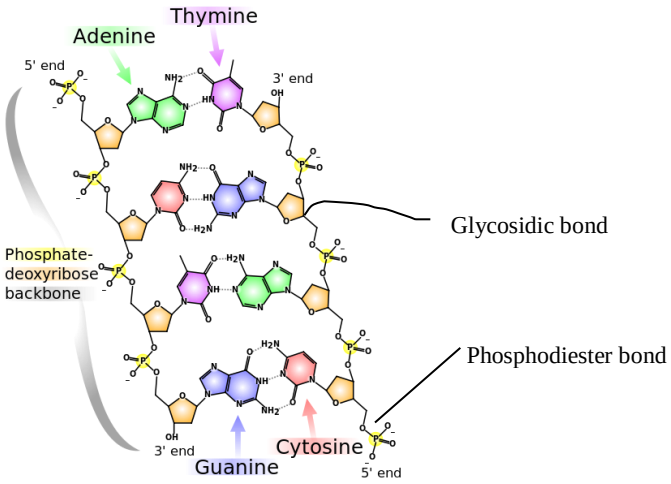

Figure 1.1. DNA strand structure.
Adapted from: http://en.wikipedia.org/wiki/File:DNA_chemical_structure.svg

The bond between a sugar and base is called a glycosidic bond. The nature of this bond allows the base to rotate freely around the bond. The sugar of each adjacent nucleotide is linked to the phosphate by a phosphodiester bond. A glycosidic bond joins nucleotides from the 3' sugar carbon through the phosphate to the 5' sugar carbon of the next nucleotide. This bond is formed during the biochemical synthesis of DNA by the enzyme DNA polymerase. The glycosidic bond gives the DNA strand a slight polarity. Double-stranded (or duplex) DNA is a right-handed helix formed by two individual DNA strands, which are aligned in an anti-parallel fashion.

A hydroxyl is a molecule group that contains one oxygen atom covalently bound to a hydrogen atom. These strands are held together via hydrogen bonds between the bases. The bases are stacked near the center of the helix, which provides extra stability to the DNA molecule. An individual base is held in place by the relative position of the base above and

below, it much as an individual coin is held in place in a stack of coins by the position of the coin above and below it.

Sugar and phosphate form the "backbone" structure of the DNA helix. Each turn of the helix is approximately ten base pairs (one base pair involves the chemical bonding of one base with another on the complementary strand) in length, in the common, or B-form (to be discussed below) of DNA (Sinden 1994). Additionally, there are two non-symmetrical grooves that spiral along the outside of the DNA double helix configuration. These are called the major and minor groove (larger and smaller one, respectively) and allow different proteins to interact with the DNA strand (Hartl and Jones 2006).

The A and T bases pair via two hydrogen bonds, while G and C pair with hydrogen bonds. The hydrogen bond is a short non-covalent bond. A non-covalent bond, in contrast to a covalent bond, does not involve the sharing of pairs of electrons and is therefore a weaker bond. These bonds can also be deformed by stretching and bending. Additionally, the hydrogen bond in DNA is weaker than most hydrogen bonds because of geometric constraints of the helix structure. The hydrogen bonds and stacking of bases provide similar amounts of stability to the DNA structure. The individual stabilization interactions are weak, but taken together, form a stable helix.

The traditional pairing of A with G, and C with T, is named after the pair of scientists credited with discovering the structure of DNA and is known as "Watson-Crick base pairing." In this scheme, each base is bonded to its complementary base on a specific part of the molecule, known as the Watson-Crick "face," or side, of the molecule. There are several other base pair schemes in which different parts of the base molecules are bonded together. In "reverse Watson-

Crick base pairing," one nucleotide is rotated 180° with respect to its complementary base. Two other base pair schemes are known as the "Hoogsteen" and "reverse Hoogsteen" pair base schemes. In each of these a different surface (the Hoogsteen bonding surface) of the nucleotide molecule is used for the bond. These different base pair schemes serve to alter the shape of the molecules, which allows different parts of the molecules to be accessed by other molecules for different chemical reactions. This change of shape alters the chemical reactivity of the DNA molecule depending on the exact shape and conformation of the molecules.

DNA can be found in various forms that have been studied using X-ray diffraction analysis. The most common and stable form of DNA is known as B-form. In the B-form, two major grooves can be distinguished—major and minor groove. The Hoogsteen bonding surface of the purines can be accessed via the major groove. The center of the helix in this form is a chemically inert place and safe for storage of genetic information due to the nature of the hydrogen bonds, base-stacking, and the hydration of the helix. In A-form DNA, the major and minor grooves are not as deep and the bases are more tilted. A-form DNA is found in a dehydrated environment. C-, D-, and T-form DNA are other subtle variations in the shape of the double helix. Finally, there is Z-form DNA, which is very different from the other variations because it is a left-handed helix. Z-form DNA is most often found in regions in which active transcription is occurring. It is thought that this shape relieves torsional stress (from twisting and untwisting) during the transcription process. A-, B- and Z-form DNA are the three most common forms of DNA and are pictured in Figure 1.2. Ultimately, the exact shape of a region of DNA depends on its base composition and the sequences flanking the region (Sinden 1994).

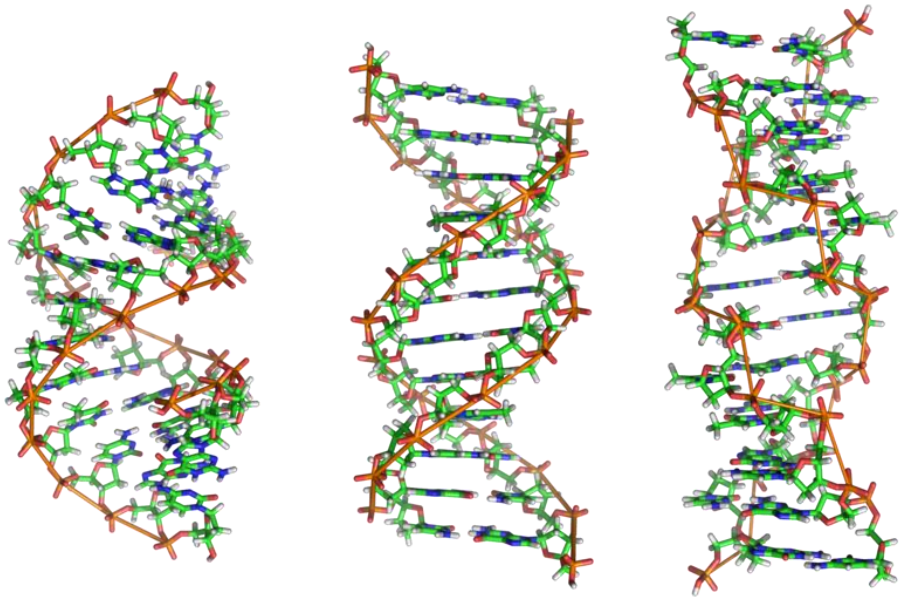

Figure 1.2. DNA Forms. From left to right: A-form, B-form and Z-form of DNA. The B-form is the most common while the Z-form form is the rarest and represents a left-handed helical structure. The A-form form is found in mostly dehydrated environments. Adapted from: http://en.wikipedia.org/wiki/File:A-DNA,_B-DNA_and_Z-DNA.png

Normal Degradation and Decay of DNA

All biological macromolecules, including DNA, are prone to spontaneous decomposition. Nucleic acids are subject to spontaneous decomposition in solution. Two main methods of decomposition are DNA hydrolysis and oxidation. Hydrolysis is a common chemical reaction in which chemicals of water are split into two smaller molecules, H^+ (protons) and OH^- (hydroxide anions). Oxidation or redox (reduction-oxidation) is a chemical process by which the oxidation status of atoms is changed. Oxidation is simply a loss of electrons leading to an increase in oxidation state, while reduction is the opposite—a gain of electrons, leading to a decrease in oxidation state. Many biological processes, such as respiration and metabolic reactions, involve these kinds of oxidation/reductions processes (Lindahl 1993).

During DNA hydrolysis, the 2’ OH- group sugar is removed, leading to instability of the glycosidic bond between the sugar and base. Guanine and adenine (the purines) seem to be liberated from the DNA structure via this process at similar rates. This loss of purines is known as depurination. Conversely, a loss of the pyrimidines is known as depyrimidination. This loss of bases is a reaction that is acid-catalyzed under physiological conditions—meaning that this can, and does, occur in the living human body under normal conditions. It has been estimated that 2,000-10,000 purine bases are lost every day due to hydrolytic depurination and subsequently repaired (Lindahl 1993). The exact depurination rate is a function of time, pH, and ionic strength of a solution. Depurination is accelerated in the presence of divalent metal ions (ions that have two additional electrons compared to the standard element) such as Mg^{2+}. Lindahl and Nyberg (1972) showed that depurination occurs at high rates in conditions resembling *in vivo* conditions. Therefore, depurination is being constantly countered by repair pathways such as base excision repair (BER) pathways throughout life.

Additionally, DNA bases are susceptible to hydrolytic deamination (removal of an amine group). The main target of this process is cytosine and 5-methylcytosine (a methylated version of cytosine). However, the double helix structure provides better protection against deamination than it does for depurination. The high deamination rate of 5-methylcytosine and slow repair mechanisms lead to spontaneous point mutations in which a G-C pair can become an A-T pair. Cytosine can be converted to uracil in a hydrolytic reaction in neutral pH, but this reaction is more serious compared to the deamination of the purines (Loeb 1989). This process occurs about 100-500 times per day in the human cell. Adenine can be converted to hypoxanthine via deamination. This conversion occurs at two to three percent of the rate of cytosine deamination. However, the product of adenine deamination is considered a mutagenic lesion because it forms

a stable base pair with cytosine instead of thymine (Lindahl 1993). The hydrolytic deamination of 5-methylcytosine can be repaired through a mismatch-specific thymine-DNA glycosylase (TDG) (Neddermann et al. 1996). Thymine-DNA glycosylase is an enzyme encoded by the TDG gene, whose function is to remove alternate thymine forms (moieties) from G/T mismatches.

Oxygen free radicals can produce damage at the same rate as depurination. In reactions with free radicals, oxygen is metabolized by a series of one electron reactions with the generation of highly active free radical intermediates (Loeb 1989). DNA oxidation is primarily carried out by the hydroxyl radical, OH-. 8-hydroxyguanine (or 8-oxoguanine) is a major mutagenic base lesion generated by the hydroxyl radical. This molecule is a form of guanine that pairs with adenine instead of cytosine, leading to a transversion mutation after replication. A type guanine (or guanine moiety) known as dGTP (deoxyguanosine triphosphate), the guanine precursor for DNA synthesis, can be oxidated to become 8-hydroxy-dGMP. Residues of this reaction can be incorporated opposite an adenine during replication, which would pair guanine with adenine. This mutation is normally effectively repaired in life. In addition to base damage, oxygen radicals can also cause major helical distortion (Lindahl 1993). It has been estimated that 10,000 oxygen free radical-induced damages occur in the DNA per cell, per day. Fortunately, there are systems in which the free radicals can be scavenged (to reduce potential damage) and the damages bases can be excised (Loeb 1989). More recent research (Cadet et al. 2003) has shown that 8-oxoguanine can cause tandem base lesions due to a single OH- radical hit. Tandem base lesions are a type of complex clustered lesions, which are mostly generated by exposure to high energy radiation such as X-ray radiation, rather than by natural processes such as cellular respiration.

Fully hydrated DNA would spontaneously degrade into shorter fragments over time at moderate temperatures. The most important method of degradation for hydrated DNA is depurination. Additionally, adsorption of DNA to hydroxyapatite results in a twofold increase in the depurination rate. The water molecules found in the grooves of the DNA double helix (the hydration layer) are structurally essential. Therefore, dehydrated DNA is more susceptible to damage because it does not retain the stable helix shape (Lindahl 1993).

Damage from ionizing radiation (such as X-rays) is very similar to that of cellular oxidation. Basu et al. (1989) found that thymine bases are the most susceptible to modification as a result of cellular oxidation. They found 5,6-dihydroxy-5,6-dihydrothymine (known as thymine glycol or t') to be the most stable product of thymine modification. T' gets paired with guanine, instead of adenine, during DNA replication, which results in a T-G wobble base pair. This mutation, in turn, changes the shape of the DNA molecule in that region, but not enough for DNA polymerases to find and repair the lesion. According to Basu et al. (1989), a t' modification only induces a T to C transition from replication of the genome. Therefore, t' lesions are only problematic in living organisms.

DNA polymerase is error prone, and the most frequent kind of error is a single base substitution. Transitions are more common than transversions, such as T-G to C-A or single base deletions. A transversion is a mutation in which a purine is substituted for a pyrimidine or vice versa. Conversely, a transition is a mutation in which a purine is replaced with another purine or a pyrimidine is replace with another pyrimidine. Transitions are less harmful than transversions, which can dramatically change the chemical structure of the DNA molecule. DNA polymerases

tend to copy past damaged DNA and insert non-complementary nucleotides opposite the site of damage (Loeb 1989).

Short Tandem Repeats (STRs)

This study utilizes short tandem repeats (STRs; also known as microsatellites) to further understand how ionizing radiation from X-rays affects a forensic genetic DNA profile. Though previous research has focused on whether radiation damages DNA, this research seeks to first, validate previous research via an independent experimental study, and second, ascertain the extent to which X-ray induced damage affects DNA markers essential to genetic profiles used in forensic identification.

An STR consists of a tandem repeat units of two to five base pairs that may be repeated within the same DNA fragment up to dozens of times. An STR genetic variant (always referred to by forensic professionals as an STR allele) represents a difference in repeat numbers. There may be anywhere from five to 20 different alleles for each STR present in a given population. Relatively short fragment lengths (from 200 to 500 base pairs) make STRs ideal for use with forensic DNA because degradative processes tend to break DNA into smaller fragments. Several STRs have been chosen for forensic use based on their distribution in the population(s) of comparison (Rudin and Inman 2001).

STR fragments are typically analyzed in a fragment analyzer machine, such as the ABI 3100 used in this study. Prior to fragment analysis, each STR is flagged with a fluorescent dye. The STR's dye fluoresces at certain wavelengths, depending on the dye color used, when excited by the fragment analyzer's laser. The machine takes this read information and translates it into a

graph of colored peaks, known as an electropherogram, and provides a corresponding table showing fragment lengths, fluorescence values (known as relative fluorescence units, or RFUs, discussed later), and scan line information. The peaks on the electropherogram are colored based on the fluorescent dye used for each target fragment. The height of each peak corresponds to the RFU value (y-axis). Taller peaks have greater fluorescence observed at that fragment length (roughly indicative of quantity of fragments). The x-axis shows the number of base pairs of the fragment or fragment lengths. Fragment lengths are derived from comparing the samples to an internal size standard that is mixed into each sample. Figure 1.3 is an example of the type of electropherogram produced from fragment analysis on an ABI 3100 machine.

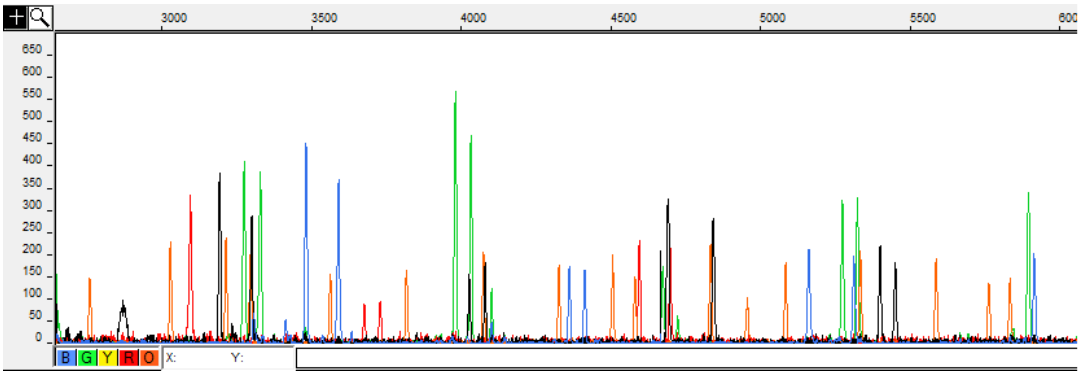

Figure 1.3. Sample electropherogram.

Five dye colors are used; blue, green, yellow, red, and orange. The orange dye is the internal size standard. Each blue, green, yellow, or red peak represents a different DNA marker fragment.

For any particular STR to be a good candidate forensic DNA marker, it needs to exhibit a high amount of variation in the target population to be able to discriminate between individual samples. Tetranucleotide repeats, or repeat units containing four base pairs, are the most commonly used because this repeat size makes it easier to resolve closely spaced heterozygotes. With a larger repeat unit (four base pairs instead of two or three), there will be more space between the peaks of a heterozygote with 12 and 13 repeats, for example. Additionally, tetranucleotide STRs exhibit fewer stutter results (amplicons that are one or more repeat units less than the true allele being amplified, discussed on page 23) than the dinucleotide and trinucleotide markers (Butler 2005).

Butler (2005) lists several screening criteria for STRs used in human identification:

1. High discriminating power, with an observed heterozygosity of 70% or greater among samples;
2. Independent chromosomal locations;
3. Robustness and reproducibility of results when multiplexed;
4. Low stutter percentages;
5. Low mutation rates;
6. Fragment sizes between 90-500 base pairs for use with degraded samples.

To explain criterion #2 further, STR markers are chosen from different chromosomes to avoid linkage between the markers. If markers are linked, then they are inherited together. For forensic purposes, linked markers would make it more difficult to discriminate between highly related individuals. Having unlinked markers also enables the use of the "product rule" when determining the uniqueness of a given DNA profile, because each marker is independent of the rest. The product rule states that you can multiple two or more probabilities to get the combined probability of all the events occurring. Each STR allele has a known frequency of occurrence

given a specific population. For each STR, the frequency of each repeat varies between populations. For example, for D2S1338 the 16 repeat allele is observed at a frequency of 4.491 in African American populations and 2.961 in Caucasian populations (Budowle et al. 2001). The product rule allows forensic scientists to combine the probabilities of an individual having several DNA markers into one probability for the entire STR profile. Forensic scientists use computer programs to obtain a "random match probability" (also, RMP), or the probability that the given STR profile belongs to only the individual in question.

Table 1.1. Random Match Probability (RMP): Demonstration of RMP calculation for a U.S "Caucasian" sample, adapted from Butler (2005).
Homozygote loci frequencies are squared and heterozygote loci frequencies are multiplied together. That sum is multiplied by two, as per Hardy-Weinberg Equilibrium (HWE). The HWE states that all genetic variants (*p* and *q*) in a population exist in predictable proportions and can be expressed as $p^2 + 2pq + q^2$. All genetic variant frequencies are then multiplied together to determine the product rule combined frequency.

Marker	**Genetic Variant 1**	**Genetic Variant 2**	**Genetic Variant 1 frequency (*p*)**	**Genetic Variant 2 frequency (*q*)**		**Expected genotype frequency**
D13S317	11	14	0.3394	0.04801	$2pq$	0.0326
TH01	6	6	0.23179		p^2	0.0537
D18S51	14	16	0.13742	0.13907	$2pq$	0.0382
D21S11	28	30	0.15894	0.27845	$2pq$	0.0884
D3S1358	16	17	0.25331	0.21523	$2pq$	0.1090
D5S818	12	13	0.38411	0.14073	$2pq$	0.1081
D7S820	9	9	0.17715		p^2	0.0314
D8S1179	12	14	0.18543	0.16556	$2pq$	0.0614
CSF1PO	10	10	0.21689		p^2	0.0470
FGA	21	22	0.18543	0.21854	$2pq$	0.0810
D16S539	9	11	0.11258	0.32119	$2pq$	0.0723
TPOX	8	8	0.53477		p^2	0.2860
VWA	17	18	0.28146	0.20033	$2pq$	0.1128
Amelogenin	X	Y				
				Product Rule Combined Frequency		1.20E-15
					1 in	8.37E +14

Table 1.1 demonstrates how the combination of several STR markers can be used to build a random match probability to determine the uniqueness of an STR profile. The product rule combined frequency is 1.20×10^{-15}, which is then inverted to determine the "1 in …" value of the profile. In this case, 1.20×10^{-15} is inverted to give a 1 in 8.37×10^{-14} chance of this profile matching another from the same population. The uniqueness of the profile allows forensic scientists to make individual identifications.

CODIS Markers

Forensic DNA markers are standardized so that jurisdictions around the world can effectively communicate. The current standard set of markers was developed at Baylor College of Medicine, in Dr. Thomas Caskey's laboratory, and at the Forensic Science Service (FSS) in England. The Promega Corporation and Applied Biosystems initially commercialized kits with the Caskey markers and FSS markers respectively. In 1996, the FBI Laboratory began an effort to establish "core" STR loci to be used in a national DNA database called Combined DNA Index System, or CODIS. Thirteen core STR loci were chosen in November 1997 and are now knows as the core "CODIS markers." When all 13 STR loci are used, there is a RMP of less than one in one trillion among unrelated individuals (Butler 2005). The 13 CODIS STRs, two additional STR markers, and the amelogenin gene are represented in the genotyping kit used in this study, the AmpFlSTR® Identifiler kit (listed in Table 1.2). The amelogenin gene provides a genetic sex estimate and is not required for a positive forensic identification.

The 13 core "CODIS makers" are used to create a DNA profile to identify individuals in forensic cases. Each person has a combination of alleles amongst all 13 markers. The uniqueness of this DNA profile is determined by the random match probability (RMP) as explained in Table 1.1. For example, at locus D13S317 an individual might have two alleles with 11 and 14 repeats, respectively. This individual will have two genetic variants, or alleles, at each of the CODIS loci. This combination of genetic variants across the CODIS loci creates an individual's forensic DNA profile. Table 1.1 represents an example of a forensic DNA profile.

Table 1.2. DNA Markers.

The following table displays all DNA markers with details such as chromosomal location, repeat motif, and known allele repeat ranges and numbers. CODIS STR markers displayed in bold.

Marker	Chromosome	Repeat Motif	Allele Size Range	# Alleles Seen
TPOX	2	GAAT	4-16	15
D2S1338	2	[TGCC][TTCC]	11-28	22
D3S1358	3	[TCTG][TCTA]	8-21	24
FGA	4	CTTT	12.2-51.2	80
D5S818	5	AGAT	7-18	15
CSF1PO	5	TAGA	5-16	20
D7S820	7	GATA	5-16	30
D8S1179	8	[TCTA][TCTG]	7-20	17
THO1	11	TCAT	3-14	20
vWA	12	[TCTG][TCTA]	10-25	28
D13S317	13	TATC	5-16	17
D16S539	16	GATA	5-16	19
D18S51	18	AGAA	7-39.2	51
D19S433	19	[AAGG][AAAG][AAGG] [TAGG][AAGG]	5.2-20	30
D21S11	21	[TCTA][TCTG]	12-41.2	82
Amelogenin	X, Y	n/a	~106-112	2 (X, Y)

Applied Biosystems provides an electropherogram with their AmpFlSTR® Identifiler kit to demonstrate the possible alleles associated with each marker and the relative lengths of each shown below in Figure 1.4.

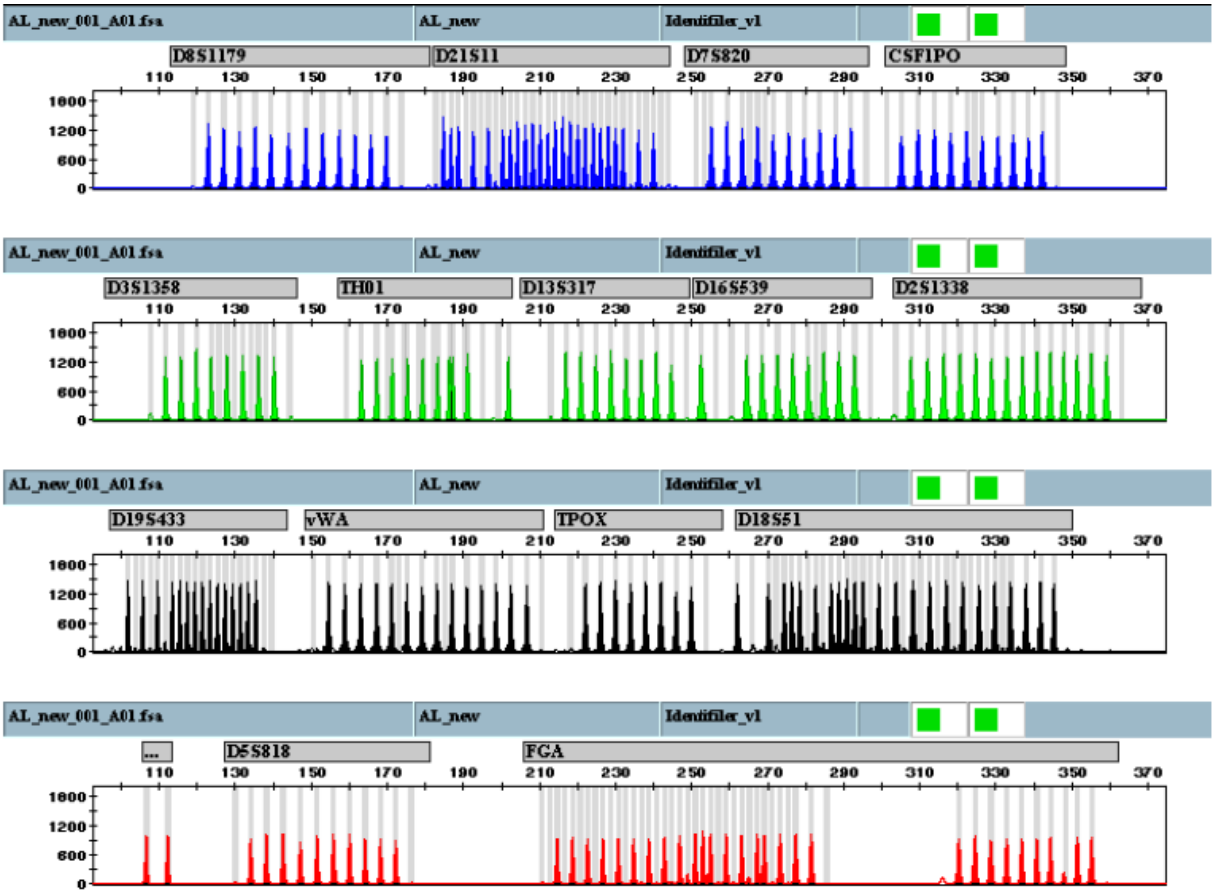

Figure 1.4. AmpFlSTR® Identifiler Allelic Ladder electropherogram. This figure shows the dye color and repeat allele peaks associated with each STR marker in the AmpFlSTR® Identifiler kit.

STR Genotyping: Relevant Issues

STR markers are the most commonly used in forensic identification applications. But as with all DNA markers, there are potential issues that the researcher must consider and account for when interpreting data. The most common issues are those of stutter, non-template addition, microvariant or off-ladder alleles, and allele drop-in and drop-out. These issues will be discussed in more detail below. But first to better understand many of the potential issues surrounding STRs, a brief explanation of how polymerase chain reaction, or PCR, works is required.

PCR – Polymerase Chain Reaction

Polymerase chain reaction, or PCR, is a technique used by researchers to duplicate a single or few copies of the desired DNA into an exponential number of copies. This process is called "amplification." At essence, PCR relies on temperature cycling, which can be performed in a very lo-tech manner – using a series of hot water bathes – or in a hi-tech manner using a machine called a "thermocycler" that automates the process. In PCR, short sequences called "primers" are used to target the DNA region of interest are mixed with a catalyst, a DNA polymerase necessary in DNA replication, extra DNA bases (deoxyribonucleotide triphosphates, or dNTPs), a buffer solution that promotes optimal reaction activity and Mg^{2+}. The DNA polymerase that is typically utilized is *Taq* polymerase, an enzyme derived from a thermophilic (heat loving) bacterium. dNTPs are necessary so that as the DNA polymerase works, it has bases to incorporate into new DNA strands.

PCR aims to imitate the natural DNA replication process in the body. Three steps are repeated anywhere from 20-40 (or as much as 60) times, depending on the protocol being employed. These three steps are denaturation, anneal and extension/elongation. The denaturation step heats the mixture enough to denature, or pull apart, the DNA creating two single-stranded DNA molecules in place of one double-stranded DNA molecule. The annealing step allows the primers to anneal to the single-stranded DNA template. The exact temperature needed for this step depends on the specific primers used. Finally, the extension/elongation step cycles to the temperature at which the polymerase experiences optimum activity (72°C is commonly used for *Taq* polymerase). It is during this step that the DNA polymerase will attach bases, from those free bases (the dNTPs) added to the mixture, to the growing copy of the template. After these

three steps have cycled enough times for a given protocol, the final step is a holding step. Generally, more cycles are used with more degraded DNA samples. The mixtures are held around 4°C for short-term storage (Innis and Gelfand 1990**)**.

Commercial kits have created protocols and reagents that optimize each step of this process for maximum results. As a result, there are many variations on the above steps, depending on the desired results.

The first three issues discussed (stutter, non-template addition and allele drop out) are all issues or additional concerns resulting from the PCR process. The final issue discussed, microvariant or off-ladder alleles, is a more general concern while analyzing STRs.

Allelic Stutter

There are several potential issues related to the analysis of STR. The most common problem is that of stutter products. Stutter products are often seen in an electropherogram as smaller peaks next to STR peaks. The stutter peaks are a result of the PCR process and thought to occur due to "slippage," or "slipped-strand mispairing." During the PCR process, a region of the primer-template becomes unpaired during the primer extension phase, which allows the primer or template to slip and one or more repeat units form a non-base-paired loop. On an electropherogram, this looks like a very small peak, approximately one repeat unit less, than the actual STR peak (Butler 2005).

Stutter can be problematic when trying to resolve DNA profiles from mixed samples. It is difficult to determine whether or not peaks are stutter or real allelic repeats from other (minor) contributors. Therefore, it is important to know how much stutter one can expect per locus. In the case of CODIS markers, there is variation in the amount of expected stutter for each locus but all

are under 15%. Longer alleles will exhibit more stutter than the smaller ones for the same locus (Butler 2005).

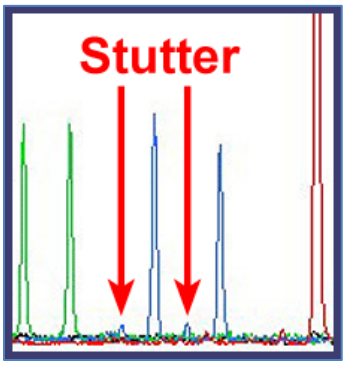

Figure 1.5. Stutter: The smaller blue peaks are an example of a stutter peak. The larger blue peaks are normal peaks. Figure from: http://www.nfstc.org/pdi/Subject06/pdi_s06_m02_05.htm

The following figures (Figure 1.6 – 1.9) show the stutter percentages for each STR locus as provided by the Applied Biosystems AmpFlSTR® Identifiler kit. The x-axis shows the individual STR marker with each number of repeats and the y-axis shows the percent of stutter seen experimentally. For example, the 8 repeat allele of D8S1179 shows approximately 2% stutter in experiments.

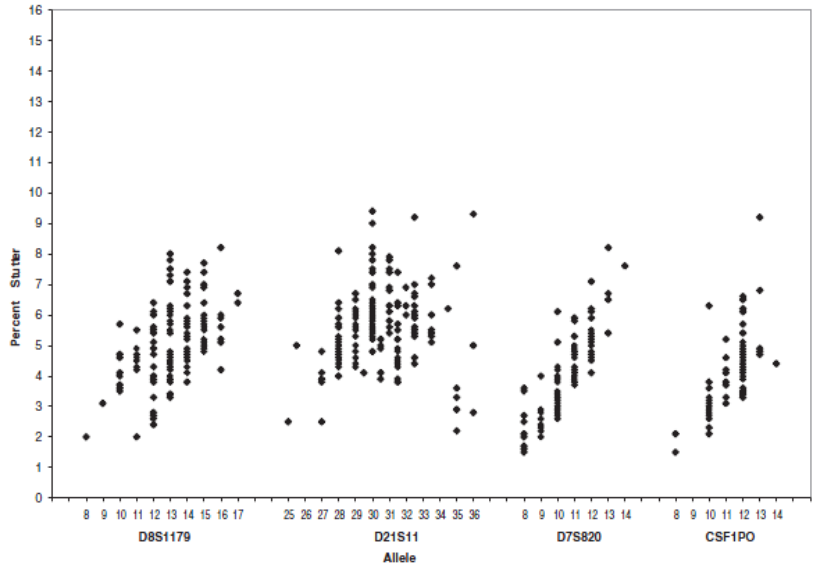

Figure 1.6. Experimentally derived stutter percentages for markers D8S1179, D2S11, D7S820 and CSF1PO.

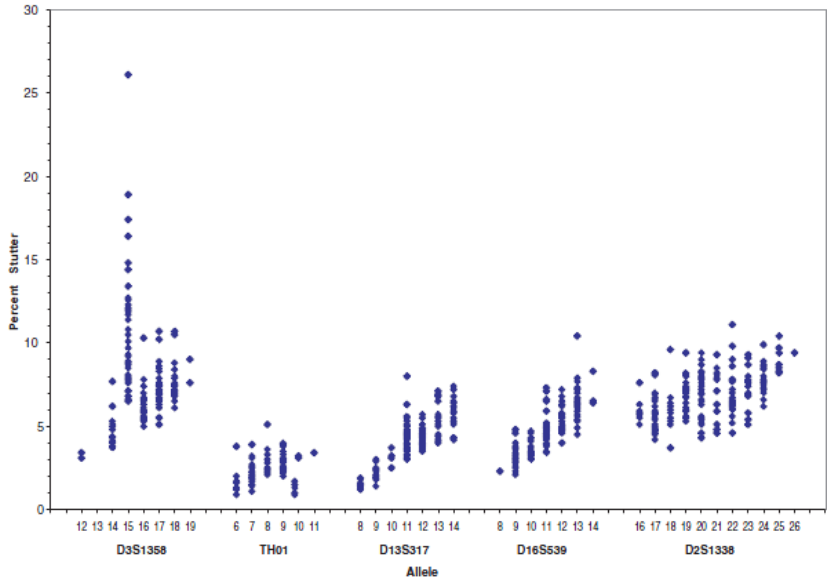

Figure 1.7. Experimentally derived stutter percentages for markers D8S1179, D2S11, D7S820 and CSF1PO.

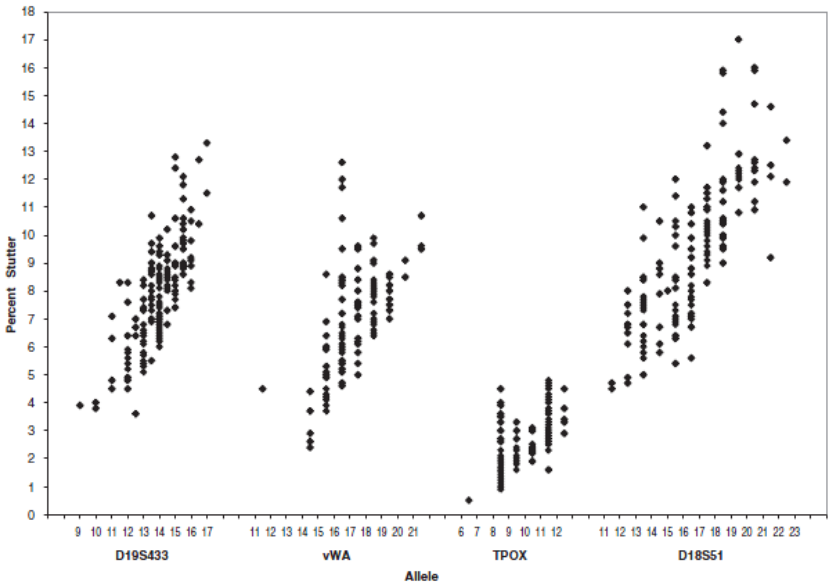

Figure 1.8. Experimentally derived stutter percentages for markers D19S433, vWA, TPOX, and D18S51.

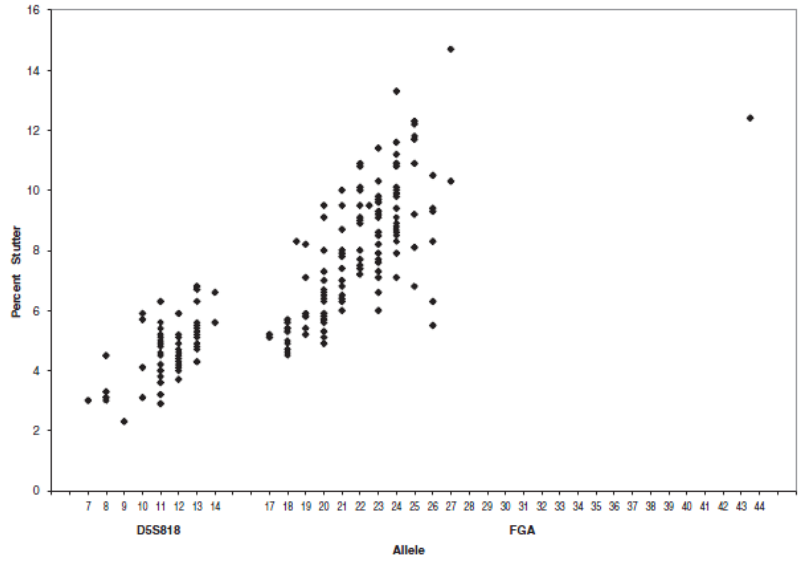

Figure 1.9. Experimentally derived stutter percentages for markers D6S818 and FGA.

STRs with longer repeat structures, such as the tetranucleotide structure of CODIS markers, tend to have reduced stutter percentages. Pentanucleotide peat loci are used in several kits and exhibit even lower stutter percentages. However, none of these loci (Penta A through Penta G) are used in the FBI's CODIS and are therefore not in the kit used in this study. Additionally, the speed of the DNA polymerase can affect the percentage of stutter. The most common DNA polymerase used by most kits has 50-60 base processivity but higher processing polymerases may be able to further reduce stutter product formation. Faster polymerases can copy the DNA strand before it has time to come apart and re-anneal (Butler 2005).

Non-Template Addition

Many DNA polymerases add an extra nucleotide to the 3' end of the PCR product. This nucleotide is usually an adenosine (A) and this process is referred to as adenylation or the +A form (Butler 2005). If all peaks for one alelle are not the same size the forensic scientist would not be able to accurately identify the correct allele for the locus (Applied Biosystems 2010).

Fortunately, the AmpliTaq Gold ® enzyme used in the Identifiler kit adenylates the PCR product. The kit promotes this adenylation with primer sequences that have been optimized for the +A form. The final extension step of 60 °C for 60 minutes also encourages this addition. The reason that this kit (and many others) is designed to promote *Taq*'s natural inclination to adenylate is to ensure that all molecules of the same allele are the same size. If the adenylation does not happen the allele might be represented by two peaks one base pair apart, as shown in the figure below.

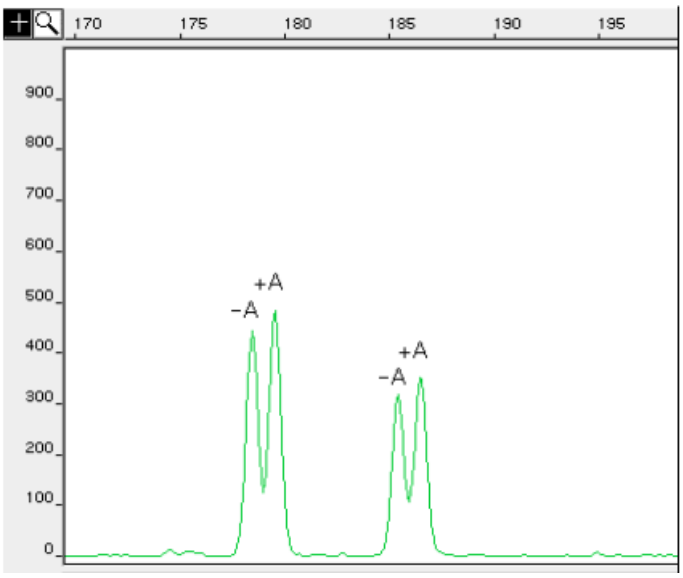

Figure 1.10. Adenylation: The graph shows peaks with and without adenylation. Non-adenylated fragments are a few bases shorter than their adenylated counterparts. This creates the double peak shown above.

Allele Dropout and Null Alleles

Allele dropout occurs when there is sequence variation in primer-binding regions or when the DNA region itself is degraded. If there is a sequence change in the primer-binding regions, then one or both primers will fail to hybridize to the appropriate part of the DNA sequence and the STR will not be amplified and therefore remain undetected. A failure to hybridize results in allelic dropout, resulting in a "null allele," which means that the STR failed to amplify. The genomic region containing the STR is present but does not appear in the analysis because it has "dropped out" due to failure of the primer to hybridize or because the template DNA is too degraded. Dropout happens very rarely with CODIS markers especially because these STRs are chosen, in part, for the stability in the flanking regions (the regions on either side of the desired fragment of DNA). The dropout phenomenon is also known as "false homozygosity" because a given locus can appear homozygous when it is in fact heterozygous with one dropped out allele.

There are a few solutions to a null allele. The first is to redesign the primer to avoid the mutation in the primer-binding region. Primer redesign is rarely done because it can result in the new primer interfering with other primers in a multiplex set. Redesigning the primers would lead to new PCR reaction optimization experiments, which are time-consuming and expensive. Second, the STR locus could be removed from the multiplex mix altogether, which is only feasible in the early development of kits. The third solution involves adding a so-called 'degenerate' primer to the primer mix that contains the known sequence polymorphism. Finally, it is possible to re-amplify the sample at a lower annealing temperature to force the null allele to be amplified. Reducing the annealing temperature allows the primer to anneal to slightly different sequences, such as the mutated primer-binding sequence in question (Butler 2005).

Allelic dropout can be very problematic for STR profiles. If even one allele is off there is a chance to have a false negative, which is why DNA databases allow modified searches to return profiles that are nearly a match (for example to return matches with 11 or 12 STR matches).

Microvariants and Off-Ladder Alleles

Microvariants, or off-ladder alleles, are not a problem with the PCR process but something to watch out for when analyzing STRs. Sometimes an allele is encountered with a slightly different sequence than those more commonly observed. These slightly different variations are called microvariants or off-ladder alleles because they do not have the same size as the reference ladder alleles. Microvariants typically have a number of full repeats followed by a partial repeat. For example, the 9.3 allele of THO1 has nine full repeats (AATG) and one partial repeat of three of the four bases of the repeating motif (ATG). These are more commonly found

in the more polymorphic loci and those with complex repeat motifs such as D18S51. Many of these microvariants have been investigated and catalogued and are taken into consideration in allele calling software. This software takes raw data obtained from fragment analyzing machines and will "call" or tell the user the exact allelic designation of each fragment. For example, an STR with eight repeats would be known as the "8 allele" of that STR. Since STRs are being named based on the number of repeat units, these should have little to no impact on building STR profiles for human identification.

Low Template DNA (LT DNA)

When DNA exists in low quantity it is referred to as "low template DNA" or LT DNA (also, "low copy number DNA" or LCN DNA). With low template DNA there is less of the DNA for the analyst to work with and the researcher needs to take special precautions. There is no official definition for low template DNA but it is generally accepted that any amount under 100 picograms (pg) is too low for typical analytical methods to be reliable. In such situations, an increase in PCR sensitivity is required in addition to different interpretation methods.

The PCR sensitivity can be improved both by increasing the number of PCR cycles as well as using a nested PCR method. The PCR cycles can be increased to as much as the researcher desires, usually up to 34 cycles in forensic analyses. However, each additional cycle has the potential to introduce greater numbers of stutter and other PCR artifacts, such as allele drop-in or dropout, which make rendering the DNA profile more difficult. In a nested PCR design, two sets of primers are used in two separate reactions. The first reaction amplifies the desired STR and flanking regions (regions on either side of the desired locus) while the second

amplifies a smaller fragment using a portion of the first PCRs product as the template. This PCR design reduces random PCR artifacts but requires transferring the PCR product into another tube, an action with the drawback of adding yet another step that could potentially exogenous, contaminating DNA into the reaction.

Experiments by Gill et al. (2000) have shown that when using DNA concentrations below 100 pg, 28-33 PCR cycles produces little DNA. However, full profiles were obtained down to 25-50 pg of DNA when using 34 PCR cycles. At concentrations below 25 pg, allele dropout occurred and full profiles were not possible. They found no advantage to using more than 34 cycles if more than 100 pg of DNA was available since the *Taq* enzyme increasingly degrades with increasing PCR cycles.

Additionally, they found that allelic stutter increased as both the cycle number and amount of template DNA was increased. This finding indicates that stutter increases largely as a product of over-amplification of the template DNA. With each increase in the number of PCR cycles there is an increasing risk of the *Taq* polymerase making a mistake, especially through slippage, which leads to stutter. Additionally, with more template DNA, there is an increased risk of mistakes during PCR amplification. These mistakes may happen because too much DNA is available relative to other chemical ingredients in the PCR mixture, which makes the reaction less efficient. There was also a general increase in the amount of imbalance in the relative allele size found in heterozygote loci with reduced DNA quantity and increased PCR cycle numbers. Imbalance refers to the relative size of the two alleles found in heterozygote loci. In a high quality DNA sample, the two allelic peaks for a heterozygote locus tend to be roughly the same size. They are imbalanced when one peak is larger than the other. This phenomenon is only a concern when trying to assess inherently problematic DNA mixtures.

Analytical Methods

Two analytical methods can be used to report and interpret DNA profiles obtained from LT DNA – biological and statistical. In the biological model, an allele is reported only if seen in more than one amplified product of the same sample extract. Each sample extract is amplified more than once and STR alleles are only counted as being present if they appear in at least two amplifications. The statistical model uses a Bayesian approach and calculates likelihood ratios by taking into account spurious bands, allelic dropout, and stutter. Using complex mathematical modeling, Bayesian statistics can determine the likelihood that a given allele is the true one and determine the probability that the profile seen under low copy number conditions is the true profile.

One complication of LT DNA is the determination of detection thresholds. When analyzing a DNA profile, the computer is instructed to call alleles above a certain threshold. If the threshold is set too low there is increased risk at including false alleles in the DNA profile. Conversely, if the threshold is set too high there is increased risk at excluding true alleles from the DNA profile. This threshold is measured in RFUs. When the fragment analysis machine, such as the ABI 3100, is reading a DNA sample, it is actually measuring the amount of fluorescence given off by the dye attached to each fragment. Higher fluorescence corresponds to higher quantities of DNA at that locus. For an allele to be reportable, it must be above a certain RFU value, known as the limit of detection (LOD) threshold, which is typically set at 50 RFUs (Gill et al. 2009 and Applied Biosystems 2010). Any peak below this LOD is considered part of the background noise of the machine. In samples with small DNA quantity, there is increased risk that true alleles will fall below this LOD because there is not enough high quality DNA to fluoresce above the threshold. Another possibility is that the allele is above the LOD but below

the low template threshold (T) known as dropout, which is typically set between 150-200 RFUs (See Figure 1.11). Alleles between LOD and T may or may not be true alleles. In low template DNA situations, there is an increasing chance the alleles will be between these two values (Gill and Puch-Solis 2009).

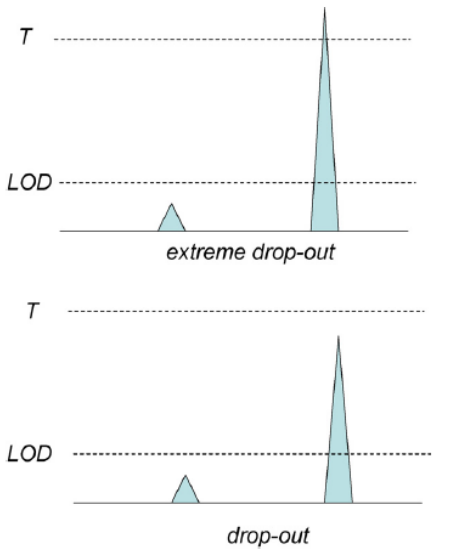

Fig. 1. When drop-out occurs, one of the alleles is below the limit of detection (*LOD*) threshold. With extreme drop-out, the present allele is above the low template threshold *T*.

Figure 1.11. Dropout: This figure shows the differences between extreme drop-out and drop-out with regards to the low template threshold and the limit of detection. (Source: Gill and Puch-Solis 2009.)

Ultimately, American Society of Crime Laboratory Directors Laboratory Accreditation Board (ASCLD/LAB) certified labs are required to determine their own threshold values. These certified forensic labs will perform repeated experiments to validate their own methods. This validation process is costly and terms of both time and money, but is required for certification to perform forensic analysis. It is important for labs to determine their own thresholds because each lab uses different pieces of equipment and different reagents. It is therefore rare for two labs to produce the exact same results due to these slight differences.

In current DNA databases, there is an option to search for allelic profiles between these two thresholds. In a legal setting it would be difficult to argue one's certainty that a low template profile below the threshold (T) is a complete match of a suspect. This low DNA quantity is problematic in the case of DNA samples obtained from skeletal material due to the amount of degradation. The current research project uses 50 RFUs as the Limit of Detection (LOD) but is not using the second threshold. All alleles falling between 50 and 150 RFUs will be noted but not excluded from the DNA profile.

Budowle et al. (2009) has outlined the limitations of LT DNA that should be considered when documenting DNA profiles. Typing low template profiles is not a perfectly reproducible technique because the analyst has to use his or her judgment when deciding what are true alleles. These results should not be used to exclude an individual, applied to post-conviction analyses, or cold cases without a lot of substantiation. It may be better to use a more concentrated sample rather than increase PCR cycles. Certain stochastic effects, allele drop-in, contamination from exogenous DNA, and allele stutter may all impact the reliability of results, particularly because there are no hard guidelines for analysts. Finally, they argue for better statistical interpretations and supporting data for probabilities to increase the reliability of LT DNA profiles. In the end,

LT profiles are more difficult, but not impossible, to define and extra care needs to be taken when DNA quantity is limited (Budowle et al. 2009).

X-rays

X-rays are a type of electromagnetic radiation that are produced when high-velocity electrons collide with materials containing atoms of high atomic numbers. X-rays are also referred to as "ionizing radiation" because they contain enough energy to detach electrons from atoms. Typically, electrons on the atom's outermost shell, or valence electrons, are most often affected by the ionizing effects of X-radiation (Dertinger 1969). A charged particle can detach secondary electrons from atoms or molecules in two ways: knock-on collisions and glancing collisions. Knock-on collisions occur when an ion is traveling much faster than the orbital speed of the atomic electron to be detached. In a glancing collision, the ion does not have to directly interact with the atom's electrons. Instead, it interacts with the atom's electrostatic field and can polarize the molecules, affecting the strength of electron bonds, causing them to detach. These glancing collisions happen more frequently than knock-on collisions (Dertinger 1969).

An X-ray machine typically consists of a vacuum tube (X-ray tube) that is capable of producing a high voltage to excite electrons, which are released by a hot cathode on one end of the tube. These high velocity-excited electrons collide with a metal target (of high atomic number), the anode, which is typically composed of tungsten or an alloy of tungsten and rhenium. This collision produces X-radiation, or X-rays.

DNA Damage from X-Ray

Two approaches to studying X-ray damage to DNA have been used. In one approach, dilute aqueous solutions are studied at ambient temperatures. Under these conditions damage is largely confined to water molecules, and the major attack on DNA involves the addition of electrons to base units and attack by OH- radicals (or free radicals) at various sites. Probably the most significant reaction of OH- radicals is the removal of a hydrogen atom from the deoxyribose sugar leading to chain breakage. In another approach, studies are conducted with "dry" DNA or in frozen aqueous solutions (Boon et al. 1984).

These and other studies have shown that ionizing radiation can have several types of mutagenic effects: single strand breaks (SSBs), altered bases, double strand breaks (DSBs) and other multiply damaged sites (Ward 1995). Multiple forms of DNA damage caused by a single ionizing radiation event are known as multiply damaged sites. When ionizing energy is introduced to a living cell, ions, free radicals, and excited molecules are created. These molecules are unstable species and react chemically, producing damage within the cell, leading to cell death and mutation. The hydroxyl radical (OH-) is involved in cell killing, DNA SSBs, and chromosomal aberrations. In cells irradiated under aerobic conditions, the hydroxyl radical accounts for 60-70% of cell killing. Experiments have shown that OH- radicals react preferentially with the bases of both single- and double-stranded DNA, though there is a possibility that the bases are sheltered inside the double helix by the sugar phosphate backbone of double-stranded DNA (Siddiqi and Bothe 1987, Swarts et al. 1992, and Ward 1981).

In experiments performed by Boon et al. (1984), oxygenated DNA solutions were irradiated at 77 Kelvin. They found that all the O_2 ions detected are formed close to DNA.

Oxygen competes directly with DNA for electrons, thereby reducing the total yield of DNA radicals. The primary radical products (G+ and T-) can lead to strand breaks. G+ and T- are damaged forms of the G and T DNA bases. Thus, the presence of oxygen results in a modest decrease in damage to DNA.

One factor that may contribute significantly to these processes is the effect of hydration on the formation and reaction of the radiation-induced radicals in and/or around the DNA. The primary hydration layer consists of ten to twelve water molecules per nucleotide, two to five of which are bound tightly to the DNA. The unique properties of the hydration layer appear to play a major role in the physical and chemical events that occur in the DNA. For example, Swarts et al. (1992) found that exposure of DNA to UV radiation (another form of ionizing radiation) altered the type and quantity of DNA damage produced as the hydration of the DNA was increased. Changes in the level of DNA hydration were also shown to affect the mobility of radiation-induced electrons in the hydration layer. The yield of DNA strand breaks and DNA-DNA crosslinks, in which two sections of DNA (intra- or inter-strand) are linked together, depends on the level of hydration. DNA crosslinks can occur between strands or on the same strand and prevent replication and lead to cell death if not repaired (Swarts et al. 1992).

Single Strand Breaks (SSBs)

The majority of radiation-induced electron interactions in DNA do not lead to damage in the form of strand breaks, and when they do occur, they are most frequently SSBs. Reactions of OH-radicals add substantially to this, both in terms of the total number of breaks and in increasing the complexity within a cluster (Nikjoo et al. 1997). There are two kinds SSBs that concern this research:

(1) immediate breaks formed soon after the formation of radicals;

(2) strand breaks that forms as a function of time after radiation (such as through slow hydrolysis).

Double Strand Breaks (DSBs)

Ionizing energy can also lead to double strand breaks, or DSBs. These have been suggested as a lethal event, and the ability of cells to repair such a break is in question. DSBs are not caused by a single reaction but rather are caused by multiple free radical reactions. It has been experimentally shown that the yield of DSBs is linear with dose of ionizing radiation. This relationship is quadratic for DSBs in aqueous solution. If an SSB lies exactly opposite to or at a small distance from another SSB in the complementary strand, the hydrogen bonding between the base pairs is broken and cleavage occurs.

Additionally, after ionizing radiation, the exact amount of radical production is inconsistent but in high local concentrations. Therefore it is not easy to predict the amount of damage caused by ionizing energy with each exposure. However, the damaging effects tend to be localized where the ionizing energy first hits the DNA strands. Most OH- radicals will react with DNA close to their point of formation (close to regions of high radical density), which is the likely method of double strand break formation caused by exposure to ionizing energy. After radiation there can be an increase in the number of DSBs even in neutral solution. A similar but lesser effect occurs even in the absence of oxygen (Siddiqi and Bothe 1987, Swarts et al. 1992, and Ward 1981).

Nikjoo et al. (1997) found that the lengths of damaged segments of DNA from individual radiation-induced electron hits tend to be short, indicating that consequent damaged sections

would be short, very seldom exceeding a few tens of base pairs. Their research shows that the characteristic feature of ionizing radiation is the ability to produce clustered damage over the dimensions of the DNA helix. Not all OH- radicals lead to strand breaks. Approximately 20% of OH- radicals react with the sugar phosphate backbone, which was deduced from counting the amount of phosphate end groups released after radiation exposure. The efficiency of SSB formation per OH- radical is about 13%. Computer simulations have shown a large variability in the types of clustered damage resulting from similar numbers of hits or quantities of energy deposited in a DNA segment. However, in long segments of DNA (216 base pairs), most segments show short hit regions, with most damage being in a single base pair, but 38% of hit segments have damage extending occasionally out to greater than 30 base pairs. Still, 33% of damaged sites have two or more lesions (damages from radiation hits). Most hits in the DNA do not lead to strand breaks, but those that do are often simple strand breaks. The more complex forms involve breaks on each side of the strand but separated by ten base pairs. The radiation is not cleaving directly through a strand of DNA but rather causing SSBs on both strands separated by several base pairs (Nikjoo et al. 1997, Sutherland et al. 2002).

Siddiqi and Bothe (1987) performed experiments to investigate the formation of DSBs. They found that DSBs are not formed linearly with radiation dose. It is possible that any linear component arises from DSBs produced from those SSBs that are already present in unirradiated DNA and therefore require only a single radiation hit to break the strand all the way through. Their experiments showed three to four times as many DBS as SSBs. A certain fraction of the radiation-induced DSBs are formed linearly, and the quadratic component of DSBs is supposed to arise through the accumulation of SSBs. Both the SSBs and the linearly formed DBSs are produced by OH- radicals from the bulk of the solution. These experiments provided evidence

for the occurrence of a radical transfer mechanism. Such a mechanism should occur after the first SSB formation, from a sugar radical at the end of the cleaved strand to the opposite strand, followed by a radical induced cleavage of the second strand. A radical transfer reaction could also proceed from an unbroken site to the opposite strand, thereby producing a strand break or another kind of damage (Siddiqi and Bothe 1987).

Damaged Bases

The level of base damage has been estimated at 2.7 times the yield of SSBs, or 2.7 x 10^3 per cell per gray (standard unit of measurement of X-ray radiation). Thymine glycol (a damaged form of thymine) represents about 10% of the total damaged bases (Ward 1995). Sutherland et al. (2002) showed that X-rays induce abasic (loss of pyrimidine sites in DNA) clusters, oxidized pyrimidine clusters, and oxidized purine clusters in DNA in human cells. Non-DSB (double strand breaks) clustered damages comprise about 70% of the complex lesions produced in cells. The relative levels of specific cluster classes depend on the environment of the DNA (presence or absence of oxygen or water).

Ionizing radiation can cause unaltered DNA bases to be released from the strand. This process may be affected by dose, extent of hydration, and the presence or absence of oxygen. The hydroxyl radical is more effective at causing SSBs than charged radicals on the bases. O_2 molecules will react differently with different forms of DNA. When DNA is in its B form (the most common form) the strand is less accessible by O_2. Experiments have shown that the base guanine (G) was released from the strand due to hydroxyl radical attack 60% more than the other three bases. It was also shown that the release of bases depended on the level of hydration and the presence or absence of O_2 molecules in addition to the form of the DNA molecule. Radiation

damage in the first 12-15 water molecules coating the DNA strand was 3.3 times less efficient in releasing DNA bases than damage sustained by the outermost water molecules (Swartz et al. 1992). The release of bases originating from radiation of the hydration waters is obtained predominately by (1) charge transfer from the direct ionization of the first 12-15 water molecules of the primary hydration layer, and (2) the attack of hydroxyl radicals generated in the outer, more loosely bound water molecules. By its proximity to the DNA, the inner layer of hydration has the ability to interact directly with the DNA. Charged molecules that are initially formed by radiation of the inner water molecules of the primary hydration layer may be transferred directly to the DNA. For the irradiated water molecules that are removed further from the DNA, it is expected that the hydroxyl radical will be the predominant damaging species (Swarts et al. 1992).

If radiation-induced electrons cause SSBs and DSBs, we can expect that some STRs will not be recoverable or will be recovered but shortened. If X-ray causes either an SSB or a DSB in the primer-binding region of an STR, the primer may be unable to bind to the correct region, causing the STR to not be amplified. If the X-ray causes an SSB or a DSB in another portion of the STR, it may be too damaged to be amplified, and if it is, it might show signs of allele stutter.

Forensic X-Ray Protocols

It is standard practice to X-ray all skeletal evidence in a forensic anthropology case. According to “Standards: Data Collection from Human Skeletal Remains” (Buikstra and Ubelaker 1994), put together by anthropologists to help streamline evidence and data collection for NAGPRA inventory requirements, standard radiographs should be taken of each skeleton.

These standard radiographs should have posterior-anterior positioning, with placement of the bones as close as possible to the film. They recommend radiographs of the cranium, long bones, and other abnormal bones (due to defects or injuries).

For the cranium, it is recommended to X-ray from a posterior-anterior and a lateral view using 24 x 30 cm film. The cranium should be oriented as it would for a photograph. Mandibles are to be subjected to three views for X-rays: one from each side and one with a posterior-anterior view. All views should maximize exposure of the dentition or dental development in the case of immature mandibles. Long bones of the same density can be X-rayed on the same film. They should be X-rayed with their anterior aspect facing the film. The closer to the central ray the bones are positioned, the less distortion there will be in the films. Finally, any bone with an abnormal condition should be X-rayed to fully document the condition.

Buikstra and Ubelaker (1994) recommend a film to tube distance of 48". The collaborators note that standard medical techniques can be easily adapted to X-raying skeletal remains, and all information concerning the techniques used should be recorded. Radiographic film is adequate for the job but some researchers have argued that using mammography film-screen combinations and techniques will allow for greater resolution (Buikstra and Ubelaker 1994).

Aside from fully documenting the skeletal evidence, X-rays can be used in positive identification of a deceased individual. X-rays are perhaps the most common diagnostic tool used in clinical practice. Therefore, X-rays represent the most common source of ante mortem information. Positive identification is done by comparing ante- and post-mortem X-rays of unusual traits that have been documented in the individual's medical and dental records. An

expert can perform a point-by-point comparison of osteological structures as well as match measurements taken on both the ante- and post-mortem radiographs. The exact number of comparison points required to make a positive identification are debated by experts (Ciaffi et al. 2011). The shape and structures of the frontal, ethmoid, and maxillary sinuses are often compared as a type of radiographic fingerprint (Christensen 2005). One can also compare the sphenoid and mastoid processes as well as the patterns of trabecular bone (Mann 1998). Finally, pathological conditions or anomalies can be compared to make a positive identification. Therefore, it is vitally important to take the appropriate X-rays of each skeleton in a forensic case in order to help make a positive identification (Byers 2001).

DNA, by design, is a stable molecule and is often protected (when not in use as in cell replication) through its shape and form. STRs are derived from non-coding regions of the genome. The STRs chosen for inclusion in the CODIS marker set (not including the amelogenin gene) are unlinked and are located on different chromosomes. X-ray radiation is known to be clustered (Sutherland et al. 2002) and therefore may only impact a few markers in a PCR sample. The stochastic nature of X-ray radiation damage will likely result in an overall decrease in the amount of template DNA available for PCR-amplification (LT DNA). The amelogenin gene will be absent if the portion of the genome where the primers bind to has been removed in every single molecule of template DNA. Furthermore, X-ray damage may allow an STR marker to be PCR-amplified but shortened due to an SSB or DSB, resulting in a stutter effect at that locus. Given this knowledge, we can expect to see a range of PCR amplification from no loci amplified to all loci amplified. Most PCR trials will likely result in partial DNA profiles. Additionally, we may see an increase in stuttering throughout the STR markers.

Chapter 2: Research Questions, Study Design, and Methods

Research Questions

The goal of the present study is to examine the effect of X-ray radiation on the recovery of DNA markers from human teeth. Given that X-ray radiation is understood to damage DNA, the following hypotheses were tested to investigate the extent to which X-ray radiation affects DNA markers and therefore compromise a resulting genetic profile:

Hypothesis I: X-ray radiation reduces the total number of recovered DNA marker alleles.

If X-ray radiation damage is occurring, we might expect to see a decrease in the total number of alleles across all DNA markers recovered from the irradiated human molars. A DNA marker allele is counted as present if it appears as an electropherogram peak in the appropriate allelic range for that marker (that is, it is not off-ladder) and at an RFU threshold above 50.

Hypothesis II: X-ray radiation causes DNA marker allele fragment lengths to shorten, producing allelic stutter.

Even if DNA marker alleles above a 50 RFU threshold and within the appropriate allelic size range are recovered, does X-ray radiation significantly damage DNA marker alleles and produce allelic stutter? The expectation is the X-ray damage should occur in irradiated samples, and that greater amounts of allelic stutter should be seen in the electropherograms.

Hypothesis III: X-ray radiation decreases the total amount of recovered DNA per marker.

As discussed in the background chapter, DNA damage from X-ray radiation is thought to be random with respect to chromosomal location (Nikjoo et. al. 1997); therefore we expect to see a uniform decrease in the total amount of DNA, as represented by RFU values, across all DNA markers.

Research Study Design

Samples

This study uses tooth samples to assess the effects of X-ray radiation on genetic profiles. Teeth are often used to extract DNA for forensic identification because they survive degradation processes longer (given their hard outer enamel) than other human bodily material, thus preserving high quality DNA. DNA can be reliably extracted from teeth exposed to environmental conditions such as high heat, humidity and varying pH levels that are often destructive to DNA extracted from bones (Schwartz et al. 1991). DNA extracted from teeth has the highest chance of being preserved and undamaged after exposure to X-ray radiation than DNA from other bones due to the hardness of the tooth enamel. Therefore, if X-ray radiation damages the DNA extracted from teeth we can extrapolate that the same or worse damage would occur to DNA from other, less protected, skeletal material.

This study used fifteen human molars from tooth extractions performed in the office of Dr. Randall Pearce, DDS. Upon extraction, these teeth were potentially stored in varying conditions such as a water and alcohol solution for preservation and disinfection, and sterilized with high pressure and heat via autoclaving. Unfortunately, the potential degradative effect of storage in such a solution is unknown, but certainly high temperatures are known to be damaging

to DNA (i.e., Arismendi et al. 2004). Additionally, it is uncertain how long the teeth had been stored since extraction, making their post-extraction age unknown. All these factors combined render it likely that degradative processes had already affected DNA quality and quantity of the teeth used in this study. In fact, nuclear DNA could not be recovered from five of the ten teeth used in this study (see Chapter 3: Results).

Study Workflow

The study's research workflow was as follows (Table 2.1 and Figure 2.1): First, fifteen first or second molars were cut in half using a Dremel tool. Second, a DNA extraction was performed on the fifteen controls using a modified silica extraction procedure (Boom et al. 1990, Hoss and Paabo 1993). Third, the control sample extracts were PCR amplified in triplicate using the AmpFℓSTR® Identifiler® PCR Amplification Kit and screened) for the presence amplified DNA using gel electrophoresis. Fourth, because five control samples failed to yield PCR-amplified DNA, only the ten experimental samples with matched DNA-positive control samples were subsequently X-rayed by technicians at the University of Tennessee Student Health Center. Next, a DNA extraction was performed on the ten experimental samples and PCR-amplified in triplicate, using the same protocols that were applied to the control samples. Subsequently, all matched control (n=30) and experimental PCR products (n=30) were run on an ABI PRISM ® 3100 Fragment Analyzer. Data were analyzed using Applied Biosystems GeneScan 3.7 software. Finally, statistical analysis of the fragment analysis results was completed; these are described below.

Table 2.1. Study workflow.

1	Fifteen human first or second molars were cut in half to create a set of control and of experimental material.
2	DNA was extracted from fifteen control sample halves.
3	The control sample extracts were PCR-amplified once using the AmpFℓSTR® Identifiler® PCR Amplification Kit.
4	PCR products visualized on gel; 10 of 15 produced recoverable DNA
5	The control sample extracts were PCR-amplified twice more using the AmpFℓSTR® Identifiler® PCR Amplification Kit, resulting in three total PCR amplifications per DNA extract (n=30).
6	The experimental sample halves that matched control samples with recoverable DNA from Step 4 were exposed to X-ray (n=10).
7	DNA was extracted from the ten experimental samples.
8	The experimental samples were PCR amplified in triplicate each using the AmpFℓSTR® Identifiler® PCR Amplification Kit.
9	Control and experimental PCR products were run on the ABI PRISM ® 3100 Fragment Analyzer.
10	ABI GeneScan 3.7 software was used to analyze results.
11	Statistical analysis of fragment analysis results was performed.

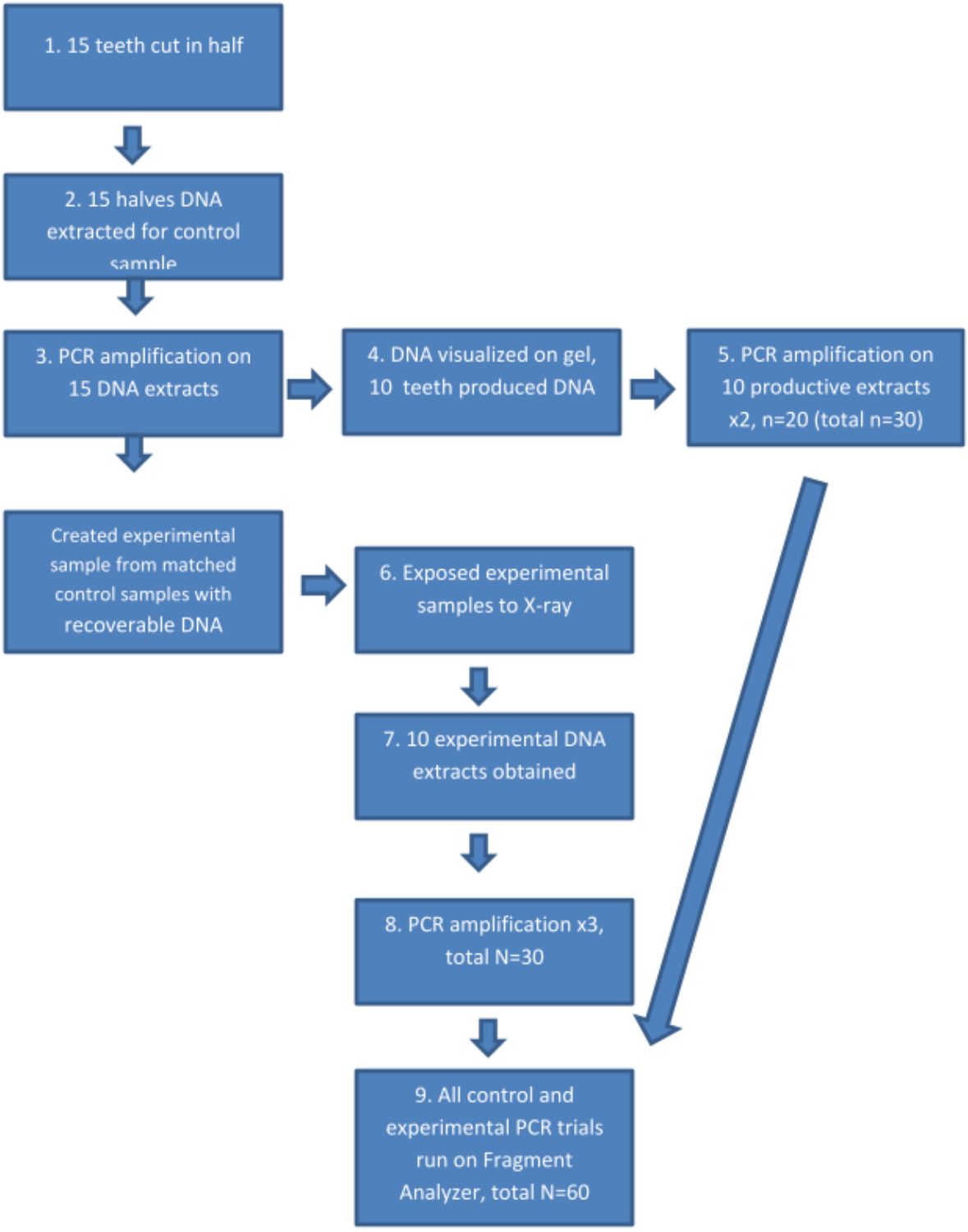

Figure 2.1. Workflow.

Experimental Methods

Contamination Controls

Samples were handled by the analyst with sterile gloves at all times. Prior to extraction, samples were stored in an upright -20°C freezer in the foyer of the Forensic Genetics Laboratory at the University of Tennessee. The Forensic Genetics Laboratory is one of two clean room labs forming part of the Department of Anthropology's Molecular Anthropology Laboratories. It is physically separate from the Ancient DNA lab and the main DNA analysis lab so as to avoid cross contamination. The Forensic DNA lab is comprised of four separate sections: a foyer, a gowning area, sample preparation and extraction room, and a PCR preparation room.

The Forensic Genetics clean room lab has its own filtration unit to prevent cross-contamination with other laboratories. HEPA-filtered air flows into the rooms through filtration pack in the ceilings and exits through separate vents. All laboratory surfaces are regularly decontaminated of exogenous DNA with 10% bleach, followed by 70% ethanol, and then a commercial DNA removal product, *DNA Away*© (Molecular BioProducts) .

The Forensic Genetics Laboratory is equipped with a biohazard hood in the sample preparation and extraction room, and a PCR hood in the PCR preparation room, both of which are equipped with blowers that blow air from inside the hood back outside to protect the sample from the researcher, and with UV lights to crosslink exogenous DNA. The biohazard hood is also equipped with a filter and vent in the top to suck the air out to protect the researcher from hazardous chemicals. The UV lights inside the hoods were turned on for a minimum of 30

minutes after each use. All PCRs were prepared in the Forensic Genetics PCR preparation room, and carried out into the Main lab to be run on ABI Veriti brand thermocyclers.

Full personal protective equipment (PPE) was worn at all times in the Forensic DNA lab clean rooms. This included two layers of gloves, full body gown, facemask, face shield, and shoe coverings. Gloves were changed when working with each new sample to help prevent cross-contamination. The clean rooms were exposed to automatic UV lights overnight and every time in between procedures to decontaminate the room from stray DNA fragments.

Sample Preparation

Tooth samples were prepared for DNA extraction as follows: Control and experimental samples were soaked in bleach for 10 minutes to remove surface contamination. All equipment was removed from the biohazard hood in the sample prep room section of the Forensic DNA clean rooms. Then, all surfaces were cleaned with a 10% bleach solution, followed by a 70% ethanol solution, and finally a DNAway©solution. A Dremel with a diamond bit attachment was cleaned with the same solutions and covered with a plastic bag with a triangle cut out to allow it to be pulled over the diamond bit attachment. Aluminum foil was placed on the bottom of the biohazard hood along with a vice and a plastic dish to collect tooth fragments and dust. Pieces of foam tape were placed on each edge of the vice followed by another piece of aluminum foil to create a valley for tooth dust and fragments to fall. The tooth sample was placed in between the edges of the vice as it was closed to hold the tooth sample in place.

On the lowest speed, the Dremel was used to slice off thin sections of the tooth. Tooth slices and dust were poured into a weigh boat (used as a plastic collection dish), which was then used to pour the tooth slices and dust into an appropriately labeled glass vial. After each sample

was processed, the aluminum foil, plastic Dremel cover, and plastic collection dish were discarded. Everything was removed from the biohazard hood and all surfaces were decontaminated again using 10% bleach solution, followed by 70% ethanol solution and finally the DNAway© solution. These steps were repeated for each tooth sample in preparation for extraction. Each labeled glass vial was then stored in a -20 ^{o} C freezer until it was ready for extraction.

Extraction Protocols

Tooth samples were processed for DNA extraction and amplification using the modified silica extraction procedures of Boom et al. (1990) and Hoss and Paabo (1993). The size-fractionated silica was prepared prior to extraction. To do this, 12g of silicon dioxide (Sigma) was mixed with Cellgro® double distilled water (ddH2O) to reach a total volume of 100 ml in a glass graduated cylinder. The graduated cylinder was then vortexed and allowed to sediment at unit gravity for 24 hours at room temperature. Then 86 ml of the supernatant was removed using a serological pipette with a 2mL pipette tip. Then ddH2O was added to the cylinder to reach a total volume of 100 ml. The cylinder was then vortexed again to resuspend the silica pellet. It was allowed to sediment again for another 5 hours at room temperature. Another 88 ml of supernatant was removed using the serological pipette. 120ul of HCl (32% wt/vol) was added to adjust the silica pH to 2. The silica was pipetted into 1.5ml eppendorf tubes for refrigerator storage. In the absence of light, the silica is stable for at least 6 months.

For this protocol two lysis buffers are necessary: L6 and L2. The buffers were prepared in the biohazard hood in the following way. For the L6 buffer, 20ml of a .1M Tris hydrochloride

solution (pH 7.4) was added to 24g of guanidinium thiocyanate (GuSCN) in a 50 ml conical tube. The tube was heated to 60-65^{o} in a microwave. Then 4.4 ml of a .2M EDTA solution and .5ml of Triton X-100 were added. The pH of the solution was adjusted with NaOH to reach a pH of 8. One and a half ml of silica was added to bind any contaminating DNA. The tube was then vortexed and centrifuged. The conical tube was covered in aluminum foil to keep light out and stored under the biohazard hood. The L2 buffer was prepared using 20ml of the .1M Tris hydrochloride solution (pH 7.4) and 24g of GuSCN in a 50ml falcon tube. The tube was then heated to 60-65 ^{o} to allow the GuSCN to dissolve into solution. Aluminum foil was placed around the L2 tube to keep out the light and stored in the biohazard hood. Both buffers are stable for at least three weeks at room temperature in the dark.

For each extraction, .25g of the powdered bone sample was added to 820 µl of L6 buffer in a 1.5ml tube. The tube was vortexed and incubated at 60C for approximately two hours with occasional vortexing. The tubes were centrifuged, and 500 µl of the supernatant was pippeted into a new eppendorf tube containing 500 µl of L6 and 40 µl of silica. The new tubes were vortexed well. These tubes were then allowed to sit at room temperature for 15 minutes to give time for the DNA to bind to the silica and then centrifuged again for at least 15 seconds. The supernatant was discarded and the pellet was washed a total of five times: twice with L2, twice with 70% ethanol and once with acetone. Each time, 1 ml of the wash was added, the silica was resuspended via vortexing, the tube was centrifuged and the supernatant discarded again. The pellet was then dried at 56 ^{o}C with open lids (lightly covered with aluminum foil) for 10 minutes or until dry. Finally, 65 µl of ddH20 was added to each tube, vortexed, allowed to sit for 10 minutes at 56 ^{o}C, centrifuged and the supernatant removed. This last step was performed twice. The final tubes were then placed in the freezer until needed for PCR.

PCR Set-Up and Amplification

In the PCR set-up chamber of the Forensic Genetics Laboratory clean room, empty PCR reagent master mix and PCR sample tubes were placed under the PCR hood and UV irradiated for a minimum of 15 minutes before use. Otherwise, all tubes were kept capped when not in use to prevent cross-contamination.

A master mix from the AmpFℓSTR® Identifiler® PCR Amplification Kit was used according to manufacturer's instructions: The master mix was prepared by combining 10.5 µl of AmpFℓSTR® PCR Reaction mix times the number of samples, 0.5 µl of AMpliTaq Gold DNA polymeras times the number of samples and 5.5 µl of AmpFℓSTR® Identifiler Primer set times the number of samples. The master mix was then vortexed for a minimum of 5 seconds. 15 µl of master mix was pipetted into each PCR tube. As per the manufacturer's instructions, ten µl of DNA was added to the appropriate sample tube, leaving two tubes without sample DNA: the positive and negative PCR controls. When done, all the PCR tubes were vortexed then carried by freshly gloved hands into the main lab for PCR amplification. In the main lab, 10 µl of control DNA were added to the positive PCR control tube which was then vortexed. All tubes were centrifuged before being added to the ABI thermocycler. The manufacturer's recommended thermal cycling conditions were used. Table 2.2 shows the thermal cycling conditions used. All samples were PCR-amplified three times for a total of 60 PCR amplifications.

Table 2.2. PCR conditions. Manufacturer recommended thermocycling conditions for PCR with AmpFℓSTR® Identifiler kit.

Initial Incubation Step	Denature	Anneal	Extend	Final Extension	Final Step
HOLD	CYCLE (28 cycles)			HOLD	HOLD
95 °C 11 min	94 °C 1 min	59 °C 1 min	72 °C 1 min	60 °C 60 min	4–25 °C (forever)

DNA Visualization

To assess whether any tooth samples yielded positive DNA results, all samples were run out on an agarose gel slab for DNA visualization. Agarose gel slabs were prepared with a 2% agarose solution (2g agarose with 100mL of Tris-borate-EDTA [TBE]) and heated in the microwave for two minutes. Three microliters of GelRed™ was added to the agarose mixture. The mixture was then poured into a casting tray with a sample comb (to create sample wells) and allowed to solidify at room temperature. The comb was then removed and the entire gel was inserted into the electrophoresis chamber and covered with additional electrophoresis buffer (the TBE) to completely submerge the gel. Exactly 5 µl of either PCR product, a positive DNA control, or a negative (blank) control (as well as the positive and negative controls) was mixed with 3 µl of loading dye before being pipetted into individual wells in the agarose gel.

Once the samples were loaded, the plastic cover was placed over the gel and the power leads were connected to the electrophoresis gel rig and run at XX V for at least 30 minutes, allowing enough time for the DNA fragments to migrate sufficiently for visualization. Once the DNA fragments migrated sufficiently, the agarose slab was removed from the electrophoresis machine and placed inside a transilluminator (an ultraviolet lightbox), which illuminates the

GelRed™ stain in the PCR-DNA in the gel. PCR products were determined to be producing enough DNA if white bands were observed in the transilluminator at the correct size ranges when compared to the manufacturer-provided allelic size ladder.

Experimental Sample Treatment: X-ray radiation

The experimental sample set was exposed to a typical dose of X-ray radiation. A 'typical' dose of X-ray radiation, for the purpose of this study, is the amount it takes to obtain one radiograph of a tooth. Twice this amount would be the amount that it takes to obtain two radiographs of that bone. The exact specifications for the X-ray machine, described below, were left to the discretion of the X-ray technician at the Student Health Center on the University of Tennessee campus, who is accustomed to X-raying forensic cases for the Forensic Anthropology Center. Standard values for obtaining a clinical head X-ray were modified slightly to produce sharper figures given the lack of flesh.

All experimental samples were X-rayed at the recommended film to tube distance of 48". The teeth halves were positioned with the cut surface down on the caps of their individual plastic sample tube caps, which were placed separately on a large piece of floral foam. The tooth halves were X-rayed for 4.9 mVs at 50kVp for 25 mAs. Peak kilovoltage or kVp is a measure of the voltage being applied across the X-ray tube. This determines how much contrast the resulting X-ray film has. Each body part takes more or less kVp to penetrate it to obtain a quality figure. Millivolts per second or mVs is how long the object was exposed to X-rays. Approximately 50 kVp is less than the normal amount used to X-ray a human head. This number was reduced from the standard because skulls have less tissue to penetrate than a fully fleshed head; therefore less voltage was required. Milliamperes per second or mAs is a measure of radiographic density and

defines how long an object was exposed to relative to a given amount of electricity. Again, this number was reduced from the medical standard used for a living head due to less tissue being present. This number is roughly the kVp divided by the mVs (Brogdon 1998, Pizzarello 1982). After X-ray treatment, each tooth half was soaked in bleach for 10 minutes to remove surface contaminants. Each experimental sample was subjected to the same preparation, DNA extraction, and PCR amplification processes as outlined above.

Fragment Analysis

After PCR and DNA visualization, all PCR amplification products (n=60) were taken to the Molecular Biology Resource Facility (MBRF) for fragment analysis. Samples were prepared for fragment analysis as recommended by the manufacturer (AmpFISTR Identifiler PCR Amplification Kit User's Manual). A master mix of Hi-Di™ Formamide and GeneScan™-600 LIZ™ Size Standard was prepared as shown:

- (Number of samples + 2) x 24.5 µl Hi-Di Formamide
- (Number of samples + 2) x 0.5 µl GeneScan-600 LIZ Size Standard

The master mix was vortexed and centrifuged. Each Genetic Analyzer sample tube was aliquoted with 25 µl of the Hi-Di Formamide/GeneScan-600 LIZ solution and 1.5 µl of PCR product (or allelic ladder). The tubes were sealed and the sample tray was vortexed and centrifuged briefly. Afterwards, the sample tray was denatured for 3 minutes at 95 ° C then chilled for 3 minutes. The MBRF lab technicians prepared the ABI 3100 Genetic Analyzer and placed the sample tray in the machine.

As the ABI PRISM ® 3100 Genetic Analyzer analyzes the samples, the information is read to the computer. ABI's GeneScan 3.7 software were then used to analyze results using the following suggested analysis parameters:

- Peak Amplitude Thresholds (PAT) equal at 50;
- Minimum peak half width set to 2 points;
- Size Call Range and Analysis Range set to "Full Range;"
- No smoothing options selected;
- Size Calling Method: Local Southern Method;
- Baseline set to 251 points.

In some cases, the software had a difficult time analyzing the information from the machine, as the amount of degradation of the DNA created a significant amount of noise in the fragment analysis process. In such instances, the parameters were adjusted until the software was able to analyze all samples. For example, in some cases the machine had to be instructed to read at different PATs or have a higher baseline depending on the amount of noise. This helped the machine to ignore the noise and only read the allelic peaks in the sample.

Figure 2.1 shows the sample flow from the initial extraction of a sample to the creation of three PCR trials and the three fragment analysis samples. Each sample (ten control and ten experimental) results in one extraction sample. Each sample was PCR-amplified three times. Each resulting PCR amplification was then run through the fragment analysis machine. In short, each sample resulted in three PCR trials and three fragment analysis samples.

Another problem was the amount of leftover primer in the samples. The manufacturer did not recommend a PCR cleanup process to remove unused primers. Unfortunately, due to the

amount of degradation, there was significant leftover primer in many samples. This created "noise" in term of primer-dimer formation, or instances in which primers – usually about 20 bases in length -- hybridize, or "dimerize." Primer-dimer formation results in fragments significantly less than 100 base pairs in length. The shortest marker in the kit is the amelogenin gene at around 105 base pairs. Fortunately then, all fragments less than 100 base pairs could be safely ignored as "noise." Figure 2.2 shows an example of this sample "noise." In the future, post-PCR clean-up processes will be utilized to remove the excess primers to ease data analysis and interpretation.

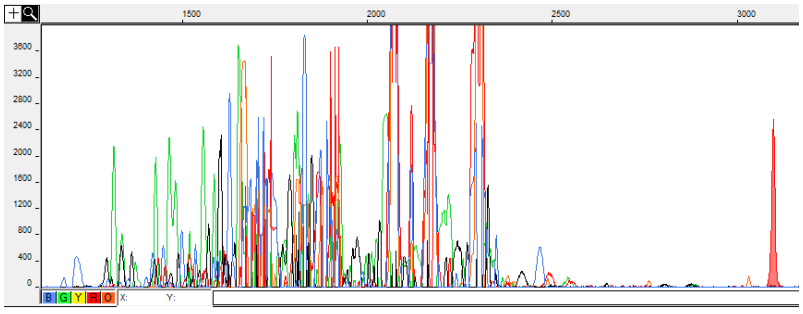

Figure 2.2. Sample Noise: Example of sample noise from primer-dimer formation. The large peaks seen on the left side of the figure are all under 60 base pairs in length, which is far shorter than any expected variant fragment. These are a result of leftover primers binding to each other in the absence of template DNA. The highlighted peak on the far right is the first marker in the kit, the amelogenin gene, at 105 base pairs in length.

Statistical Design & Methods

This research assumes that X-ray radiation will damage DNA markers, and predicts that that damage will manifest in three ways:

(1) A reduction in the total number of genetic variants recovered;

(2) A reduction in fragment sizes, seen as allelic stutter;

(3) A reduction in the amount of DNA recovered per marker.

All statistical analyses were performed using IBM SPSS Statistical software version 21 for Windows. A significance level of p=0.05 is used for all statistics. The asymptotically estimated p-values are reported in all cases.

Missing loci were analyzed visually as well as statistically via a chi-square test. A chi-square analysis was conducted to test for differences in frequencies of missing loci. This test will show if any locus is more frequently found missing in a sample or not being amplified. That is to say, is any locus (or loci) more frequently dropping out of the consensus DNA profiles.

Consensus Profiles

A Wilcoxon signed-rank test was conducted for each sample to examine consistency between trials. The Wilcoxon signed-rank test, as a non-parametric test, compares median differences between groups of data. In all cases, no significant differences were found amongst all three PCR trials for each sample (control and experimental). Therefore, the use of consensus profiles is statistically justified, should the test warrant its use

Consensus profiles were used to generate some descriptive statistics, as well as to test Hypothesis III. All three PCR trials of each sample were averaged into a consensus profile for statistical analyses. If the same genetic marker was present in two or three trials of the same sample, an average fragment length for that marker was calculated for inclusion in the consensus profile. Similarly, if potential stutter was observed, the stutter allele was counted as part of the profile only if it was observed in more than one amplification of the same extract, as per the

biological model for reporting LT DNA profiles described in Chapter 1. See Appendix 1 for fragment sizes and corresponding RFU values for each consensus sample.

Hypothesis Testing

Hypothesis I: X-ray radiation reduces the total number of recovered DNA marker alleles.

A DNA marker is counted as present if it appears as an electropherogram peak in the appropriate allelic range for that marker (i.e., not an "off-ladder" allele, as determined by the Genescan v. 3.7 software) at an RFU threshold above 50. A reduction in recovered DNA markers is expected to occur as a result of DNA damage. To test this hypothesis, a Wilcoxon signed-rank test was used to compare the number of markers recovered across all the matched control-experimental samples from all PCRs

Hypothesis II: X-ray radiation causes DNA marker allele fragment lengths to shorten and produce allelic stutter.

To test whether if the X-rays significantly increased the amount of allelic stutter, the amount of stutter from each PCR trial of each sample was counted and pooled into a control group and an experimental group. The amount of stutter was then compared using the Mann-Whitney *U* test, which is designed to compare the medians between two groups and makes no assumptions about normality. This non-parametric test was required because the data were found to be non-normally distributed. Significant differences in fragment lengths are expected to be found because X-ray radiation damage is known to cause SSBs and DSBs. These kinds of damages are expected to manifest in the form of allelic stutter. A radiation-induced electron may

cause a DSB in one or more fragment but other copies of the same fragment may be unaffected. This might lead to stuttering at that DNA marker.

Hypothesis III: X-ray radiation decreases the total amount of recovered DNA per marker.

A higher RFU for a given marker indicates that there are more copies of that marker present. It is expected that the control samples will produce, on average, higher RFU values. The better the available DNA template, the more successful are any PCR runs using that template; the end result is more amplified fragments per marker. A Mann-Whitney *U* test is used to find if there are any significant differences in the RFU values for each marker, between the control consensus profile and experimental consensus profile. The experimental samples are expected to be more degraded due to the X-ray exposure, produce fewer DNA fragments, and therefore lower RFU values) for each marker.

Chapter 3: Results

First, descriptive statistics and the derived consensus profiles are described and characterized to give a broad understanding of the data obtained in this study. The three hypotheses of this study are described and tested. Non-parametric statistics are used in all cases. Sample 5 is excluded from statistical analysis because experimental sample 5 produced no amplified DNA. Hypothesis I is tested via the Wilcoxon signed-rank test and uses all three PRC trials of each control and experimental sample. Hypothesis II is tested via a Mann-Whitney *U* test to examine differences in the amount of stuttering seen between all three PCR trials of the control and experimental samples. Hypothesis III is tested using the Mann-Whitney *U* test and uses the consensus samples for the control and experimental groups. Finally, a *post-hoc* test examining potential dye biases is explained and performed.

Data Description and Descriptive Statistics

Ten of fifteen teeth produced nuclear DNA material and were amplifiable with the AmpFℓSTR® Identifiler® PCR Amplification Kit. All ten control samples used and nine experimental samples produced either complete or partial profiles in the sense that at least one of 15 total markers were represented at above a 50 RFU threshold in at least two out of three PCR runs, or trials. Experimental sample five did not produce a genetic profile in any of the three trials. Table 3.1 shows how many total genetic variants were identified (we can expect anywhere from16-32 genetic variants depending on the number of heterozygote loci) in the consensus sample of each control and experimental sample.

Table 3.1. Number of variants recovered from all cases.

Case	# Variants – Control (consensus)	# Variants – Experimental (consensus)	# Present in Control & Missing from Experimental	# Missing in Control & Present in Experimental
1	28	13	15	0
2	28	15	7	6
3	30	30	2	2
4	35	34	3	2
5	38	0	38	0
6	32	23	12	3
7	38	31	13	6
8	29	29	3	2
9	29	28	3	2
10	29	5	25	1

Table 3.1 shows how the number of genetic variants comprising each case in both the control and the experimental groups. It also shows how many genetic variants were present in the consensus control profiles but were absent in the consensus experimental profiles ("# Present in Control & Missing from Experimental") as well as how many extra genetic variants the consensus experimental profiles contained that were not present in the corresponding consensus control profiles ("Missing in Control, & Present in Experimental"). In some instances, the extra loci found in the consensus experimental profile represent missing loci from the control profile.

Table 3.2. Descriptive statistics for fragment lengths.

		Mean	Median	St. Dev.	25%	75%	Normality
Case 1	**Control**	216.67	226.32	72.61	149.94	278.23	0.078
	Experimental	199.89	172.72	70.31	128.91	272.68	0.200
Case 2	**Control**	215.87	217.93	72.47	146.98	279.70	0.200
	Experimental	181.75	173.02	57.47	132.10	233.45	0.124
Case 3	**Control**	214.65	218.93	72.97	145.34	282.47	0.200
	Experimental	209.41	218.97	72.17	133.44	276.91	0.200
Case 4	**Control**	204.70	198.73	70.27	134.58	274.17	0.079
	Experimental	202.89	180.85	71.35	132.89	274.52	0.052
Case 5	**Control**	205.57	204.76	66.16	146.09	251.75	0.192
	Experimental	n/a	n/a	n/a	n/a	n/a	n/a
Case 6	**Control**	203.08	198.71	71.19	130.58	264.99	0.154
	Experimental	199.70	171.83	76.92	123.74	279.23	**0.043**
Case 7	**Control**	203.60	168.53	87.91	133.06	275.99	**0.000**
	Experimental	214.84	221.21	69.28	148.98	277.22	0.200
Case 8	**Control**	204.85	184.03	72.85	136.38	275.26	0.148
	Experimental	204.85	184.03	72.85	136.38	275.25	0.148
Case 9	**Control**	201.70	184.05	76.70	123.10	276.72	0.077
	Experimental	211.16	213.98	73.00	138.28	277.51	0.200
Case 10	**Control**	206.09	206.70	66.63	145.59	270.70	0.200
	Experimental	214.12	172.84	104.23	123.66	325.23	0.200

Table 3.2 reports the descriptive statistics for fragment sizes for all consensus profiles in the control and the experimental groups. The mean, median, standard deviation and quartiles are provided to characterize the range and variation seen in the data. In many cases, these numbers look similar between the control and experimental consensus profile of each case. Normality was tested with the Kolmogorov-Smirnov test. All significant values are highlighted in red and indicate a departure from normality. Because two consensus profiles are non-normally distributed, all consensus profiles must be tested with non-parametric statistics for consistency.

Table 3.3. Descriptive statistics for RFU values.

		Mean	Median	St. Dev.	25%	75%	Normality
Case 1	**Control**	2316.34	1434.33	2271.18	485.13	4011.17	**0.007**
	Experimental	70.95	74.00	15.44	56.50	83.00	0.200
Case 2	**Control**	2337.90	1693.84	1620.41	1334.75	3408.75	**0.031**
	Experimental	76.76	62.00	50.17	53.00	81.50	**0.001**
Case 3	**Control**	3588.36	3248.00	2875.34	1001.67	6162.26	**0.009**
	Experimental	213.95	143.67	194.27	96.75	244.71	**0.001**
Case 4	**Control**	2456.26	1257.33	2596.25	573.00	3456.33	**0.000**
	Experimental	767.85	604.25	659.86	323.25	991.00	**0.017**
Case 5	**Control**	1311.14	1102.25	1311.95	344.50	1767.75	**0.005**
	Experimental	n/a	n/a	n/a	n/a	n/a	n/a
Case 6	**Control**	133.50	113.09	94.22	61.00	163.74	**0.035**
	Experimental	89.80	81.00	37.96	65.00	115.67	0.195
Case 7	**Control**	2449.04	1336.00	2643.36	436.13	3830.75	**0.000**
	Experimental	178.25	150.00	116.45	91.50	197.50	**0.000**
Case 8	**Control**	413.17	251.00	561.99	143.50	438.00	**0.000**
	Experimental	413.17	251.00	561.98	143.50	438.00	**0.000**
Case 9	**Control**	1765.09	1259.67	1513.72	677.09	2320.59	0.056
	Experimental	395.40	330.25	350.44	200.25	454.17	**0.000**
Case 10	**Control**	275.80	249.00	117.25	171.67	366.00	0.200
	Experimental	52.20	55.00	6.76	46.00	57.00	0.200

Table 3.3 reports the descriptive statistics for RFU values for all consensus profiles in the control and the experimental groups. The mean, median, standard deviation and quartiles are provided to characterize the range and variation seen in the data. In many cases, these numbers do not look similar (unlike the fragment sizes) between the control and experimental consensus profile of each case. Normality was tested with the Kolmogorov-Smirnov test. All significant values are highlighted in red and indicate a departure from normality. Because all but five consensus profiles are non-normally distributed, all consensus profiles must be tested with non-parametric statistics for consistency. Figure 3.1 and Figure 3.2 provide boxplots comparing the control and experimental groups by fragment size and RFU values respectively.

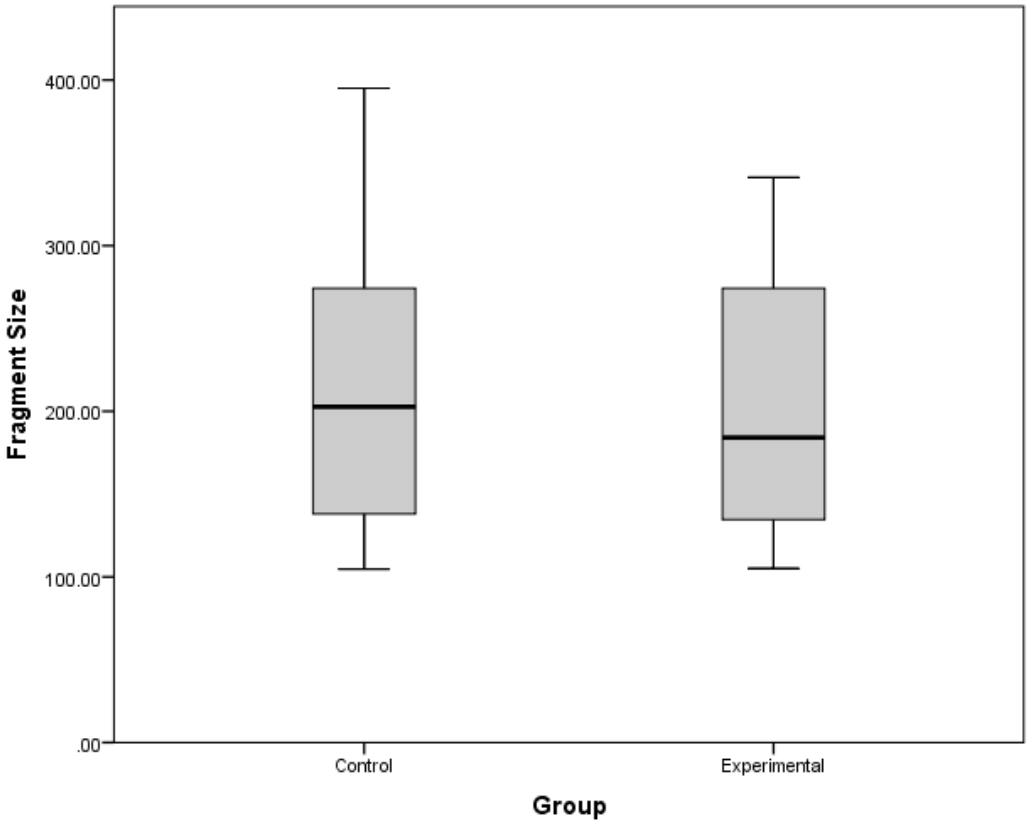

Figure 3.1. Boxplot of fragment sizes, separated by group. The quartiles of the control and experimental consensus profiles look roughly equivalent. The control consensus group looks more symmetrical than the experimental.

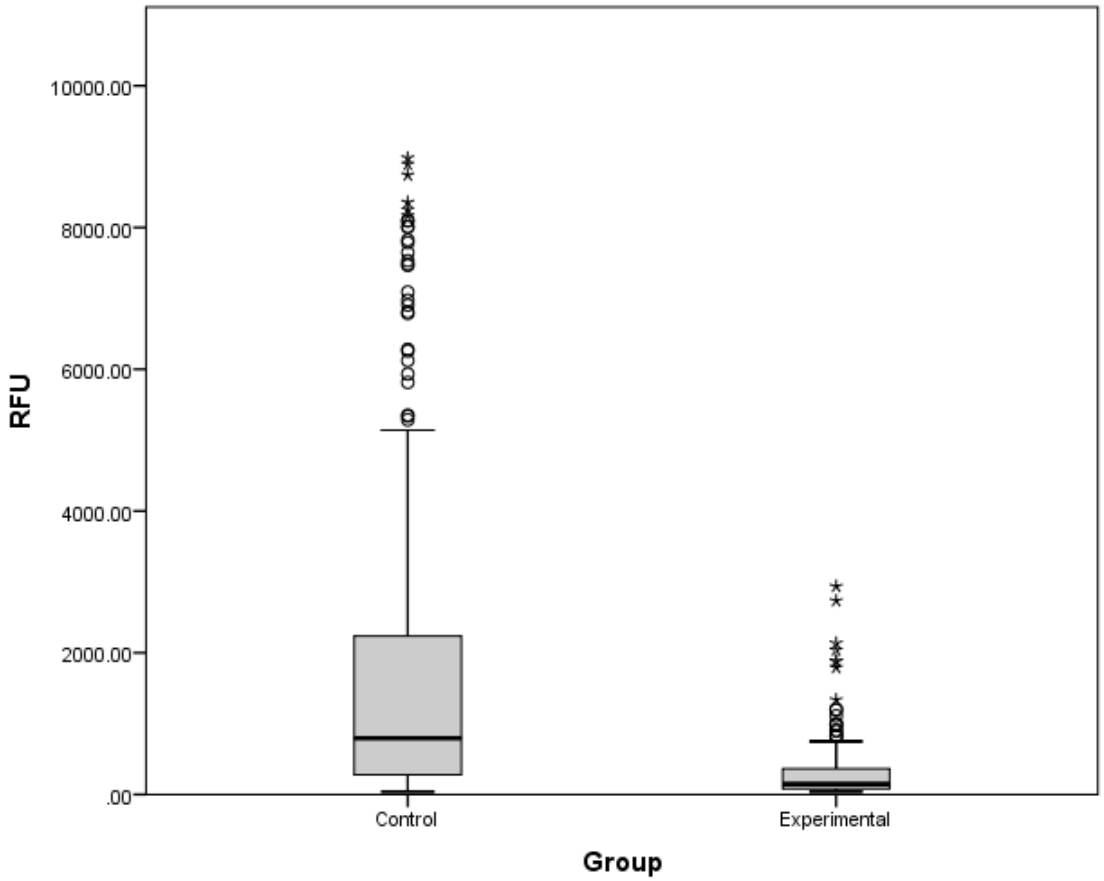

Figure 3.2. Boxplot of RFU values separated by group. This boxplot demonstrates the differences in range and quartiles between the control and the experimental consensus profiles. The control consensus profiles exhibit a larger range of variation, whereas the majority of the experimental consensus RFU values are close together (under 500).

Control and Experimental Profile Description

For ease of comparison, each locus in the Identifiler kit was assigned a unique number (Table 3.4). Loci in bold are part of the 13 CODIS STRs used in forensic identification. Only three loci used in this kit (D2S1338, D19S433, and amelogenin) are not included in the CODIS STR marker set.

Table 3.4. Identifiler Kit Loci: All loci found in the Identifiler kit with appropriate dye color and number identifier.

Dye	STR	Locus
Blue	**D8S1179**	1
	D21S11	2
	D7S820	3
	CSF1PO	4
Green	**D3S1358**	5
	TH01	6
	D13S317	7
	D16S539	8
	D2S1338	9
Yellow (appears as black)	D19S433	10
	vWA	11
	TPOX	12
	D18S51	13
Red	**D5S818**	14
	FGA	15
	Amelogenin	16

Missing Loci

Table 3.5. Frequency of missing loci: this table demonstrates which loci are missing from all the experimental samples and the frequency of each missing loci.

Locus	1	2	3	4	5	6	7	8	9	10	11	12	13	14	15	16
Case 1		yes		yes	yes		yes						yes	yes	yes	
Case 2		yes		yes			yes	yes	yes							
Case 3							yes									
Case 4																
Case 5	yes	yes	yes	yes	yes	yes	yes	yes	yes	yes	yes	yes	yes	yes	yes	yes
Case 6			yes				yes								yes	yes
Case 7																
Case 8																
Case 9																
Case 10		yes	yes	yes	yes		yes	yes		yes	yes	yes	yes	yes	yes	
Frequency	1	4	3	4	3	1	6	3	2	2	2	2	3	3	4	2

Table 3.5 shows that locus 7 is the most commonly missing locus in the experimental consensus profiles (missing from six experimental consensus profiles). Loci 2, 4, and 15 are the next more commonly missing loci (missing from four experimental consensus profiles). Locus 7 is also missing from three control consensus profiles. However, when this locus is missing from a control consensus profile it is found present in the corresponding experimental consensus profile. This indicates that locus 7 may have a problematic recovery in general due to the already degraded nature of these samples. A Chi-square goodness of fit test showed no significant associations between any locus and whether or not it was missing ($p < 0.05$).

Loci with blue or green dye were found to have stutter products. Stutter can sometimes be an indication of a mixed sample or contamination. However, when stutter is found in these

samples, it is not widespread. For example, there is stutter at locus 5 (D3S1358) in only the first PCR of control sample 7. This locus does not demonstrate stutter in the other two PCRs for this sample and no other locus in this sample shows stuttering. If this stutter represented a mixed sample or contamination, one would expect to see stutter at this locus in all the PCRs or more stuttering throughout the samples. Additionally, all the PCR blanks and negative controls in the fragment analysis step remained blank, indicating a lack of contamination.

Sample 5 was the most problematic sample overall in terms of fragment recovery. Two of the three control PCRs were successfully analyzed by the ABI 3100 Fragment Analysis machine. The electropherograms show stuttering throughout the sample. This stuttering may be due to the degradation of the sample prior to this study. Figure 3.3 shows the incidences of stuttering seen in sample 5. The three PCR trials of experimental sample 5 were not successfully analyzed by the ABI 3100 Fragment Analysis machine. No peaks, aside from the internal size standard, were detected and no electropherograms were produced. The presence of the internal size standard indicates that the fragment analysis detection worked properly, but no labeled fragments were found. X-ray radiation treatment further degraded this sample such that none of the DNA markers in the Identifiler kit were able to be amplified.

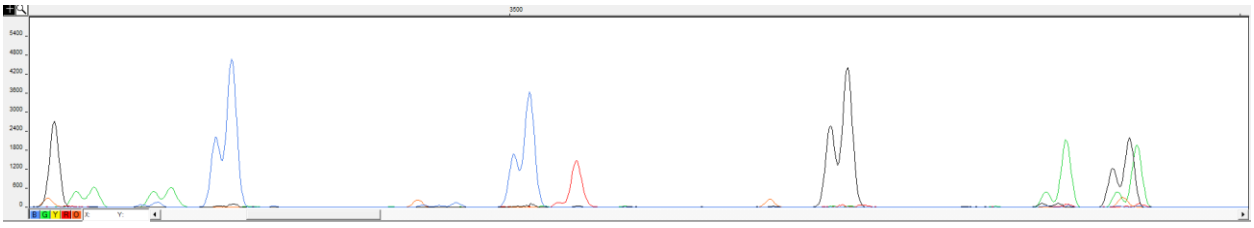

Figure 3.3. Electropherogram of control sample 5. The peaks on this electropherogram represent genetic variants between 105 and 180 base pairs. Nearly all peaks show stutter, shown as the smaller peaks directly to the left of the larger peaks in this electropheorgram. Allelic stutter is either due to contamination or degradation of the template DNA.

Table 3.6. Missing Loci and Allelic Drop-in and Drop-out.

Consensus Profile	Loci Missing from Experimental	Allelic Drop-in	Allelic Drop-out
1	2 ,4, 5, 7, 13, 14, 15	none	10
2	2, 4, 7, 8, 9	none	5, 12, 13, 14, 15
3	7	10	4, 6
4	none	none	7, 12
5	all	none	none
6	3, 7, 15, 16	none	2, 6, 10
7	none	none	1, 10
8	none	none	none
9	none	none	1
10	2, 3, 4, 5, 7, 8, 10, 11, 12, 13, 14, 15	none	1, 6

Table 3.6 shows which loci (as defined in Table 3.4) are present in the control consensus profile but absent in the experimental consensus profile for each case. “Allelic Drop in” characterizes the false heterozygosity seen in the experimental consensus samples. A false heterozygote, or allelic drop in, is seen when the loci is characterized as homozygous in the control consensus profile but heterozygous in the experimental consensus profile. “Allelic Dropout” characterizes the false homozygosity seen in the experimental consensus samples. A false homozygote, or allelic dropout, is seen when the loci is characterized as heterozygous in the control consensus profile but homozygous in the experimental consensus profile.

Locus 7 (D13S317) is missing from the control consensus profiles for cases 7, 8 and 9 but present in the corresponding experimental consensus profiles.

Hypothesis Testing Results

Hypothesis I: X-ray radiation reduces the total number of recovered DNA marker alleles.

The number of DNA marker alleles recovered in all three PCR runs of each control sample, was compared to the number of genetic variants recovered in all three PCR runs of each experimental sample, using a Wilcoxon signed-rank test. Data from all three PCR trials were used to increase sample size and statistical power. All genetic variants included were within acceptable size ranges (i.e., none were "off ladder" alleles) to prevent inclusion of spurious peaks.

This test compares the difference in medians between two paired samples, or repeated measures, when the samples cannot be assumed to come from a normal distribution. A repeated measures test was used because the data are coming from multiple PCRs of the same sample. This test found a significant difference ($p < 0.05$) between the median number of control genetic variants across all three PCRs and the number of experimental genetic variants across all three PCRs. The median number of genetic variants across three PCR trials from the control group is 27 and the median number of genetic variants from the experimental group is 10. These results indicate that the control sample PCRs produced more genetic variants than the experimental sample PCRs. Therefore, the results of this test support the hypothesis that X-ray radiation reduces the total number of recovered DNA marker alleles.

Hypothesis II: X-ray radiation causes DNA marker allele fragment lengths to shorten, producing allelic stutter.

The amount of stutter was counted for each PCR trial for each sample. All control samples were pooled and all experimental samples were pooled. Statistical analysis comparing the overall amount of stutter found in all three control samples versus the corresponding three experimental samples was performed with the Mann-Whitney *U* test. This test assesses whether or not the medians from two groups are statistically different from one another. The Mann-Whitney *U* test was used instead of the *t*-test because the *t*-test's assumption of normality was not met. The Kolmogorov-Smirnov statistic was significant for both the control and the experimental groups $p < 0.05$). A significant Kolmogorov-Smirnov statistic indicates that the data are not normally distributed. The Mann-Whitney *U* test found significant differences ($p < 0.05$) in the occurrences of stutter between the control and experimental samples. However, as can be seen in Table 3.7, the experimental samples all show significantly reduced occurrences of stutter as compared to the control samples. Most experimental samples have no stutter. This information supports the rejection of the above hypothesis; X-ray radiation reduces the amount of allelic stutter seen.

Table 3.7. Amount of Stutter: Table showing the counts of stutter seen in each sample. Samples are labeled as follows: the first number identifies the PCR trial (1, 2 or 3) and the second number identifies the sample number. For example, Sample 3-7 represents the third PCR trial for the seventh sample.

Sample	# Stutter - Control	# Stutter - Experimental
1-1	15	0
2-1	10	1
3-1	11	0
1-2	17	1
2-2	8	0
3-2	17	0
1-3	12	0
2-3	13	0
3-3	13	1
1-4	8	10
2-4	11	2
3-4	12	0
1-5	0	0
2-5	7	0
3-5	8	0
1-6	0	0
2-6	0	0
3-6	0	0
1-7	11	1
2-7	7	0
3-7	0	0
1-8	0	0
2-8	2	0
3-8	3	0
1-9	18	3
2-9	13	0
3-9	1	1
1-10	1	0
2-10	1	0
3-10	1	0
Total	220	20

Hypothesis III: X-ray radiation decreases the total amount of recovered DNA per marker.

Consensus profiles were used in the testing of this hypothesis. Statistical analysis comparing the RFU values found in the control profile versus the corresponding experimental profile found significant differences throughout. This analysis was performed with the Mann-Whitney *U* test, which assesses whether or not the medians from two groups are statistically different from one another. The Mann-Whitney *U* test was used instead of the *t*-test because the *t*-test's assumption of normality was not met. The Kolmogorov-Smirnov statistic was calculated for each sample and found to be significant in most cases (see Table 3.2 and Table 3.3 for exact significance values). A significant Kolmogorov-Smirnov statistic indicates that the data are not normally distributed. Table 3.8 shows the results of the Mann-Whitney *U* tests comparing the RFU values. N is the number of fragments compared in each test. All tests show significant differences in RFU values between the control and the experimental group. The results of this test support Hypothesis III and suggest that X-ray radiation does decrease the total amount of recovered DNA per marker.

Table 3.8. RFU Comparisons: Results of Mann-Whitney *U* tests comparing RFU values between the control and the experimental consensus profiles. Significant results are highlighted in red.

		N	Median	St. Dev	Significance
1	Control	13	3582.3338	1883.51439	**0.000**
	Experimental	13	70.9485	15.44046	
2	Control	15	2800.9667	1893.53161	**0.000**
	Experimental	15	67.9333	19.35188	
3	Control	27	3580.0004	2754.79599	**0.000**
	Experimental	27	229.2407	199.10171	
4	Control	32	2648.7291	2632.24373	**0.000**
	Experimental	32	790.3594	668.74406	
5	Control	38	1311.1447	1311.95261	
	Experimental	0	0	0	**0.000**
6	Control	20	164.3830	105.71983	**0.011**
	Experimental	20	88.0250	39.29057	
7	Control	25	2686.5068	2780.13559	**0.000**
	Experimental	25	192.6264	123.88538	
8	Control	26	443.5896	586.51075	**0.030**
	Experimental	26	209.3146	107.22381	
9	Control	26	1901.8662	1538.32047	**0.000**
	Experimental	26	409.8331	356.96698	
10	Control	4	413.6675	61.61440	**0.029**
	Experimental	4	51.2500	7.41058	

Post-Hoc Test: Dye Bias Testing

Due to observations of the fragment analysis data, it was deemed necessary to investigate any potential dye biases that might affect detection of certain markers. Commercial kits are optimized to promote equal fragment detection across all dyes. However, a cursory glance of the data showed that in many cases the missing markers were commonly from the blue or green dye type. Therefore it was judged worth investigating whether the use of certain dye(s) improved or reduced the chances of fragment detection in this set of samples. If dye biases are present, they

may influence any statistically significant differences found in RFU values between the corresponding control and experimental consensus profiles.

A Kruskal-Wallis test, a non-parametric analysis of variance text, was performed to examine differences in RFU values based on dye color for each sample. The Kruskal-Wallis test assesses whether or not the medians from two or more groups are statistically significant from each other. If significant differences are found, *post hoc* tests may be performed to discover where those differences exist. The parametric ANOVA test has three assumptions: the data must be independent, normally distributed, and have homogeneity of variances. Homogeneity of variances can be tested using Levene's test. If the results of Levene's test are significant then one cannot assume that population variances are equal and therefore the data cannot be considered to have homogeneity of variances. The Kolmogorov-Smirnov test statistic has been used to test the normality of the data (please refer to Table 3.2 and Table 3.3 for normality data). If this statistic is significant, the data are non-normally distributed and a non-parametric test must be used. Due to several samples exhibiting non-normality, a Kruskal-Wallis test was used in all cases.

These Kruskal-Wallis tests were done to ascertain any existing biases in RFU values based on the dye color use for a fragment. Only sample 7 produced significant differences amongst dye colors and therefore *post hoc* tests were performed for only this sample. Table 3.9 shows the results of the Kruskal-Wallis tests for the control samples.

Table 3.9. Control Dye Bias results: RFU values by dye color results for control samples. Significant values highlighted in red.

Case	Kruskal-Wallis	Significance
1	2.891	0.409
2	8.748	0.033
3	5.984	0.112
4	1.721	0.632
5	4.884	0.180
6	5.278	0.153
7	12.408	0.006
8	1.266	0.737
9	4.066	0.254
10	2.048	0.562

Table 3.9 shows the results of the Kruskal-Wallis tests for the control profiles. For the control consensus profiles, no significant differences were found in RFU values based on dye color, except in case 7. Case 7 showed some stutter peaks, which may be reflected in this test result, because there are extra green labeled genetic variants represented in the sample. Pairwise comparisons were performed with Mann-Whitney *U* tests to explore this further. Significant results were obtained when comparing RFU values with blue dye to green dye ($p < 0.05$) and blue dye to yellow dye ($p < 0.05$). There are several stutter genetic variants with green dye in this case. The significant difference in RFU values between the blue and the yellow labeled genetic variant may be partially a function of sample size (blue n=14, yellow n=6). The dye bias seen in control case 7 is found in a significant difference between the blue and green dye and the blue and yellow dye. This may indicate that the significant differences in RFU values found between the control and experimental profiles for case 7 are at least partially a result of this dye bias. A bias towards blue dye labeled markers might result in increased RFU values in the control profile as compared to the experimental profile.

Table 3.10 shows the results of the Kruskal-Wallis tests for the experimental profiles. No significant differences were found in RFU values based on dye color among the experimental samples. Therefore there is no observed dye bias in the experimental samples.

Table 3.10. Experimental Dye Bias results: RFU values by dye color results for experimental samples.

Case	Kruskal-Wallis	Significance
1	1.555	0.460
2	0.880	0.830
3	0.246	0.970
4	1.501	0.682
5	n/a	n/a
6	3.266	0.352
7	1.573	0.666
8	3.646	0.302
9	1.456	0.693
10	2.133	0.344

Chapter 4: Discussion

This chapter discusses the study results in light of the overall questions being addressed in this thesis; that is, in terms of how DNA may be affected by the X-ray exposure in terms of the CODIS markers and forensic genetic identification. All three hypotheses and the *post-hoc* dye bias test are discussed. This chapter also discusses the issues of missing loci, allelic dropout, and the RFU cutoff, as missing loci and allelic dropout were seen throughout the experimental samples.

Hypothesis I: X-ray radiation reduces the total number of recovered DNA marker alleles: SUPPORTED

It was expected that X-ray radiation would decrease the total number of identifiable DNA markers. The Wilcoxon signed-rank test found significant differences between the numbers of genetic variants recovered in the control versus the experimental groups.

Overall, more genetic variants were identified in the control versus the experimental groups. It seems that X-ray radiation damaged or degraded the experimental DNA enough to render it less amplifiable, though it is still uncertain what kind of damage occurred (SSB, DSB, or individual base damage).

Hypothesis II: X-ray radiation causes DNA marker allele fragment lengths to shorten, producing allelic stutter: REJECTED.

Mann-Whitney *U* test found significant differences in the median amount of stutter across all PCR trials. However, the control samples contained significantly more stuttering than the experimental samples. Therefore X-ray radiation did not cause an increased amount of stutter;

rather it was decreased. The incidence of stutter is known to increase with degraded DNA and LT-DNA (Gill et al. 2000). Therefore it is surprising to not see an increase in the stuttering in the experimental samples. In the experimental samples, genetic variants seem to drop out altogether rather than show up shortened or as stutter. In this case, X-ray damage is not responsible for stutter effects. X-ray radiation is not causing the kind of damage that would lead to PCR slippage and therefore result in stutter. Rather, X-ray radiation damages DNA enough to prevent amplification. This is also evident in the RFU value results discussed below.

Hypothesis III: X-ray radiation decreases the total amount of recovered DNA per marker: SUPPORTED.

Significant differences were found in RFU values between the control and the experimental consensus profiles. Control consensus profiles had larger average RFU values than experimental consensus profiles. A larger RFU value for a certain peak indicates that there were more fragments at that location. Therefore, the experimental consensus profiles, on average, had fewer fragments that were recovered at each peak. This indicates that the X-ray radiation caused significant damage to the DNA markers, which caused less DNA to be recovered overall. In other words, where X-ray radiation caused DNA damage it manifested in a lack of amplification rather than a shortening of fragments (stuttering).

Post-Hoc *Analysis Results: Dye Biases*

Does dye bias affect recovery of certain fragments? In all but one case, there were no significant differences in RFU values between each of the four dyes. Only control consensus profile 7 had significant differences in RFU values between the dye colors. Further analysis revealed that the significant differences in RFU values were between the blue and green dyes and

the blue and yellow dyes. These differences may have been a result of the stuttering seen in that sample or a result of unequal (and low) sample sizes. Commercial kits are calibrated in such a way as to prevent dye biases so this may just be an anomaly. Further research may be able to shed some more light on this question.

Allelic Dropout or False Homozygosity

Missing loci in a forensic DNA profile are not as problematic as false homozygotes (allelic dropout) or false heterozygotes. A 100% match at all CODIS marker loci is not always necessary for a positive identification. Partial profiles (at least 10 of the 13 CODIS loci) can still be uploaded to the state of federal DNA database (Butler 2005). However, false homozygous or heterozygous loci lead to mismatches. While missing loci can decrease the power of the forensic identification based on DNA, the allelic dropout seen in the experimental consensus profiles lead to incorrect labeling at the dropped out locus. A complete and accurate profile gives the greatest chance of success at correctly identifying an individual.

Among all the experimental consensus profiles, 16 false homozygotes and one false heterozygote were found. A total of 17 loci would have been misidentified when compared to the control consensus profile. Only experimental consensus case 8 contained no false homozygous or false heterozygous loci. This case would have produced a partial match, with no misidentified loci, when compared to the control consensus profile. The match would be partial because experimental consensus case 8 has one additional peak (locus 7) that does not appear in the control. This additional peak was most likely missing from the control due to DNA degradation.

RFU Cutoffs

Additionally, it is important to note that the RFU cutoff value used in this study (minimum RFU of 50) is lower than that can be used in actual forensic casework. Laboratories that generate forensic DNA profiles determine and validate their own RFU thresholds. This is because each laboratory has different equipment, reagents and testing environments that may affect the analysis of genetic testing. For example, Bode Technology Group, Inc., a company that performs forensic genetic testing law enforcement agencies, has set their RFU threshold at 75 for heterozygote genetic variants and 200 for homozygote genetic variants (Jen Sampson and Heather Cunningham, personal communication, February 11, 2013). Houston Police Department requires a minimum threshold of 200 RFUs for a single source (non-mixed) sample and 50 RFUs for a mixed sample ("Standard Operating Procedures: DNA").

Since the purpose of this study was to assess the nature and extent of damage caused by X-ray radiation, a relatively low RFU threshold was used to ensure comparable control and experimental data from these samples.

Other Considerations

As discussed in Chapter 1, DNA can be found in various forms, but most commonly exists in the B-form. However, dehydrated DNA is typically in the A-form. If the DNA molecules in this study were in another, more vulnerable form (like the A-form), they may have been more susceptible to X-ray radiation damage. Additionally, the level of hydrolysis of the DNA molecules may have affected the amount of damage sustained in each sample (or each molecule of each sample). Hydration surrounding the DNA molecule serves to protect the

molecule. However, the increased amount of oxygen creates more chances for oxygen radical formation and therefore more chances at clusters of ionizing damage from the X-ray radiation. Finally, the DNA in this study can be considered Low Template because of the degradation prior to X-ray radiation. Some of these results may be an artifact of this pre-existing degradation. However, the results still indicate differences between the control and experimental samples therefore not all the degradation occurred prior to X-ray radiation.

Recommendations for Forensic Practitioners

Given the results from this study, it is recommended that X-rays should be taken after skeletal material (including dental material) has been processed for DNA analysis. At the very least, a portion of the remains should be kept aside, and not X-rayed, for later DNA extraction and identification. Once the skeleton has been X-rayed, DNA is still recoverable but it is damaged and may not produce an accurate profile. Another type of marker or a combination of different marker types may be better suited for identification if the sample has already been X-rayed. This study has shown that the X-ray process causes sufficient allelic dropout, or false homozygosity, which would lead to a misidentification at those loci.

Recommended Follow-Up Research

Follow-up research could examine the effects of multiple X-ray exposures, given that x-ray irradiated human remains are often exposed to multiple X-ray dosage events. The remains are therefore potentially subject to even further DNA degradation due to X-rays radiation than

seen in this study. If one X-ray exposure produces the results mentioned above, multiple X-ray exposures should produce further degradation.

In this study, the presence or absence of the target DNA markers (mostly STRs) was used to demonstrate changes caused by X-ray radiation. Future research should look at sequence data to see precisely how the X-rays are causing these changes. It would be more informative to compare direct sequences to see how DNA bases are being modified, if at all, and where DNA strands are excised, if at all.

It would also be interesting to investigate whether damage from X-ray radiation increases as the level of degraded template DNA increases? Future research into this question should also quantify the amount of template DNA available both before and after X-ray radiation. In addition to quantifying DNA template, X-ray crystallography should be performed to investigate the relationship between the shape and form of the DNA molecule between control and experimental samples.

This study only examined changes in a limited set of DNA markers due to X-ray radiation. Future research should examine changes in other regions of the human genome, such as mitochondrial DNA, other STRs, and even other types of markers such as SNPs (single nucleotide polymorphisms).

In fact, some researchers are working on validating SNPs for forensic identification purposes. In 2007, the 22nd Congress of the International Society of Forensic Genetics (ISFG) held a panel discussion on the future of SNPs and their use in forensic identification. The panelists agreed that SNPs may not replace STRs anytime soon, but they should continue to be explored as SNPs can be used as adjuncts to STRs in problematic samples (Butler et. al. 2008).

If SNPs are to be used in future forensic identification efforts, it is important to examine potential degradation effects from various sources, including X-ray radiation.

Conclusions and Future Considerations

The dosage of X-ray radiation used on the human molars in this experiment was found to be damaging to the nuclear DNA. There was a significant difference in the number of genetic variants that were recovered between the control and the experimental groups. This indicates that the X-ray radiation damaged DNA enough to cause allelic dropout throughout the samples. However, there did not appear to be an increase in stutter effects, as examined visually as well as statistically, looking for average differences in fragment length. Additionally, statistically significant differences were found in the average RFU values between samples.

Taken together, the results demonstrate that damage from X-ray radiation renders the DNA markers used in this study unrecoverable due to drop-out from the sample. Without further testing, it is not clear whether this dropout is being caused by damage to individual bases (which could change the configuration of the primer binding site) or to DNA strands (from SSBs or DSBs). Regardless of the mechanism of damage, it is clear that X-rays have caused damage to STR-DNA and the amelogenin gene in these samples. Enough damage occurred that the forensic profiles before and after X-ray differed significantly.

If a sample has already been X-rayed, it may be better to use another type of DNA marker or a combination of DNA markers instead of the standard CODIS markers. One such alternative marker, the Single Nucleotide Polymorphism (SNP), will be discussed below.

Single Nucleotide Polymorphisms (SNPs)

A Single Nucleotide Polymorphism, or SNP, is a genetic variant in which only one nucleotide is different from the parent sequence and is polymorphic (highly variable) in the target population). For example, a cytosine (C) may be replaced with a thymine (T) (Figure. 5.1). SNPs tend to occur in non-coding regions because natural selection is not necessarily acting on these regions and fixating genetic variants, and many are found near STRs.

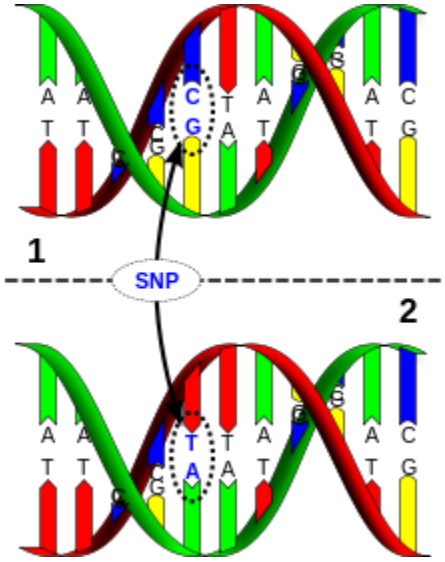

Figure 5.1: SNP example. Adapted from: http://en.wikipedia.org/wiki/File:Dna-SNP.svg

Over the last ten years, various laboratories have been attempting to build SNP sets to use in forensic DNA identification. Researchers argue that SNPs are ideal for human identification for several reasons. First, SNPs have lower mutation rates than STRs, making relatedness testing (paternity testing) easier because the sequences are more consistent for a greater number of generations. SNPs can be typed with much smaller DNA fragments, making them ideal for

degraded DNA or low-copy number (LCN) analysis, which is frequently encountered in anthropological (ancient DNA) and forensic applications. These kinds of markers can be typed with the high-throughput technology found in larger laboratories performing forensic DNA casework, which can type hundreds of DNA profiles in a shorter time span. Because there are only four possible genetic variants per SNP locus (versus STRs, that can have multiple variants each), they are easier to validate, produce frequency estimates for and interpret (Musgrave-Brown et al. 2007, Phillips et al.2008, and Kidd et al. 2012).

Researchers such as Sanchez et al. (2006) and Musgrave-Brown et al. (2007) have recommended the use of 40-60 SNPs for the same level of discriminatory power as the CODIS core loci. Most laboratories have been developing a suite of about 50 unlinked SNPs with high heterozygosity (two different genetic variants at one genetic marker) to reach a similar level of discrimination. Some SNPs are highly polymorphic in one population yet monomorphic in another population; therefore more population specific studies are being done to select SNPs that are polymorphic across most if not all populations (Sanchez et al. 2006, Musgrave-Brown et al. 2007).

SNPs, being one base pair long, are obviously shorter than STRs. The primers sets designed to locate these markers are also shorter, tending to be 59-115 base pairs in length. The longest SNP primer set is about the same length as the shortest CODIS marker (amelogenin at 106-112 base pairs in length). CODIS markers range from 106-350. The advantage in these small fragment sizes is that highly degraded DNA produces shorter fragments. So the shorter the fragment, the less likely you are to be able to amplify and analyze longer fragments (Sanchez et al. 2006).

SNPforID Consortium

The SNPforID (http://www.snpforid.org) Consortium in Europe has been performing much recent SNP research. Their goal is to test, validate and implement SNPs for use in forensic DNA identification. They see SNPs as the realistic alternative to STRs in situations where DNA evidence is in low quality and/or quantity. They believe SNPs should be used to augment or replace STRs when DNA is highly degraded. In cases such as X-rayed material, SNPs use might be more effective and reliable than STR kits due to their smaller size (Sanchez et al. 2006).

This SNPforID consortium has developed and validated a 52-plex assay for forensic identification. To validate this 52 SNP assay, 40 extracts were sent to a total of five different laboratories. Each sample was tested using the SNP assay and a commercial STR kit (Promega Powerplex ® 16). Three types of extracts were chosen to mimic forensic casework samples: LCN extracts (testing sensitivity), degraded extracts, and LCN + degraded extracts. In tests of sensitivity (the LCN extracts), the commercial STR kit out-performed the 52 SNP assay in terms of number of correctly assigned genetic variants and number of genetic variants dropping-in (extra, incorrect genetic variants being identified or contaminant genetic variants). These results conflicted with a previous study and may indicate lack of training and primer stock quality as well as interactions during the PCR step. In terms of degraded samples, both the commercial STR kit and the 52 SNP assay produced good results with large fragment sizes. As fragment size was smaller, the SNP assay performed better than the STR kit. Results were mixed for samples that were both in low copy number and degraded. But overall, the SNP assay performed better than the STR kit. However, genetic variant drop-in was still a larger problem with the SNP

assay. The researchers noted that the laboratories with the least successful typing results on the SNP assay were also the ones that showed the most amount of drop in. This finding suggests that better training, facilities, and reagents are necessary when using SNP assays over STR kits (Musgrave-Brown et al. 2007).

Recent Research in Forensic SNP Use

Research performed by Lou et al. (2011) compared the use of 44 SNPs to the AmpFℓSTR® Identifiler® PCR Amplification Kit. Fifteen (ten naturally degraded and five dry blood stains) degraded samples were typed with both the SNP kit they developed as well as the STR kit, and the results compared. All ten naturally degraded samples (EDTA-blood samples preserved in tubes placed in the natural environment during summer for 20 weeks) returned partial profiles with no peaks detected for genetic variants larger than 200 base pairs when using the STR kit. The shorter genetic variants were only observed below the genotyping threshold (50 RFUs). The remaining five samples (dry blood stains preserved on gauze for more than 20 years) showed no results using the STR kit. The SNP method successfully typed 36-44 loci in all 15 samples. The SNP markers used in this study were amplifiable in degraded samples (shorter fragments lengths) better than the commercial STR kit (Lou et al. 2011).

The usefulness of SNPs with degraded DNA indicates that further research and validation with SNP assays should be performed. In situations in which the DNA has been degraded by X-ray radiation, it might be useful to include a SNP assay to obtain a complete and reliable DNA profile. Further testing and validation on these assays needs to be performed in order for the results to be admissible in a forensic casework setting. Once SNP results are legally acceptable in

a court of law they can be used to augment or replace existing STR kits for better DNA identification.

List of References

Applied Biosystems. 2010. AmpFℓSTR® Identifiler® PCR Amplification Kit: Users Manual. Applied Biosystems.

Arisemendi, Jacquel L., Baker, Lori E., and Karla J. Matteson. 2004. Effects of processing techniques on the forensic DNA analysis of human skeletal remains. Journal of Forensic Science. 49(5):1-5.

Bar, Walter, Kratzer, Adelgunde, Machler, Marco and Werner Schmid. 1988. Postmortem Stability of DNA. Forensic Science International. 39, 59-70.

Basu, A.K., Loechler, E.L., Leadon, S.A., and J.M. Essigmann. 1989. Genetic effects of thymine glycol: Site-specific mutagenesis and molecular modeling studies. Proceedings of the National Academy of Sciences of the United States of America. 85(20): 7677-7681.

Boom, R., Sol, C.J.A., Salimans M.M.M., Lansen, C.L., Wertheim-Van Dillen, P.M.E., and J. Van Der Noordaa. 1990 Rapid and simple method for purification of nucleic acids. J Clin Microbiol. 1990 March; 28(3): 495-503

Boon, Philip J., Cullis Paul M., Symons Martyn C.R. and Brendan W. Wren. 1984. Effects of ionizing radiation on deoxyribonucleic acid and related systems part 1. The role of oxygen. Journal of the Chemical Society, Perkin Transactions II 3, 1393-1787.

Brogdon, Bruce G. 1989. Forensic Radiology. Boca Raton: CRC Press.

Budowle, Bruce, Collins, Patrick J., Dimsoski, Pero, Ganong, Constance K., Hennessy, Lori K., Leibelt, Craig S., Rao-Coticone, Sulekha, Shadravan, Farideh, and Dennis J. Reeder. 2001. Population Data on the STR Loci D2s1338 and D19S433. FBI: Forensic Science Communications. http://www.fbi.gov/about-us/lab/forensic-science-communications/fsc/july2001/budowle2.htm/ [Accessed 5 February 2013].

Budowle, Bruce, Eisenberg, Arthur J., and Angela van Daal. 2009 Validation of Low Copy Number Typing and Applications to Forensic Science. Croatian Medical Journal. 207-217.

Buikstra, Jane. E and Ubelaker, Douglas H. Standards: For Data Collection from Human Skeletal Remains, 1994, Eds: Jane E Buikstra and Douglas H. Ubelaker. Proceedings of a Seminar at The Field Museum of Natural History.

Butler, John M. 2005. Forensic DNA Typing: Biology, Technology and Genetics of STR Markers. Elsevier Academic Press.

Butler, J.M., Budowle, B., Gill, P., Kidd, K.K., Phillips, C., Schneider, P.M., Vallone, P.M., and N. Morling. 2008. Report on ISFG SNP Panel Discussion. Forensic Science International: Genetics Supplement Series. 1:471-472.

Byers, Steven. 2001. Introduction to Forensic Anthropology: A Textbook. Boston: Allyn and Bacon.

Cadet, Jean, Douki, Thierry, Gasparutto, Didier and Jean-Luc Ravanat. 2003. Oxidative damage to DNA: formation, measurement and biochemical features. Mutation Research. 531, 5-23.

Ciaffi, R., Gibelli, D., and C. Cattaneo. 2011. Forensic radiology and personal identification and unidentified bodies: a review. La Radiological Medical. 116:960-968.

Christensen, Angi M. 2005. Testing the reliability of frontal sinuses in positive identification. Journal of Forensic Sciences. 50:1-5.

Dertinger, Hermann. 1969. Molecular Radiation Biology. Berlin: Springer-Verlag.

Franklin County, New York. http://www.franklincony.org/content/Departments/View/15:field=documents;/content/Documents/File/430.pdf Accessed 5 May 2013.

Fuciarelli, A.F. and Zimbrick J.D. 1995. Radiation Damage in DNA: Structure/Function Relationships at Early Times. Columbus: Battelle Press.

Gill, Peter, Whitaker, Jonathan, Flaxman, Christine, Brown, Nick and John Buckleton. 2000. An investigation of the rigor of interpretation rules for STRs derived from less than 100 pg of DNA. Forensic Science International. 112(1):17-40.

Gill, P., Puch-Solis R., and J. Curran. 2009. The low-template DNA (stochastic) threshold – its determination relative to risk analysis for national DNA databases. Forensic Science International Genetics. 3:104-111.

Gotherstrom, Anders, Fischer, Cornelia, Linden, Karin and Kerstin Liden. 1995. X-raying ancient bone: A destructive method in connection with DNA analysis. Laborativ Arkeologi. 8:26-28.

Granier, Robert and Gambini Denis-Jean. 1990. Applied Radiation Biology and Protection. New York: Ellis Horward.

Grieshaber, Britta M., Osborne, Daniel L., Doubleday, Alison F., Kaestle, Frederika A. 2008. A pilot study into the effects of X-ray and computed tomography exposure on the amplification of DNA from bone. Journal of Archaeological Science 35, 681-687.

Grosovsky, Andrew J., De Boer, Johan G., De Jong Pieter J., Drobetsky, Elliot A., and Barry Glickman. 1987. Base substitutions, frameshifts, and small deletions constitute ionizing radiation-induced point mutations in mammalian cells. Proceedings of the National Academy of Sciences 85, 185-188.

Hada, Megumi and Betsy M. Sutherland. 2006. Spectrum of complex DNA damages depends on the incident radiation. Radiation Research 165, 223-230.

Hartl, Daniel and Elizabeth Jones. 2006. Essential Genetics: A Genomic Perspective. Sudbury, MA: Jones and Bartlett Publishers.

Houston Police Department. 2013. Standard Operating Procedures: DNA. http://www.houstontx.gov/police/crimelab/pdfs/DNA/14_01_Statistics_092412.pdf [Accessed 14 March 2013].

Hoss, M., and Pääbo, S. 1993. DNA extraction from Pleistocene bones by a silica-based purification method. Nucleic Acids Research, 21(16):3913-3914.

Hutchinson, Franklin. The molecular basis for radiation effects on cells. Cancer Research. 1966. 26, 2045-2052.

Innis, Michael A. and David H. Gelfand. 1990. Optimization of PCRs. In: PCR Protocols: A guide to methods and applications. Edited by: Michael A Innis, David H. Gelfand and John J. Sninsky. San Diego: Academic Press, Inc.

Kidd, Kenneth K., Kidd, Judith R., Speed, William C., Fang, Rixun, Furtado, Manohar R., Hyland, F.C.L., and Andrew J. Pakstis. 2012. Expanding data and resources for forensic use of SNPs in individual identification. Forensic Science International: Genetics. 6:646-652.

Lindahl, Tomas and Barbro Nyberg. 1972. Rate of depurination of native deoxyribonucleic acid. Biochemistry. 11(19): 3610-3618.

Lindahl, Tomas. 1993. Instability and decay of the primary structure of DNA. Nature. 362:709-715.

Lou, C., Cong, B., Li, S., Fu, L., Zhang, X., Feng, T., Su, S., Ma, C., Yu, F., Ye, J. and Li Pei. A 2011. SNaPshot assay for genotyping 44 individual identification single nucleotide polymorphisms. Electrophoresis. 32:368-378.

Mann, R.W. 1998. Use of bone trabeculae to establish positive identification. Forensic Science International. 98:91-99.

Musgrave-Brown, E., Ballard, D., Balogh, K., Bender, K., Berger, B., Bogus M., Borsting, C., Brion, M., Fondevila, M., Harrison, C., Oguzturun., Parson, W., Phillips, C., Proff, C., Ramos-Luis, E., Sanchez, J.J., Sanchez Diz, P., Sobrino Rey, B., Stradmann-Bellinghausen, B., Thacker, C., Carracedo, A., Morling, N., Scheithauer, R., Schneider, P.M., and Denise Syndercome Court. 2007. Forensic Science International: Genetics. 1:186-190.

Neddermann, Petra, Gallinari, Paola, Lettieri, Teresa, Schmid, Daniel, Truong, Oanh, Hsuan, J. Justin, Wiebauer, Karin and Josef Jiricny. 1996. Cloning and Expression of Human G/T Mismatch-specific Thymine-DNA Glycosylase. The Journal of Biological Chemistry. 271:12767-12774.

Nikjoo, H., O'Neill, P., Goodhead, D.T., and M. Terrissol. 1997. Computational modellling of low-eneergy electron-induced DNA damage by early physical and chemical events. International Journal of Radiation Biology. 71 (5), 467-483.

Nikjoo, H., O'Neill, P., Wilson, W.E., and D.T. Goodhead. 2001. Computational approach for determining the spectrum of DNA damage induced by ionizing radiation. Radiation Research 156, 577-583.

Nikjoo, H., Bolton, C.E., Watanabe, R., Terrissol, M., O'Neill, P. and D.T. Goodhead. 2002. Modelling of DNA damage induced by energetic electrons (100 eV to 100 keV). Radiation Protection Dosimetry. 99, 77-80.

Ostling O and K.J. Johanson. 1984. Microelectrophoretic study of radiation-induced DNA damaged in individual mammalian cells. Biochemical and Biophysical Research Communications 123(1), 291-298.

Paredes, Ursula, Prys-Jones, Robert, Adams, Mark, Groombridge, Jim, Kundu, Samit, Agapow, Paul-Michael and Richard Abel. 2012. Micro-CT X-rays do not fragment DNA in preserved bird skins. Journal of Zoological Systemics and Evolutionary Research. 50(3):247-250.

Phillips, C., Fondevila, M., Garcia-Margarinos, M., Rodriguez, A., Salas, A., Carracedo, A., and M.V. Lareu. 2008. Resolving relationship tests that show ambiguous STR results using autosomal SNPs as supplementary markers. Forensic Science International: Genetics. 2:198-204.

Pizzarello, Donald J. 1982. Radiation Biology. Boca Ration: CRC Press.

Putkonen, Mikko T., Palo, Jukka U., Cano, Jose M., Hedman, Minttu, and Antti Sajantila. 2010. Investigative Genetics. 1-9.

Rudin, Norah and Keith Inman. 2001. An Introduction to Forensic DNA Analysis. Boca Raton: CRC Press.

Sampson, Jen and Heather Cunningham. Personal communication. February 11, 2013.

Sanchez, J.J., Phillips, C., Borsting, C., Balogh, K., Bender, K., Berger, B., Bogus, M., Fondevila, M., Harrison, C.D., Musgrave-Brown, E., Salas, A., Syndercombe-Court, D., Schneider, P.M., Carracedo, A., and Niels Morling. 2006. A multiplex assay with 52 single nucleotide polymorphisms for human identification. Electrophoresis. 27:1713-1724.

Schwartz, Ted R., Schwartz, Elayne E., Mierszerski, Laura, McNally, Lorah and Lawrence Kobilinsky. 1991. Characterization of deozyribonucleic acid (DNA) obtained from teeth subjected to various environmental conditions. Journal of Forensic Sciences. 36(4):979-990.

Semenenko, V.A. and Stewart, R.D.. 2004. A fast Monte Carlo algorithm to simulate the spectrum of DNA damages formed by ionizing radiation. Radiation Research. 161(4), 451-457.

Siddiqi M and Bothe E. 1987 Single- and double-strand break formation in DNA irradiated in aqueous solution: dependence on dose and OH- radical scavenger concentration. Radiation Research 112, 449-463.

Sinden, Richard. 1994. DNA Structure and Function. San Diego: Academic Press.

Shafirovich, Vladimir and Nicholas E. Geacintov. 2010. Role of free radical reactions in the formation of DNA damage. In: The Chemical Biology of DNA Damage. Eds: Nicholas E. Geacintov and Susan Broyde. Germany:Wiley-Vch.

Sutherland, Grant R. and Robert I. Richards. 1995. Simple tandem DNA repeats and human genetic disease. Proceedings of the National Academy of Sciences. 92, 3636-3641.

Sutherland, Betsy M., Bennett, Paula V., Sutherland, John C. and Jacques Laval. 2002. Clustered DNA damages induced by X-rays in human cells. Radiation Research 157, 611-616.

Swarts, Steven G., Sevilla, Michael D., Becker, David, Tokar, Christopher J. and Kenneth T. Wheeler. 1992. Radiation-induced DNA damage as a function of hydration. Radiation Research 129, 333-344.

Ward, John F. 1981. Symposium on radical processes in radiobiology and carcinogenesis: some biochemical consequences of the spatial distribution of ionizing radiation-produced free radicals. Radiation Research 98, 185-195.

Ward, J.F., Jones, G.D.D. and J.R. Milligan. 1994. Biological consequences of non-homogeneous energy deposition by ionising radiation. Radiation Protection Dosimetry. 52, 271-276.

Ward, J.F. 2005. Radiation Mutagenesis: The initial DNA lesions responsible. Radiation Research. 142(3): 362-368.

Wolff, Sheldon. 1967. Radiation genetics. Annual Review of Genetics. 1, 221-244

Appendices

Appendix One: Consensus Sample Data

Control Sample 1:

Consensus	Dye	Size	RFUs
1C	R	105.0933	2508
1C	Y	120.98	1482.333
1C	G	122.4267	3309.667
1C	Y	125.265	1592.667
1C	B	128.4667	4245
1C	B	146.3	5934
1C	R	148.9033	389
1C	R	153.0367	361.3333
1C	G	168.7467	6809.333
1C	Y	168.24	230
1C	G	172.49	4773
1C	B	216.7433	1295
1C	G	172.68	8251
1C	R	225.22	743
1C	G	227.42	513.5
1C	Y	228.7767	5352.667
1C	G	231.4133	340.6667
1C	R	233.3933	677.3333
1C	Y	244.8867	5104.667
1C	B	270.2033	1386.333
1C	G	275.2367	2564.667
1C	G	279.22	2182.667
1C	Y	293.3	538
1C	Y	305.15	475.6667
1C	G	312.65	1833.333
1C	B	322.7033	356.6667
1C	B	326.7933	359
1C	G	341.14	1249

Control Sample 2:

Consensus	Dye	Size	RFUs
2C	R	105.08	1602.333
2C	Y	117.12	1768
2C	Y	122.34	2377.333
2C	G	126.4233	3370
2C	G	134.5967	3151
2C	B	142.1567	5813.333
2C	B	146.31	5287.667
2C	R	148.97	405.3333
2C	R	153.0467	305
2C	G	172.8033	4964.667
2C	G	176.8833	4698.333
2C	Y	180.595	4463.5
2C	B	202.77	1379.333
2C	B	210.7167	1333
2C	R	225.1433	638
2C	R	229.11	770.3333
2C	Y	240.8033	3467.333
2C	Y	244.9267	3421.667
2C	G	267.2567	3159.667
2C	B	270.2033	1474.667
2C	G	275.2033	2936.333
2C	Y	281.2	324
2C	B	282.2467	1340
2C	Y	289.27	312
2C	G	308.8233	2089.667
2C	B	322.6667	1619.667
2C	B	326.69	1452
2C	G	341.11	1537

Control Sample 3:

Consensus	Dye	Size	RFUs
3C	R	105.0767	2607.667
3C	R	111.0033	3938.333
3C	Y	116.3033	8892
3C	B	121.7767	8091.667
3C	G	122.4567	4682.333
3C	B	129.8267	7825.333
3C	G	134.5933	4526.333
3C	R	148.9233	719.3333
3C	R	153.0167	692.6667
3C	Y	164.23	6122.667
3C	Y	180.55	3396.333
3C	G	183.8333	8981.333
3C	G	184.37	8740
3C	B	206.73	1611.667
3C	B	212.68	1518.333
3C	R	225.18	1021
3C	G	227.26	1082
3C	R	237.3033	856.6667
3C	Y	240.7567	6787
3C	Y	244.9267	6281
3C	B	270.2	1519
3C	G	275.1767	3640.333
3C	B	282.2367	1256
3C	G	283.1667	3099.667
3C	Y	289.28	321.6667
3C	Y	301.3067	303.6667
3C	G	312.7567	3749
3C	B	322.6233	943.6667
3C	G	325.1033	3516.667
3C	B	326.6867	927.3333

Control Sample 4:

Consensus	Dye	Size	RFUs
4C	R	105.04	1923.333
4C	R	110.96	2219
4C	G	122.4633	3851
4C	Y	124.2767	3392.333
4C	Y	126.3067	3475.667
4C	G	126.5867	3456.333
4C	B	129.8633	505.6667
4C	B	133.9067	8164.333
4C	G	134.5767	112.6667
4C	B	146.3	573
4C	B	150.47	7531.667
4C	G	151.2033	84.33333
4C	R	153.05	922.6667
4C	Y	168.33	222.6667
4C	G	172.7767	8099
4C	Y	176.4267	252
4C	G	180.91	7786.333
4C	B	198.7333	1368
4C	B	208.6867	1257.333
4C	Y	219.1233	289.3333
4C	R	221.17	790.6667
4C	G	231.38	785.3333
4C	G	234.67	1012.667
4C	Y	235.3167	6258.333
4C	R	237.45	919
4C	G	271.2233	522.6667
4C	B	274.1733	1502
4C	G	275.2733	7465
4C	B	278.2533	1364.667
4C	Y	289.2633	602.6667
4C	Y	297.2867	567.3333
4C	G	312.7733	3275
4C	B	318.53	1104.667
4C	B	322.6667	1079.333
4C	G	325.0633	3233

Control Sample 5:

Consensus	Dye	Size	RFUs
5C	R	105.09	7088.5
5C	Y	112.465	2495.5
5C	Y	120.305	2274.5
5C	G	121.975	562
5C	G	122.53	500
5C	G	126.55	545.5
5C	B	128.99	1205
5C	B	129.785	3536
5C	B	145.41	873
5C	B	146.305	1761.5
5C	R	148.93	1153
5C	Y	163.41	1596
5C	Y	164.37	3400.5
5C	G	175.77	351
5C	G	176.815	1754.5
5C	G	179.82	325
5C	Y	180.42	2211
5C	G	180.89	1606.5
5C	B	202.75	104
5C	B	206.755	2069
5C	G	227.28	1913
5C	Y	227.84	590
5C	Y	228.775	1786.5
5C	G	231.395	1581
5C	Y	235.88	498
5C	B	236.59	233
5C	Y	236.815	1607
5C	R	241.59	1197.5
5C	R	245.615	190
5C	B	270.19	1051.5
5C	B	270.15	214
5C	G	275.155	940
5C	B	278.23	89
5C	G	287.105	703.5
5C	Y	289.205	315
5C	B	322.53	200
5C	B	326.67	107
5C	G	341.055	1195.5

Control Sample 6:

Consensus	Dye	Size	RFUs
6C	R	105.04	92.33333
6C	R	110.83	72
6C	Y	116.4367	156
6C	G	118.57	146.3333
6C	B	121.07	44
6C	G	122.4533	166.3333
6C	B	129.27	40
6C	Y	130.28	148.6667
6C	B	131.46	44
6C	B	146.3433	305.6667
6C	B	150.4933	303.6667
6C	R	153.065	111.5
6C	G	168.7033	459.3333
6C	Y	176.4333	252.6667
6C	G	183.13	50
6C	B	194.6733	71
6C	B	202.7433	92.66667
6C	G	215.205	85.5
6C	Y	228.7467	187.6667
6C	R	229.34	59
6C	G	231.43	56
6C	Y	244.8533	180
6C	R	250	50
6C	B	258.1567	114.6667
6C	G	267.27	236.3333
6C	B	274.25	119.5
6C	G	279.23	152
6C	Y	293.255	76.5
6C	Y	297.27	57
6C	G	316.9467	135.3333
6C	G	325.07	139.3333
6C	B	326.77	67

Control Sample 7:

Consensus	Dye	Size	RFUs
7C	R	104.6767	3275
7C	Y	108.39	393
7C	Y	112.46	4032.5
7C	R	113.07	85
7C	B	120.92	240
7C	B	128.99	453
7C	B	127.1433	548.6667
7C	B	129.76	8007.5
7C	G	130.455	1576.5
7C	B	133.915	595
7C	G	134.575	1414.5
7C	B	137	307
7C	B	137.9233	5142.667
7C	R	148.95	364
7C	R	153.06	314
7C	G	158.67	3839
7C	G	162.64	8355
7C	G	166.84	3579
7C	G	168.66	3828
7C	Y	168.39	2235
7C	G	172.83	7482
7C	Y	176.54	1599
7C	G	176.94	6906
7C	B	206.74	433.5
7C	B	216.725	392
7C	Y	228.66	8008
7C	Y	240.77	7646.5
7C	B	270.19	437
7C	G	275.27	1257.5
7C	B	278.17	250
7C	G	283.145	1039.5
7C	G	312.735	1654
7C	G	316.87	1471
7C	B	322.63	830
7C	B	326.7	800
7C	R	395.09	2457
7C	B	395.09	938
7C	G	395.09	878

Control Sample 8:

Consensus	Dye	Size	RFUs
8C	R	105.075	514
8C	G	118.49	300
8C	Y	120.415	265
8C	B	125.84	125.5
8C	Y	126.34	290
8C	B	129.895	2733.5
8C	G	134.65	307
8C	B	138.105	91.5
8C	B	142.245	1884.5
8C	R	149.01	231.5
8C	R	153.07	251
8C	Y	172.395	675.5
8C	G	172.7267	183.3333
8C	Y	176.42	586.5
8C	G	184.03	206.5
8C	B	202.795	254
8C	B	212.72	221.5
8C	Y	228.775	656
8C	R	235.405	127.5
8C	R	245.7	103.5
8C	B	270.21	146
8C	G	271.28	493
8C	G	279.225	383
8C	B	282.355	141
8C	Y	285.42	98
8C	Y	297.365	127
8C	G	312.785	166
8C	B	326.74	269
8C	G	341.19	151

Control Sample 9:

Consensus	Dye	Size	RFUs
9C	R	105.0533	700.6667
9C	Y	112.455	175.5
9C	G	114.59	164
9C	Y	116.45	2512.5
9C	G	118.52	2236.5
9C	B	120.9167	921.6667
9C	B	121.865	6974
9C	Y	124.33	2355.5
9C	G	132.65	653.5
9C	G	134.66	2958
9C	R	148.98	361
9C	R	157.04	334
9C	Y	172.4633	1554.667
9C	Y	180.5667	1214.667
9C	G	184.05	5340.667
9C	B	206.725	1877.5
9C	R	221.085	1214
9C	Y	228.7867	3294.667
9C	R	229.23	1252.5
9C	Y	240.82	3065.333
9C	B	266.145	1210.5
9C	G	275.21	2285.667
9C	B	278.23	1130
9C	G	283.15	2044.667
9C	Y	289.34	553.5
9C	Y	305.13	489
9C	B	318.565	1437.5
9C	G	325.0967	1616.333
9C	G	337.11	1259.667

Control Sample 10:

Consensus	Dye	Size	RFUs
10C	R	105.0167	379.6667
10C	Y	112.4833	374.6667
10C	G	118.5267	426.3333
10C	Y	120.3533	292.3333
10C	G	122.4767	357.3333
10C	B	133.9	559
10C	B	142.2333	438.6667
10C	R	148.9367	141.3333
10C	R	152.9967	153
10C	G	172.78	487.3333
10C	Y	176.3667	241
10C	G	176.83	406.3333
10C	Y	180.51	229
10C	B	202.7333	175
10C	B	206.6867	157
10C	R	221.07	226
10C	G	227.365	150.5
10C	Y	228.7467	301.3333
10C	R	229.2667	249
10C	G	231.23	114.5
10C	Y	240.83	290.3333
10C	B	266.1833	197.6667
10C	G	275.22	296.6667
10C	B	278.3	182
10C	G	279.23	325
10C	Y	285.2567	179.6667
10C	Y	289.2933	150.3333
10C	G	325.1567	349
10C	B	326.72	168.3333

Experimental Sample 1:

Consensus	Dye	Size	RFUs
1E	B	120.85	66
1E	G	122.535	87.5
1E	Y	128.29	56
1E	B	129.5333	73.33333
1E	B	146.29	77
1E	G	168.72	77
1E	Y	172.715	74
1E	Y	228.91	87
1E	Y	242.78	94.5
1E	B	270.22	43
1E	G	275.14	57
1E	G	279.73	51
1E	G	312.89	79

Experimental Sample 2:

Consensus	Dye	Size	RFUs
2E	R	105.04	93.5
2E	Y	116.58	53
2E	Y	122.48	65.5
2E	G	129.98	57
2E	R	129.98	283
2E	B	134.21	67
2E	B	142.2067	80
2E	B	146.3167	83
2E	B	150.79	50
2E	R	153.04	50
2E	G	173.02	105
2E	G	177.065	65.5
2E	Y	180.71	51
2E	G	181.53	58
2E	G	227.33	73
2E	R	229.29	53
2E	R	237.68	62
2E	Y	237.6	99
2E	B	270.21	56.5
2E	B	282.33	45
2E	Y	289.25	62

Experimental Sample 3:

Consensus	Dye	Size	RFUs
3E	R	105.08	163.5
3E	R	110.98	99.5
3E	Y	112.51	55
3E	Y	116.4733	471
3E	B	121.8833	502.6667
3E	B	129.8833	528
3E	G	122.475	126.5
3E	G	134.63	149
3E	R	148.89	103
3E	R	153.015	99
3E	Y	164.3	82
3E	Y	180.46	90
3E	G	184.1067	979
3E	B	206.775	88
3E	B	212.705	101
3E	R	225.22	367
3E	R	237.46	215.5
3E	B	234.01	90
3E	Y	240.84	212.3333
3E	Y	244.9833	257.3333
3E	B	270.22	293.5
3E	B	282.3	240.5
3E	G	275.11	179
3E	G	283.155	103
3E	Y	289.27	219.6667
3E	Y	301.27	216
3E	G	312.7033	138.3333
3E	G	325.0333	121.6667
3E	B	322.61	43.5
3E	B	233.85	84

Experimental Sample 4:

Consensus	Dye	Size	RFUs
4E	R	105.02	466
4E	R	110.92	464.5
4E	G	118.58	69
4E	G	122.49	1204
4E	Y	124.27	749
4E	Y	126.31	893.5
4E	G	126.59	1336
4E	B	129.88	142
4E	B	133.885	2134
4E	B	146.28	147
4E	B	150.48	2038
4E	R	153.02	818
4E	Y	168.32	87
4E	Y	172.41	988
4E	G	172.905	725
4E	Y	176.57	112
4E	Y	180.62	908.5
4E	G	181.075	746.5
4E	B	198.76	407.5
4E	B	208.725	403.5
4E	R	221.08	243
4E	G	231.3	390
4E	Y	236.815	2936.5
4E	R	237.4	288
4E	G	271.16	159
4E	B	274.3	834
4E	G	275.19	1878.5
4E	B	278.3	819
4E	Y	289.315	366
4E	Y	297.31	335
4E	G	312.715	1000
4E	B	318.555	483.5
4E	B	322.655	424.5
4E	G	325.115	1111

Experimental Sample 5: No data

Experimental Sample 6:

Consensus	Dye	Size	RFUs
6E	Y	116.4	162
6E	G	118.43	149
6E	G	122.44	65
6E	B	123.2	44
6E	B	123.74	46
6E	B	146.32	115.6667
6E	B	150.4833	85
6E	R	153.28	50
6E	G	168.75	182
6E	R	171.83	68
6E	Y	176.51	81
6E	B	194.91	67
6E	Y	228.9	99.33333
6E	Y	244.955	76
6E	G	267.24	116
6E	G	279.23	70
6E	Y	293.21	50
6E	Y	297.45	53
6E	G	316.99	89
6E	G	325.07	90
6E	B	326.76	70.5
6E	R	123.2	109
6E	R	123.81	128

Experimental Sample 7:

Consensus	Dye	Size	RFUs
7E	R	105.06	312
7E	Y	112.455	603.5
7E	B	129.9167	395.3333
7E	G	130.475	150
7E	B	133.94	66
7E	G	134.665	161.5
7E	B	137.9833	412.3333
7E	R	148.975	88
7E	R	153.125	91.5
7E	Y	168.395	143.5
7E	G	172.8	148
7E	G	176.925	201
7E	Y	176.53	74
7E	B	206.755	90
7E	B	216.74	81.5
7E	R	221.205	139.5
7E	G	223.2	66
7E	Y	228.735	250.5
7E	G	227.43	65
7E	Y	240.775	197.5
7E	R	249.87	111
7E	B	270.34	229.5
7E	G	275.21	167
7E	Y	277.215	191.5
7E	B	278.33	189
7E	G	283.115	154
7E	Y	301.12	137
7E	G	312.685	170
7E	G	316.83	168.5
7E	B	322.575	140
7E	B	326.605	131.5

Experimental Sample 8:

Consensus	Dye	Size	RFUs
8E	R	105.0267	205
8E	G	118.55	157
8E	Y	120.46	351
8E	Y	126.37	330.5
8E	B	129.92	468
8E	G	134.68	238.5
8E	B	142.2467	492.3333
8E	R	149.035	85.5
8E	R	153.125	85
8E	Y	172.4467	103
8E	G	172.855	307
8E	Y	176.5033	88.66667
8E	G	184.13	304
8E	B	202.86	82.5
8E	B	212.75	146.5
8E	G	227.48	63
8E	Y	228.84	449.6667
8E	G	231.33	82
8E	R	235.365	171.5
8E	R	245.7	135
8E	B	270.275	288.5
8E	G	271.23	190
8E	G	279.13	204
8E	B	282.32	239
8E	Y	285.3067	145.6667
8E	Y	297.2867	145.6667
8E	G	312.6767	132.6667
8E	B	326.7867	205.3333
8E	G	341.18	183

Experimental Sample 9:

Consensus	Dye	Size	RFUs
9E	R	105.11	363
9E	Y	112.66	57
9E	Y	116.485	521.5
9E	G	118.55	320.5
9E	B	121.91	1191.333
9E	Y	124.2967	320
9E	G	134.7	275.5
9E	R	149.015	162
9E	R	157.23	146
9E	Y	172.465	115
9E	Y	180.655	113
9E	G	184.1867	1791
9E	G	202.75	43
9E	B	206.795	493
9E	R	221.15	403
9E	G	227.265	372.5
9E	Y	228.8933	534.6667
9E	R	229.24	330
9E	Y	240.8433	577.3333
9E	B	266.295	376
9E	G	275.1533	234
9E	B	278.285	330.5
9E	G	283.1267	230
9E	Y	289.2367	327
9E	Y	305.2167	364
9E	B	318.5033	190.3333
9E	G	325.1567	463.3333
9E	G	337.1567	426.6667

Experimental Sample 10:

Consensus	Dye	Size	RFUs
10E	R	105.04	55
10E	B	142.28	41
10E	G	172.84	58
10E	G	325.2	56
10E	G	325.26	51

Appendix Two: Electropherograms

All samples are labeled as follows: the first number identifies the PCR trial (1, 2 or 3) and the second number identifies the sample number. For example, Sample 3-7 represents the third PCR trial for the seventh sample. The C or E after each sample number identifies it as belonging to the control (C) or experimental (E) group.

Sample 1-1C:

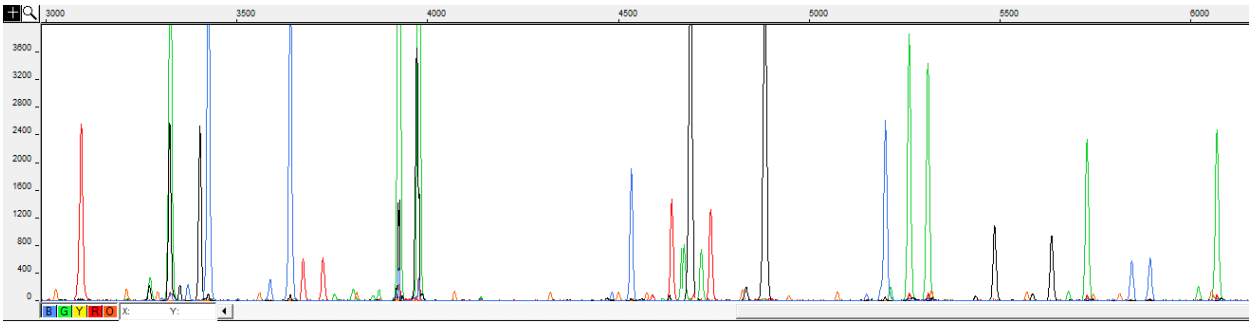

Sample 2-1C:

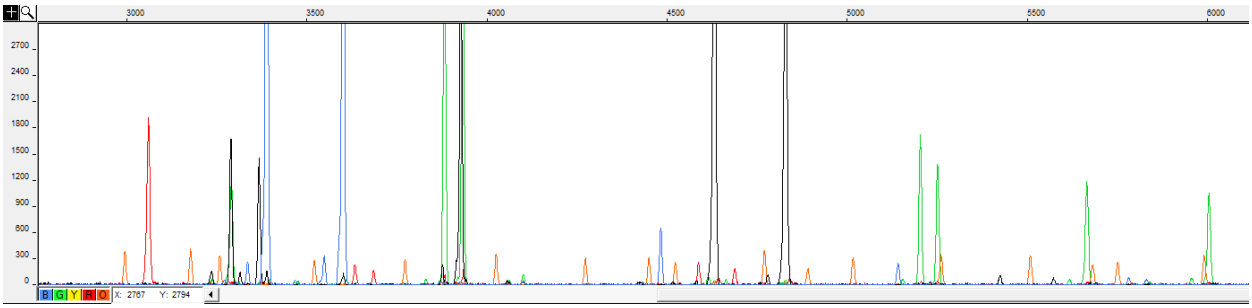

Sample 3-1C:

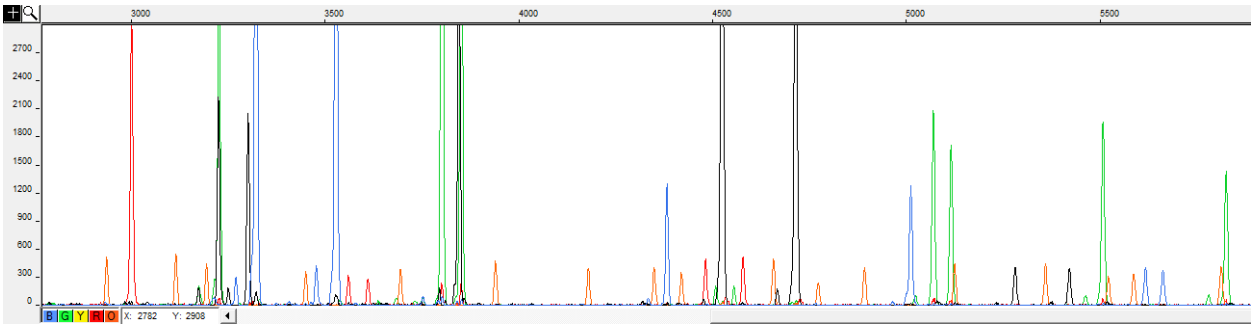

Sample 1-2C

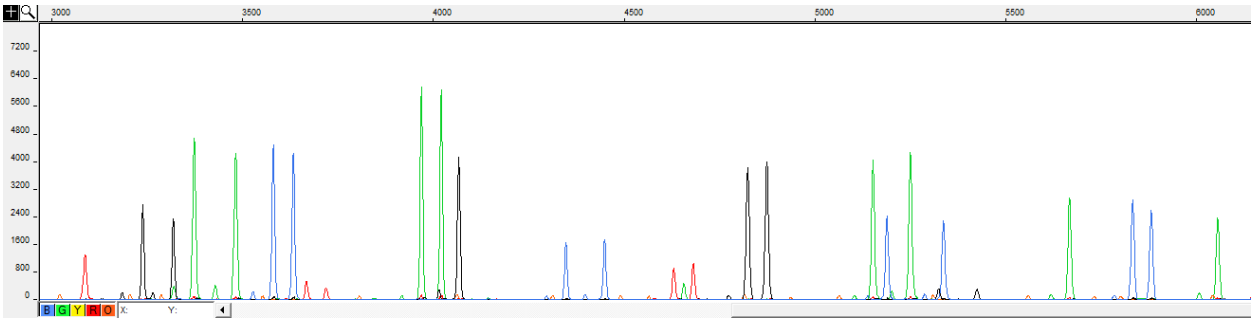

Sample 2-2C:

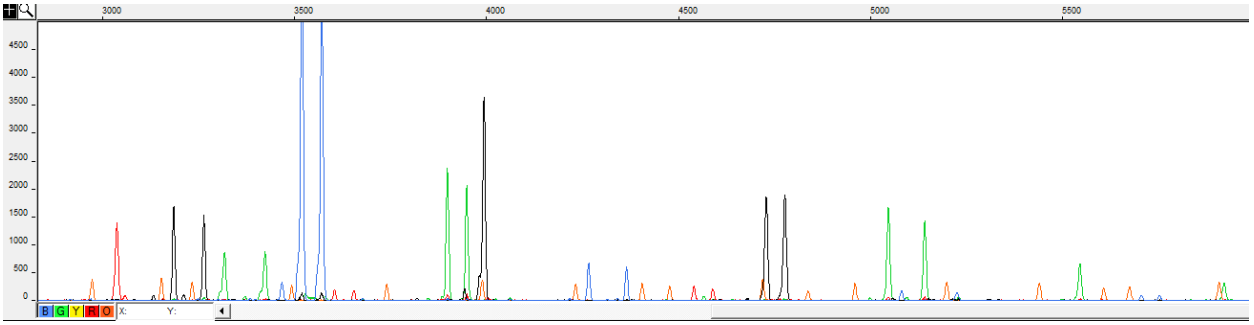

Sample 3-2C:

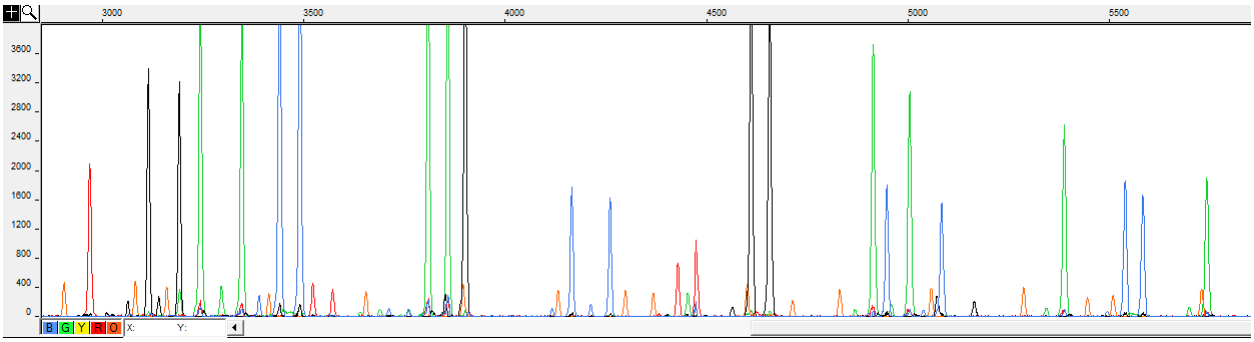

Sample 1-3C:

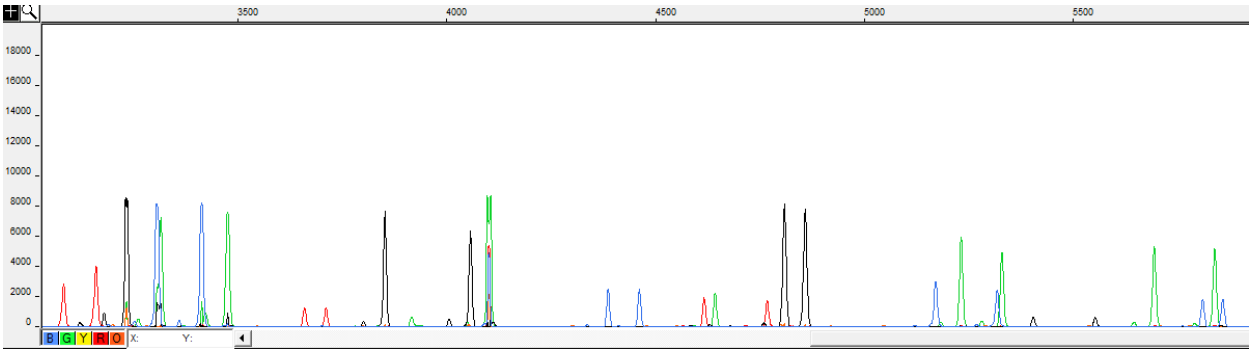

Sample 2-3C:

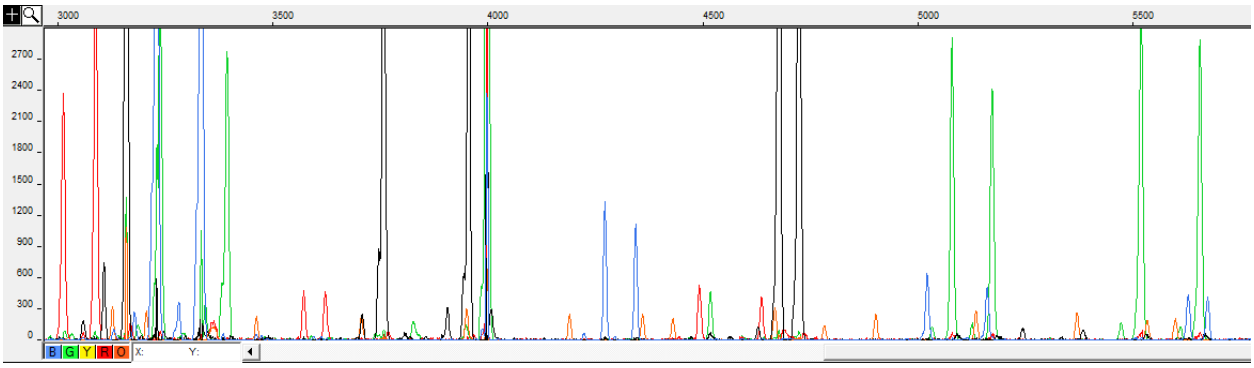

Sample 3-3C:

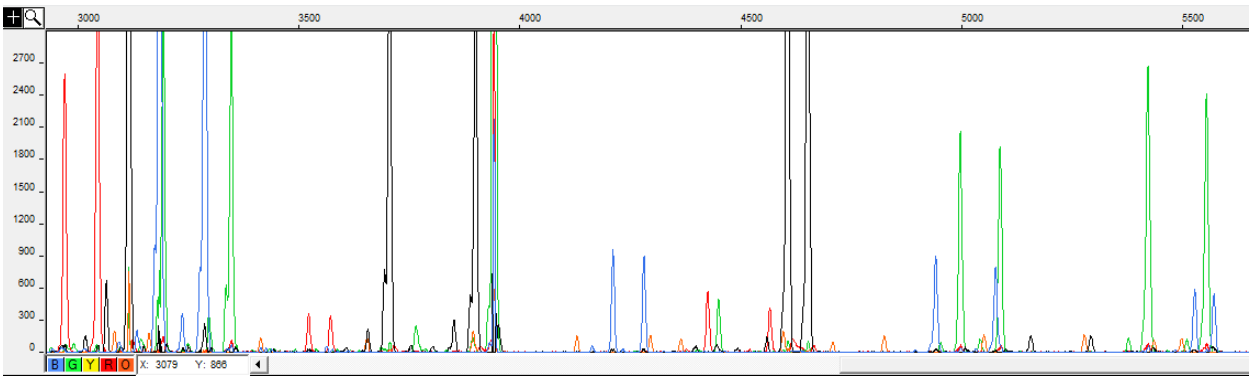

Sample 1-4C:

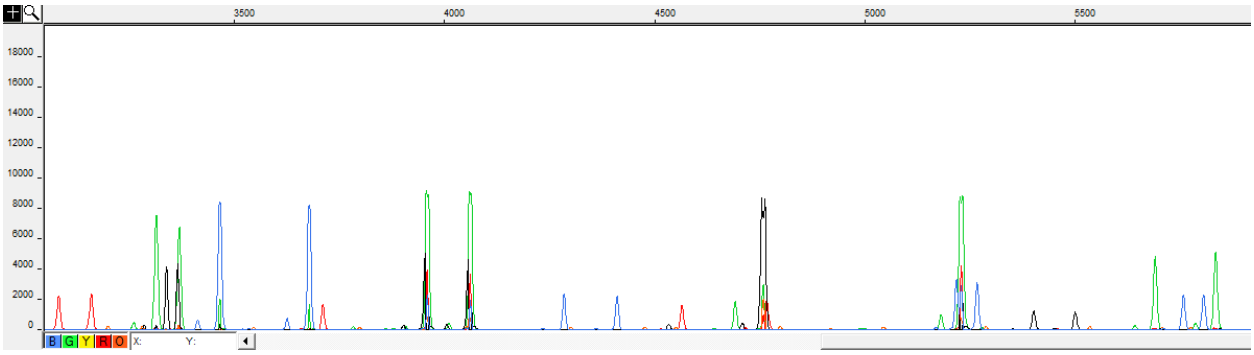

Sample 2-4C:

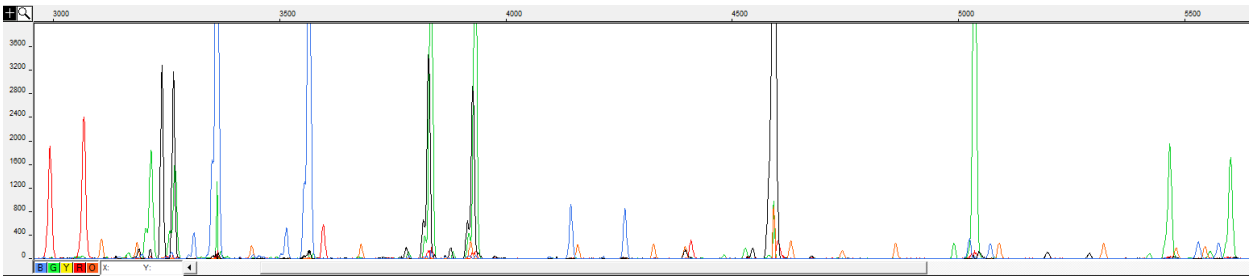

Sample 3-4C:

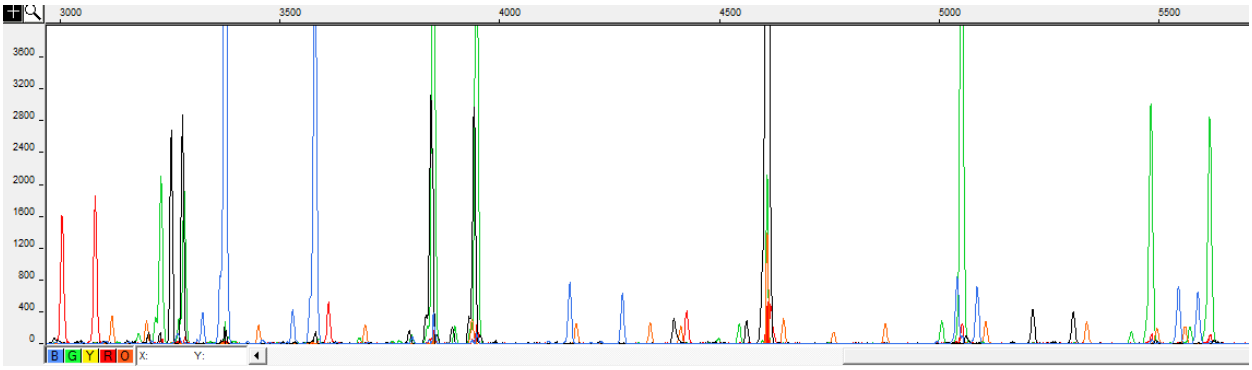

Sample 1-5C:

No electropherogram.

Sample 2-5C:

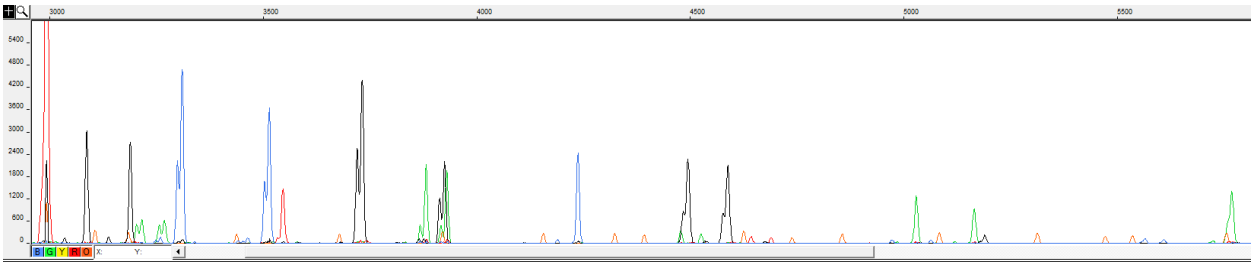

Sample 3-5C

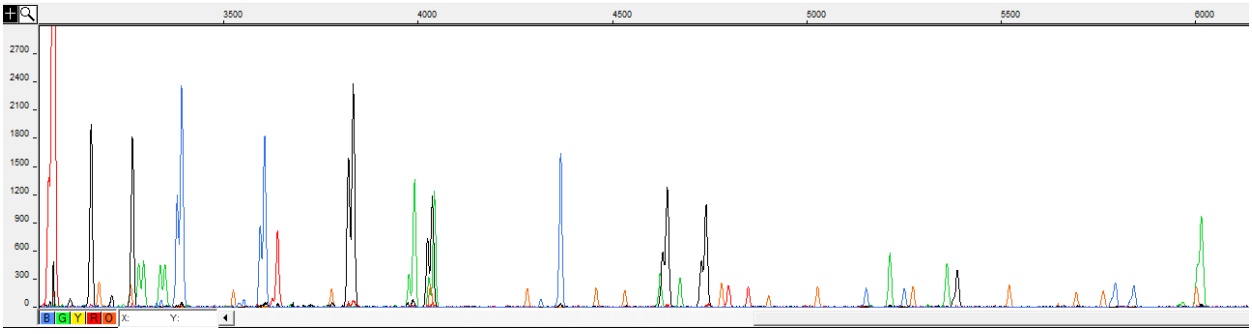

Sample 1-6C:

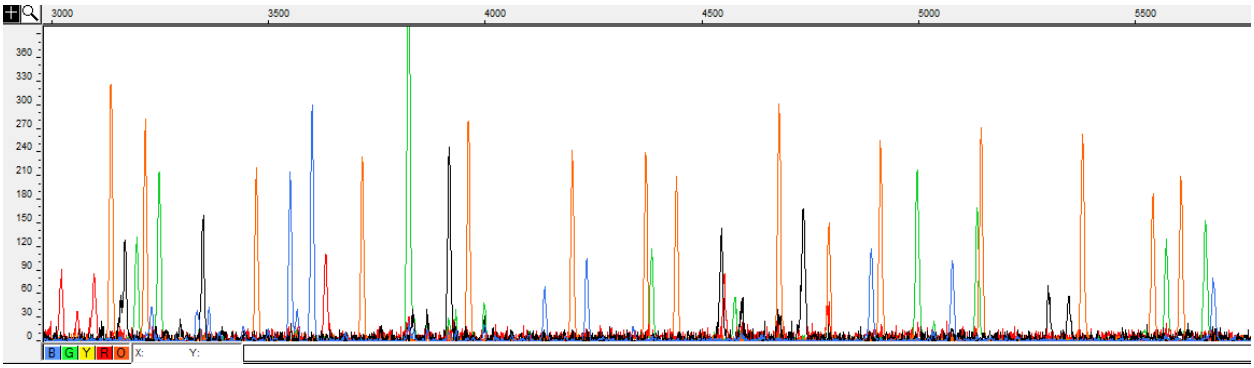

Sample 2-6C:

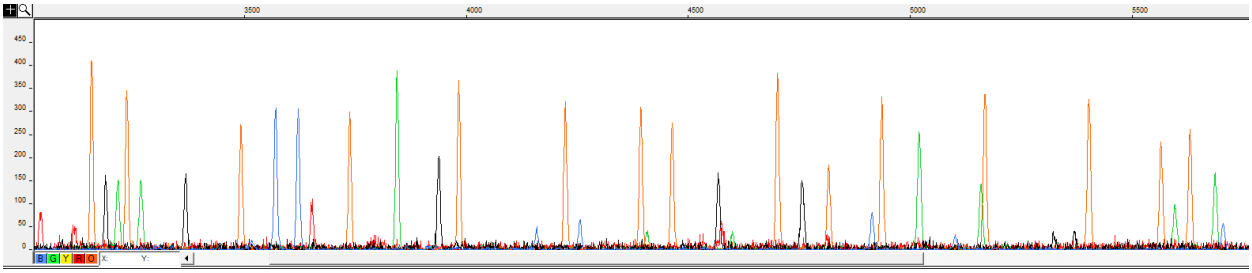

Sample 3-6C:

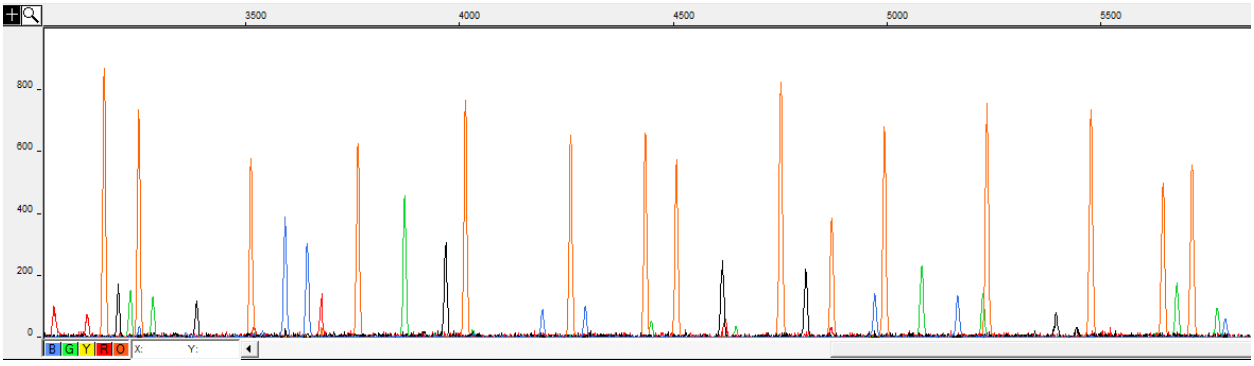

Sample 1-7C:

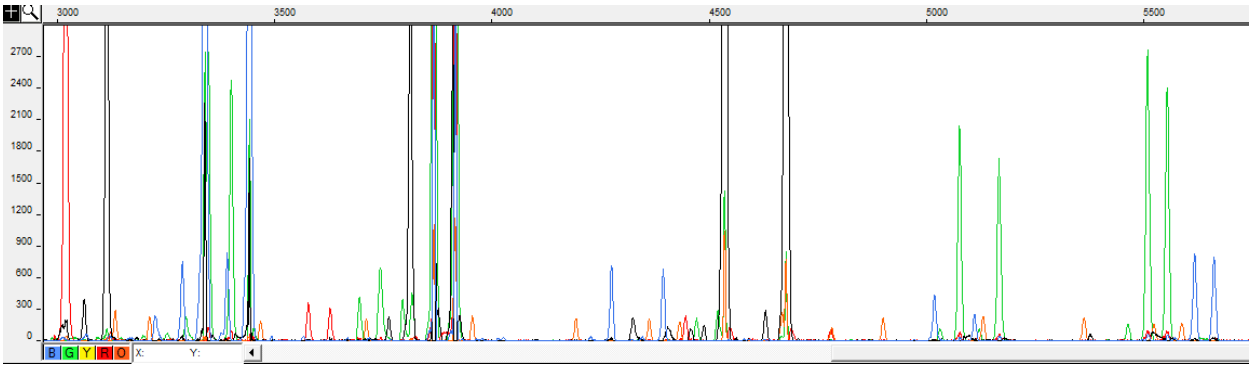

Sample 2-7C:

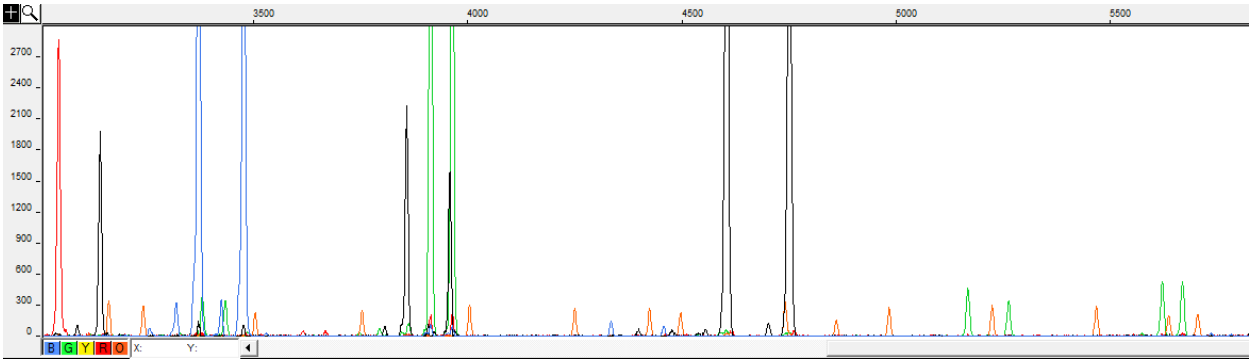

Sample 3-7C:

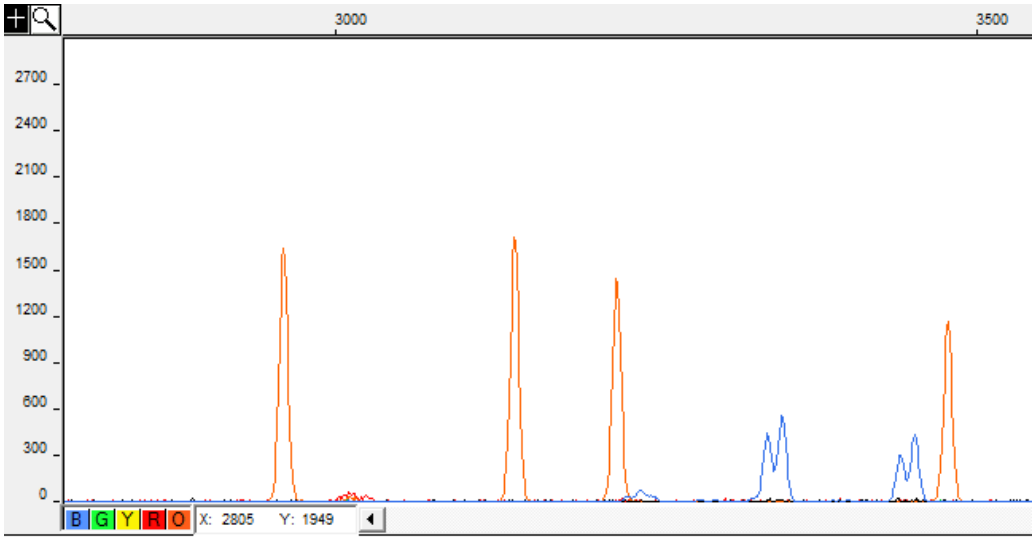

Sample 1-8C:

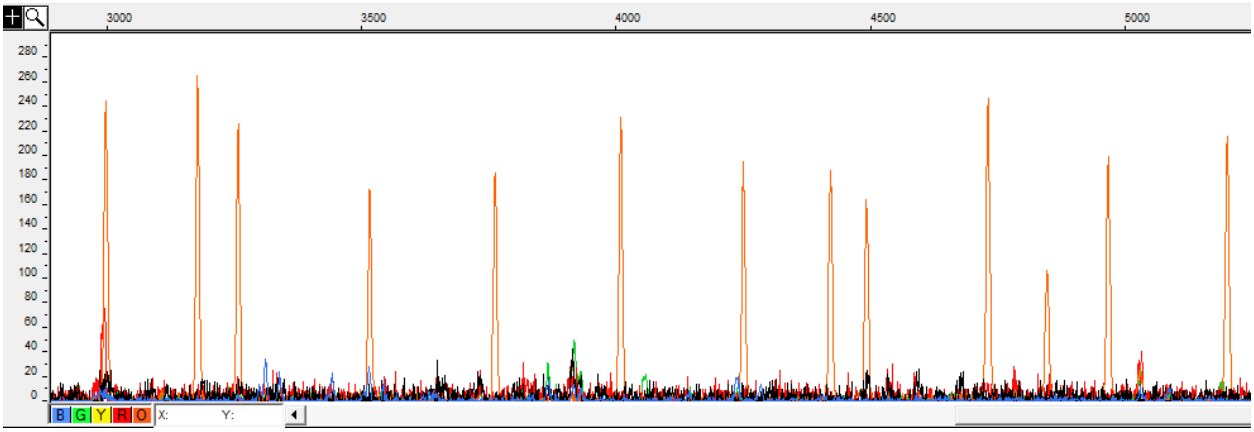

Sample 2-8C

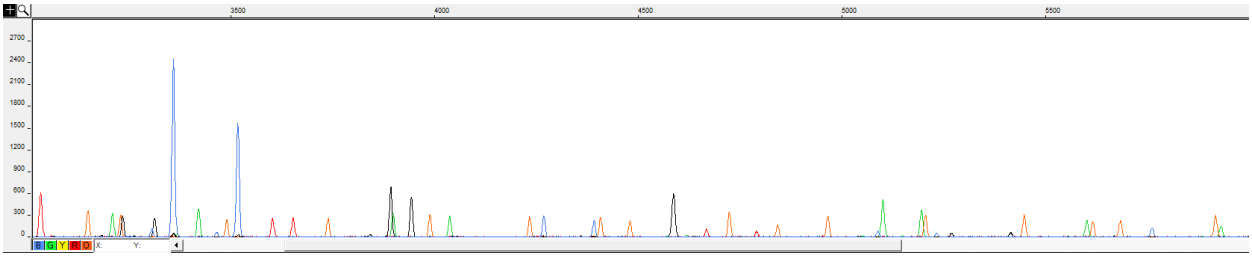

Sample 3-8C:

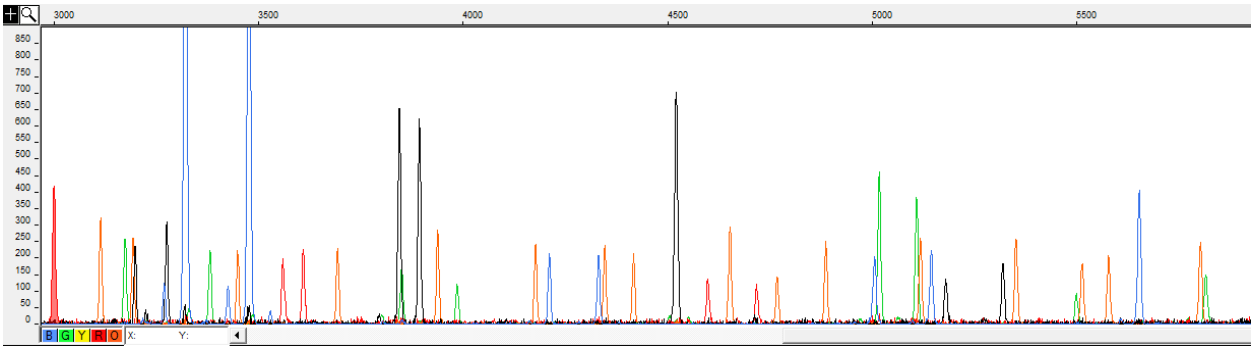

Sample 1-9C:

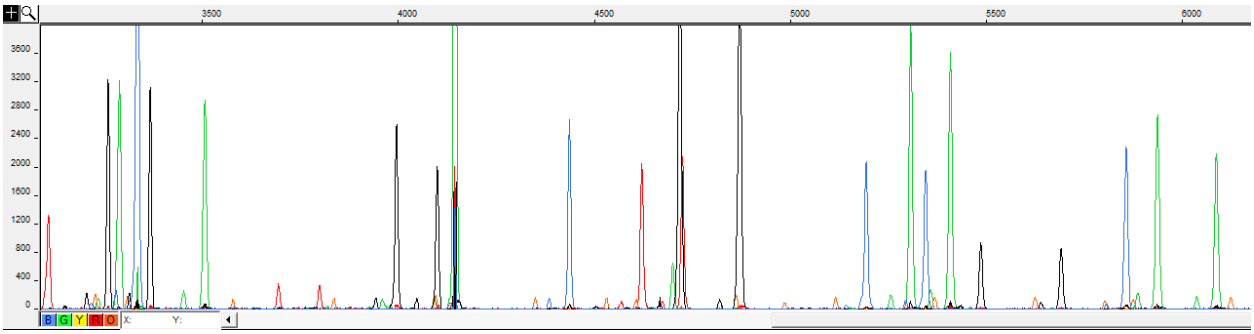

Sample 2-9C:

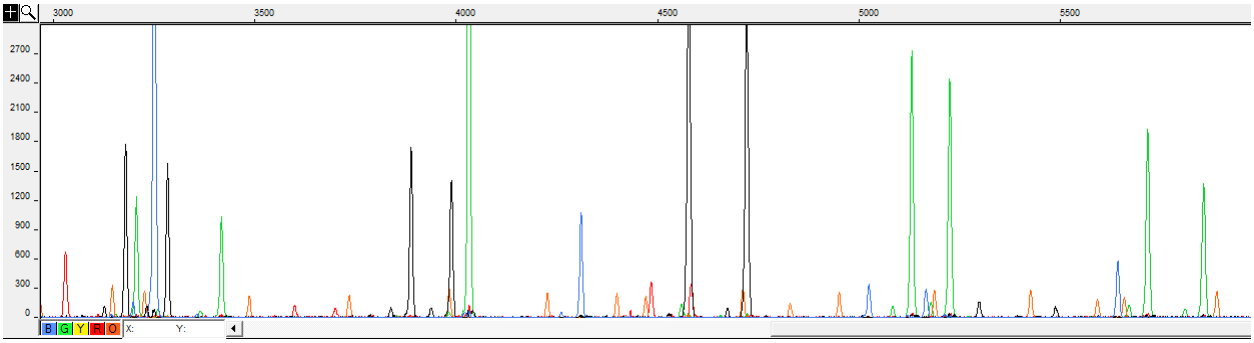

Sample 3-9C:

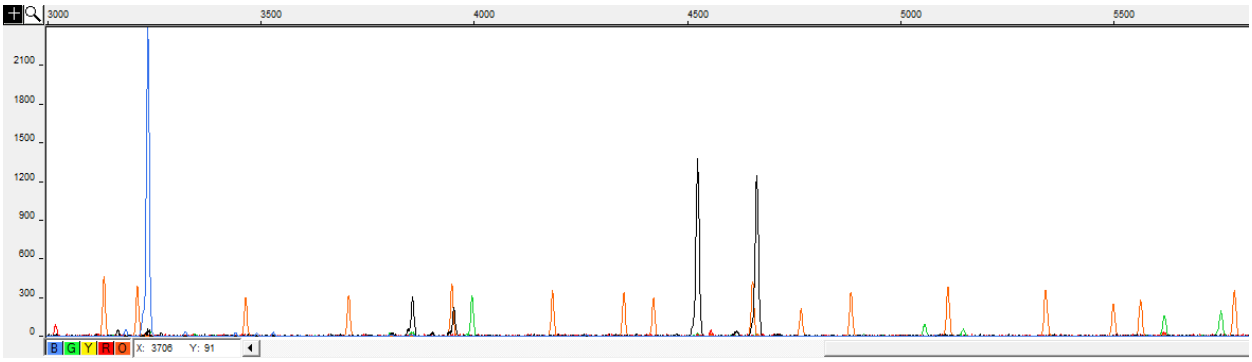

Sample 1-10C:

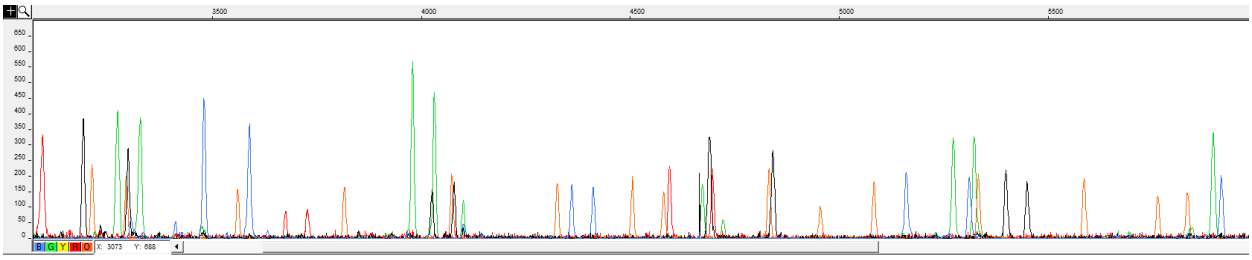

Sample 2-10C:

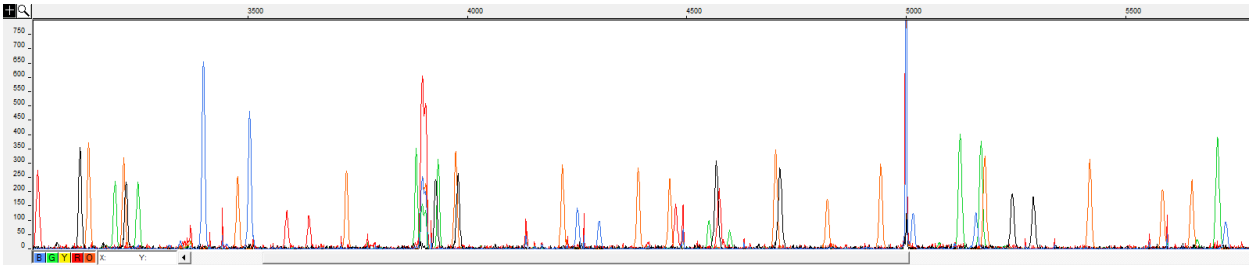

Sample 3-10C:

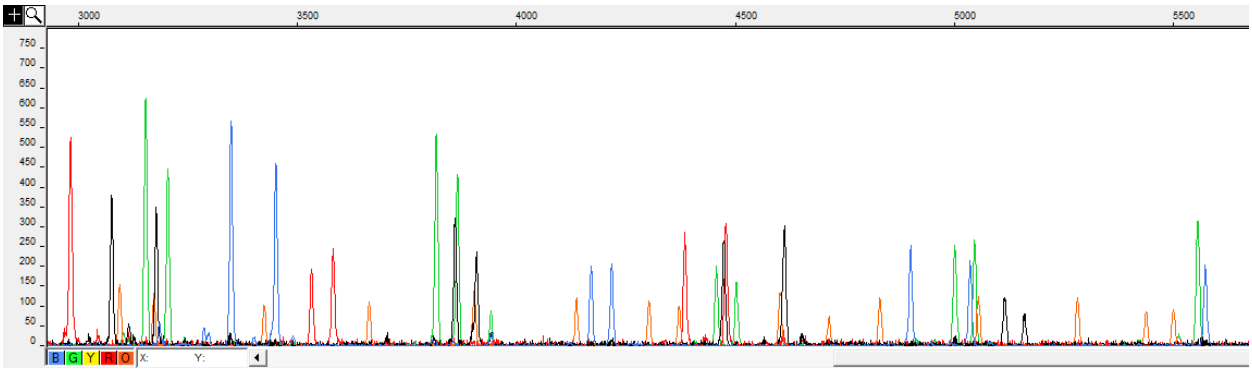

Appendix Three: Control Sample Electropherograms

Sample 1-1E:

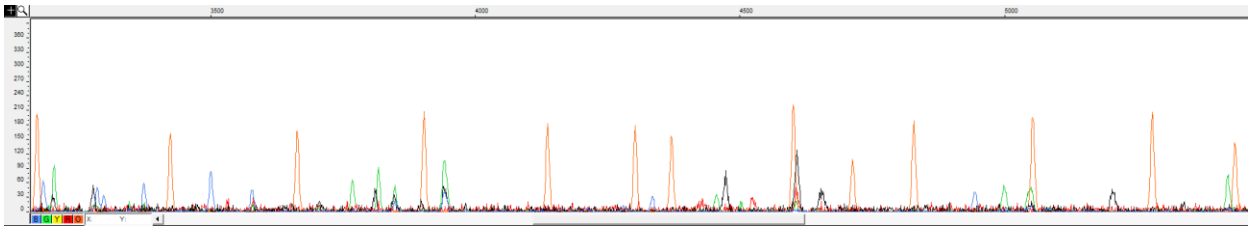

Sample 2-1E:

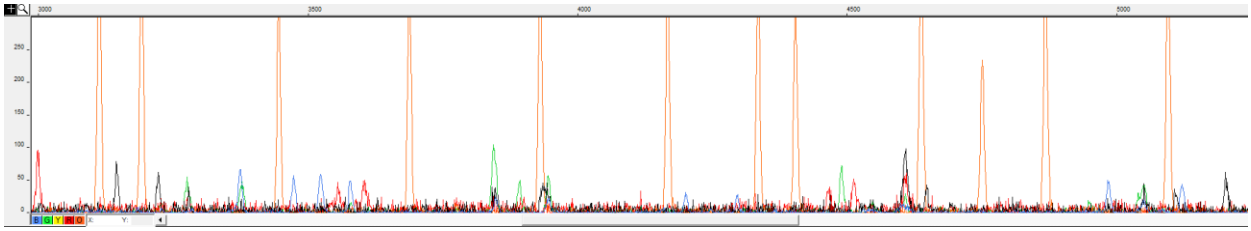

Sample 3-1E:

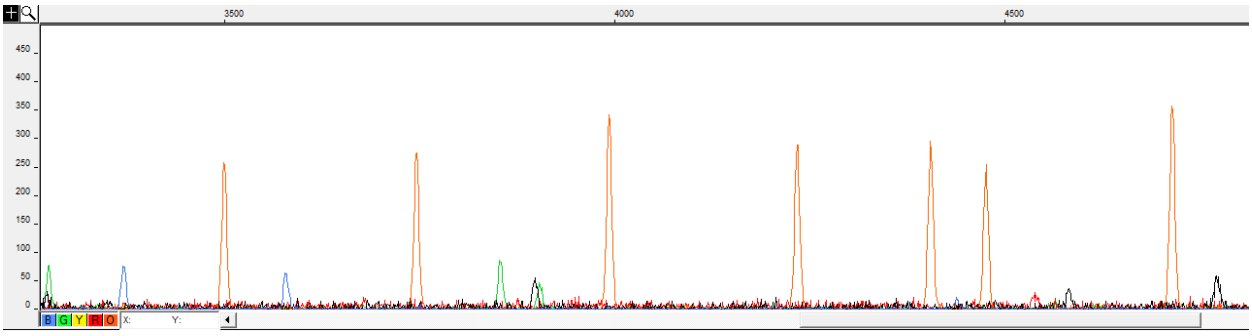

Sample 1-2E:

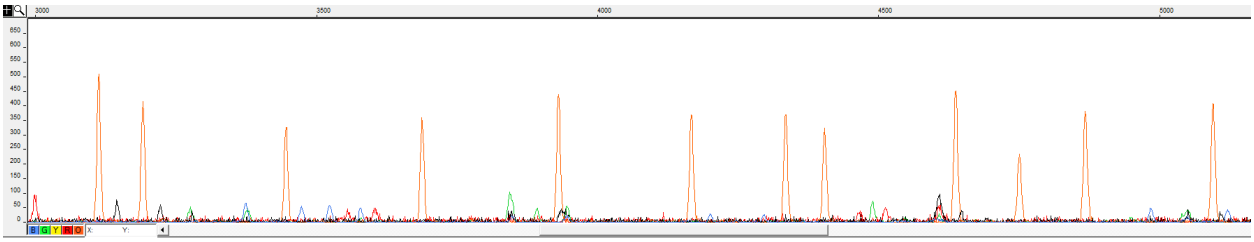

Sample 2-2E:

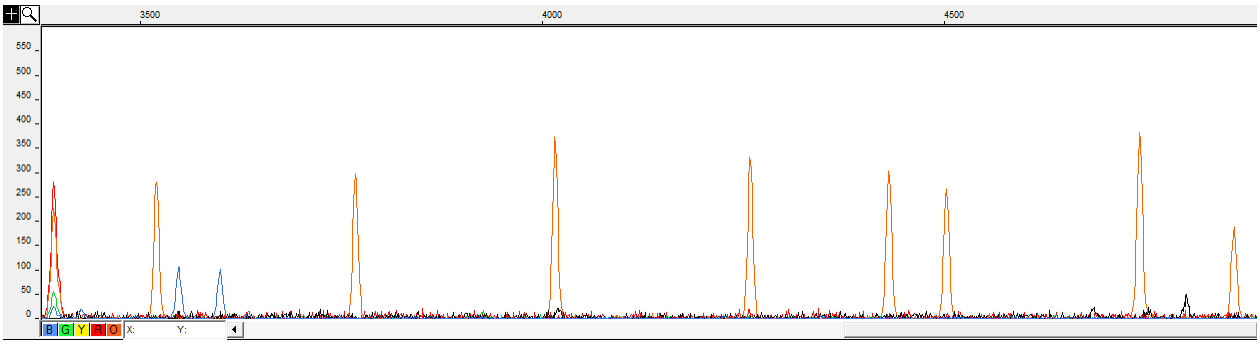

Sample 3-2E:

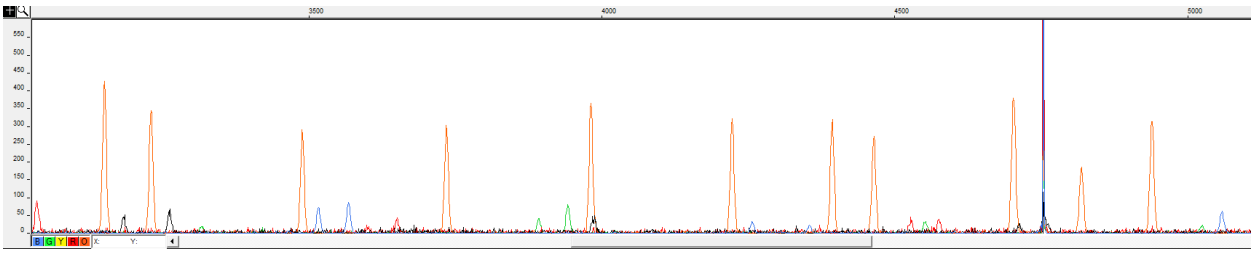

Sample 1-3E:

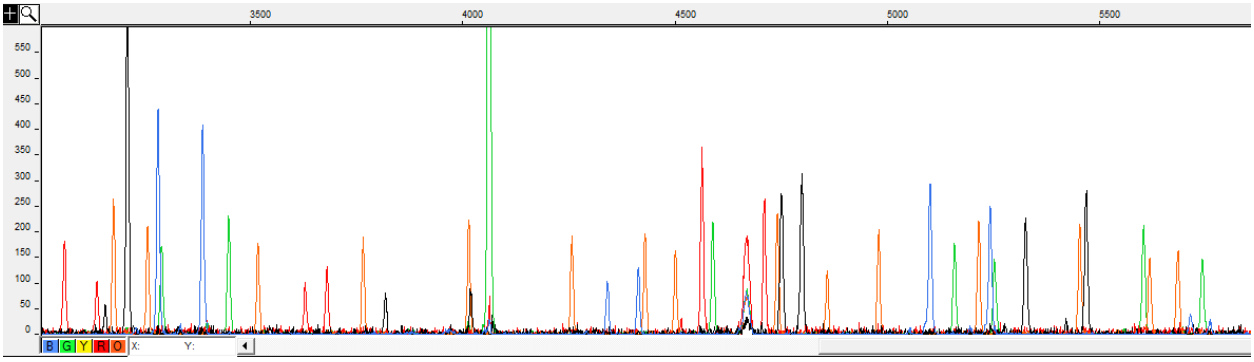

Sample 2-3E:

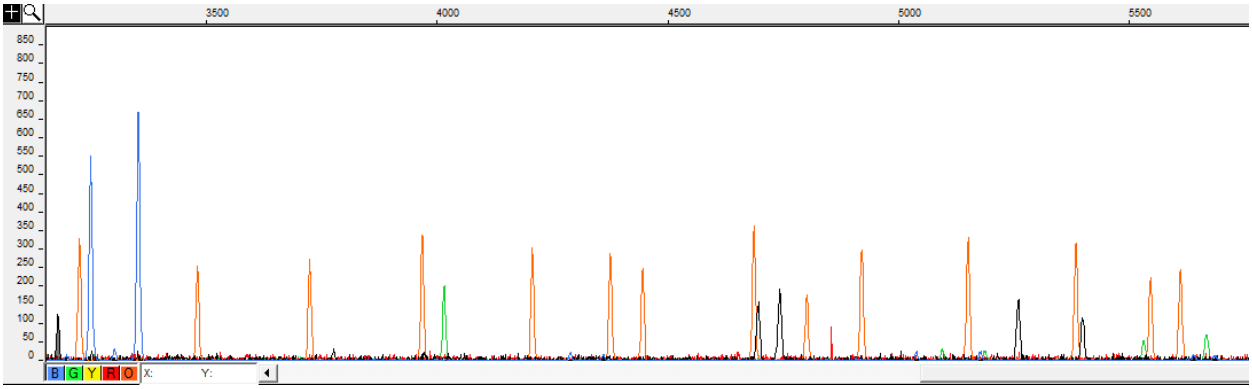

Sample 3-3E:

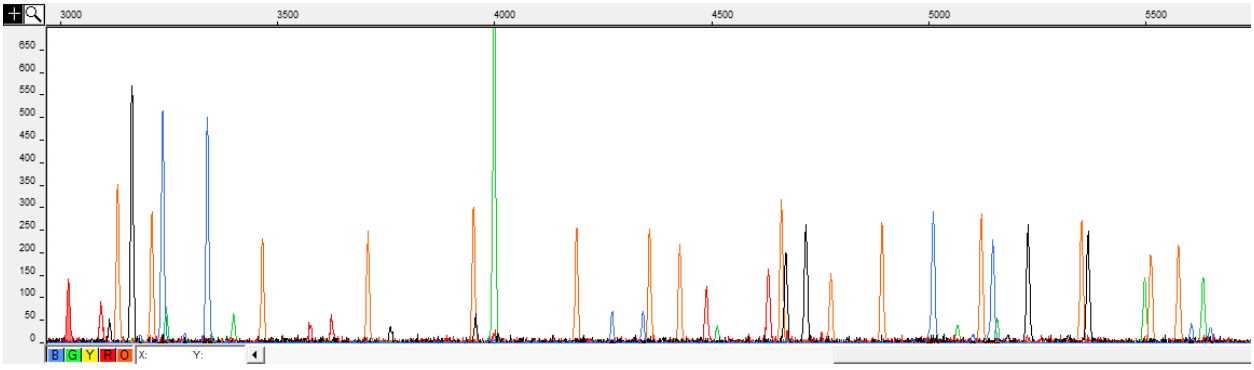

Sample 1-4E:

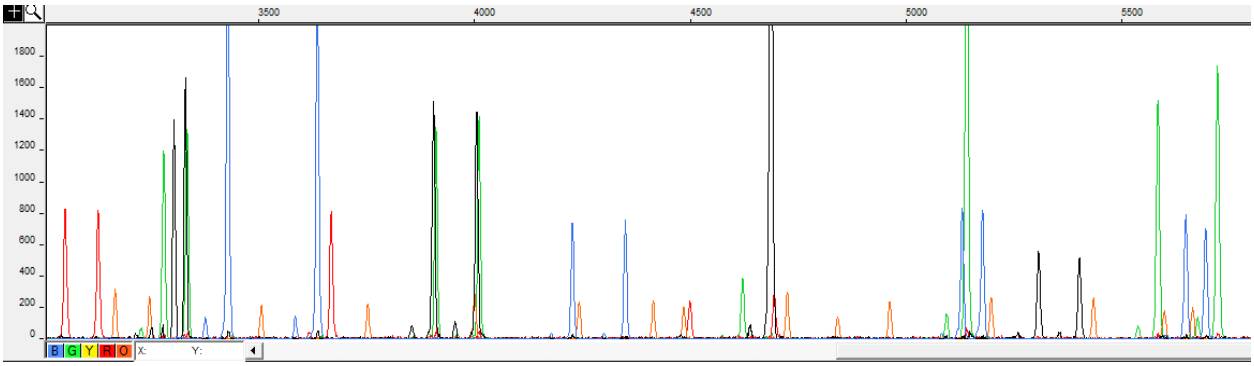

Sample 2-4E;

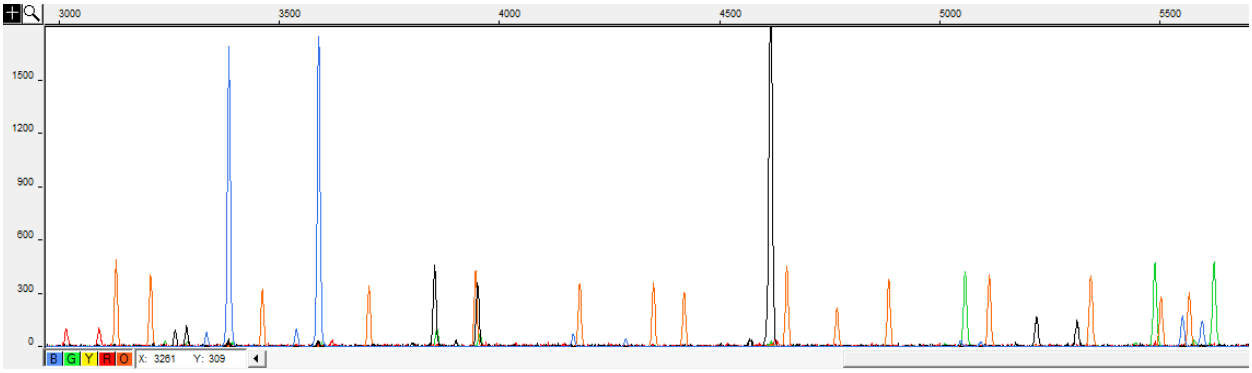

Sample 3-4E:

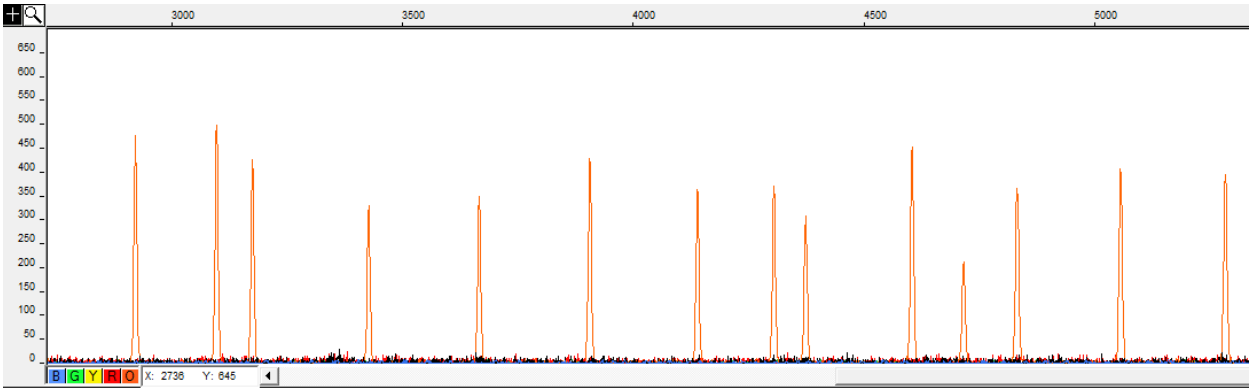

Sample 1-5E:

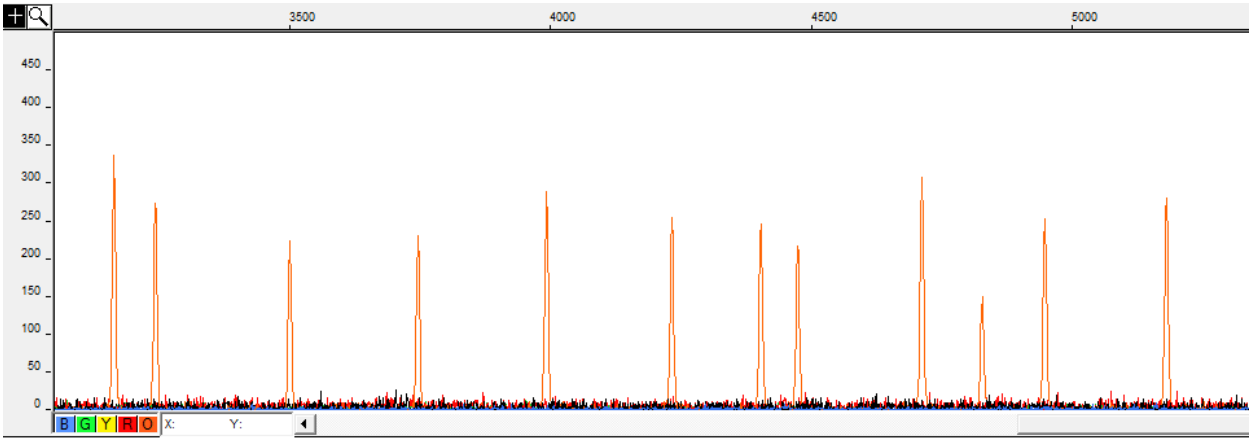

Sample 2-5E:

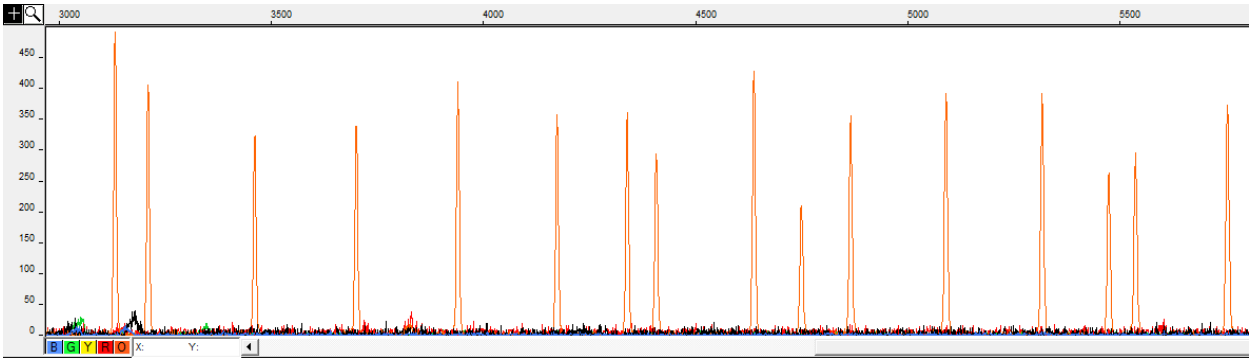

Sample 3-5E:

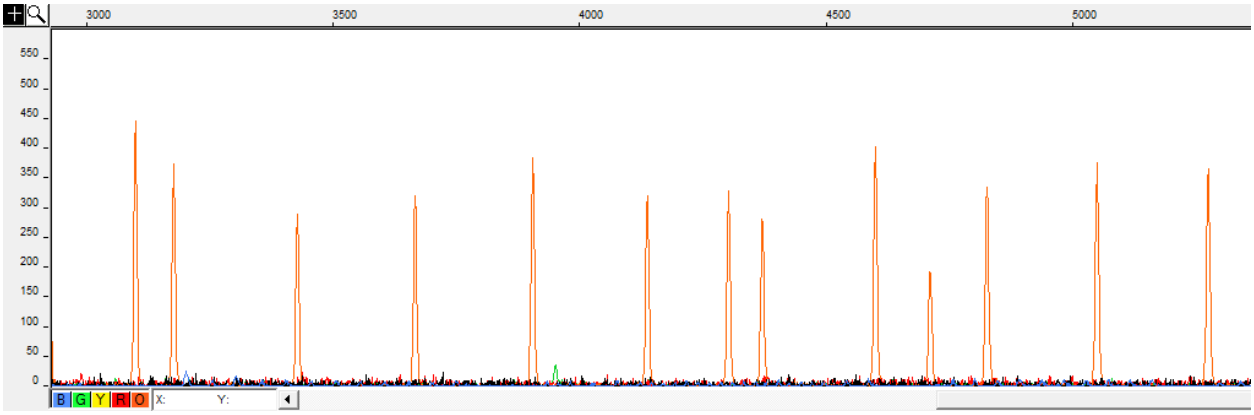

Sample 1-6E:

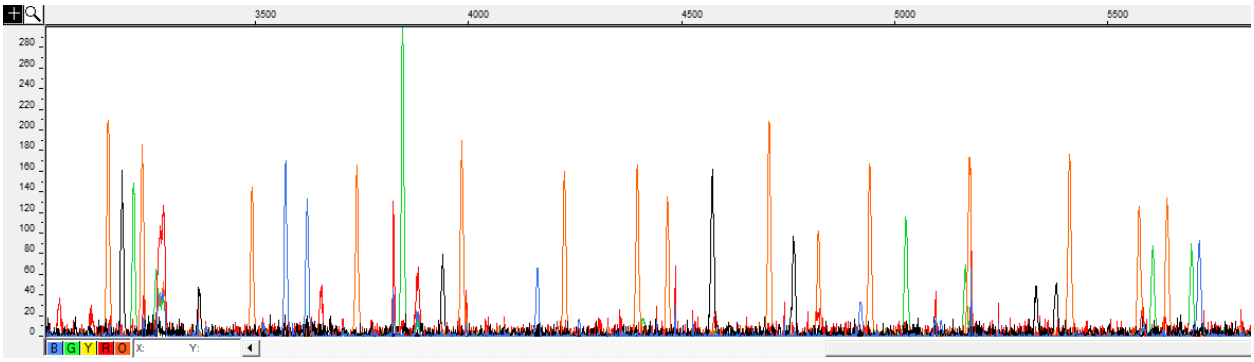

Sample 2-6E:

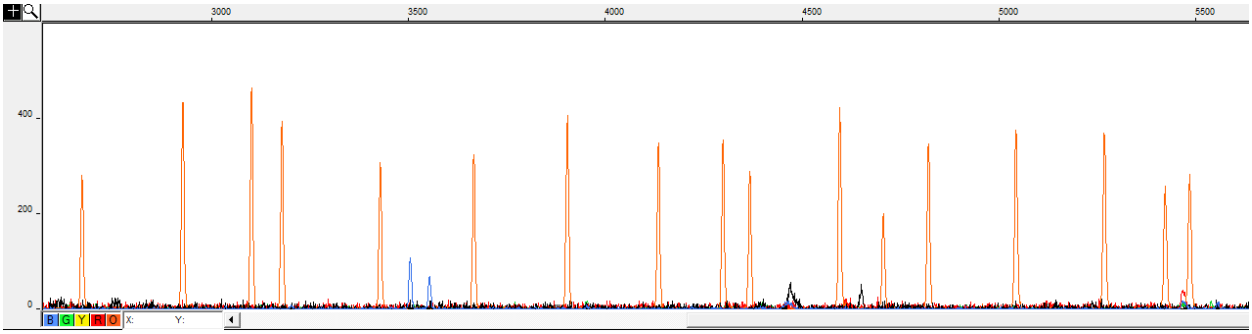

Sample 3-6E:

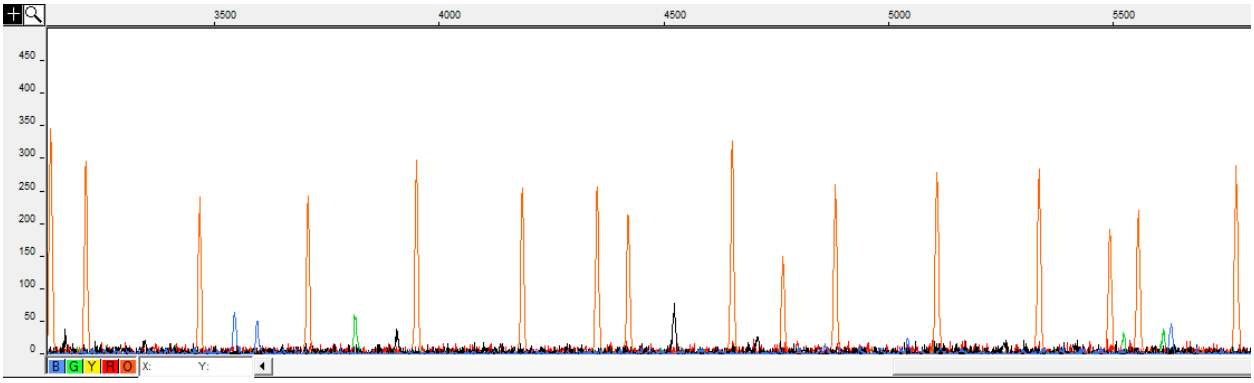

Sample 1-7E:

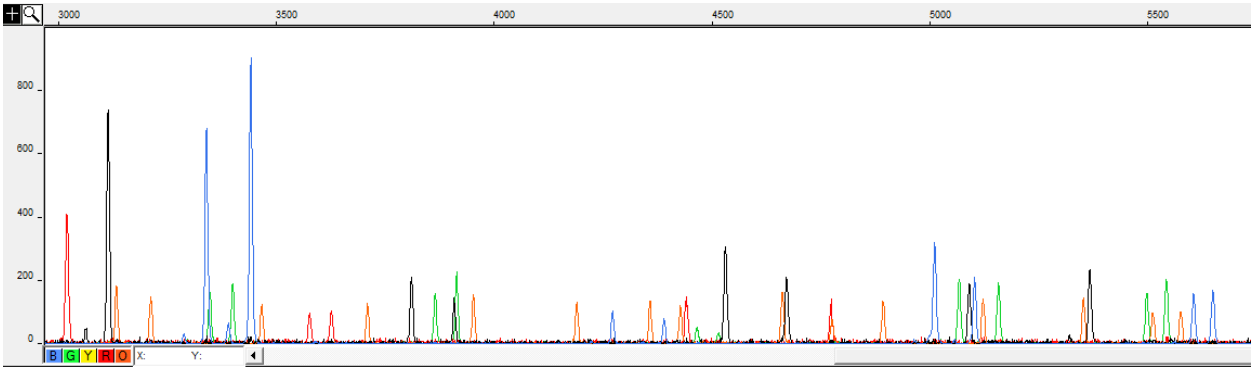

Sample 2-7E:

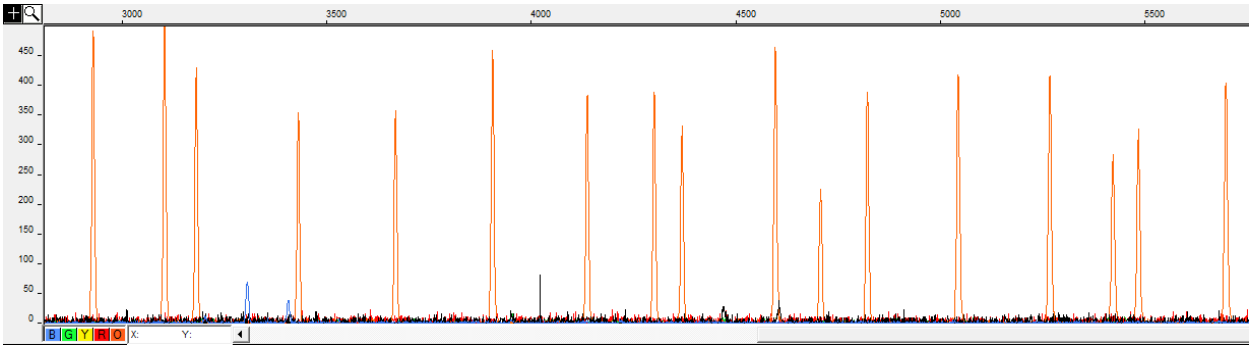

Sample 3-7E:

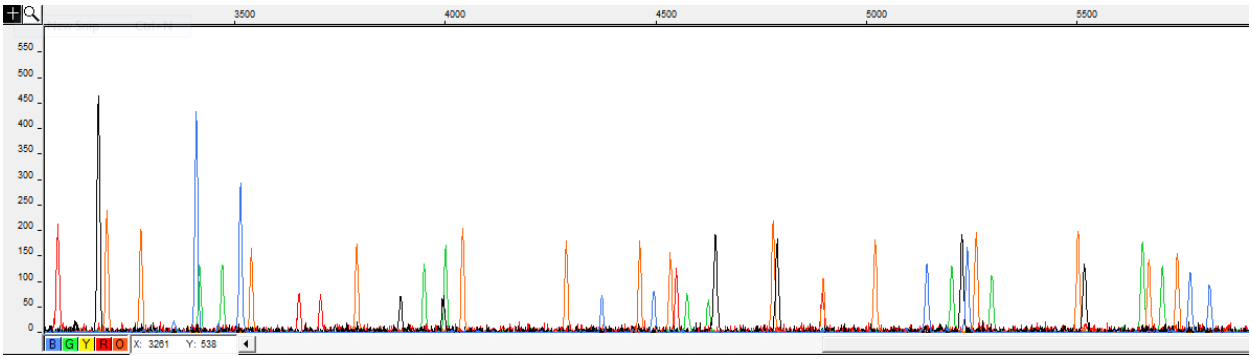

Sample 1-8E:

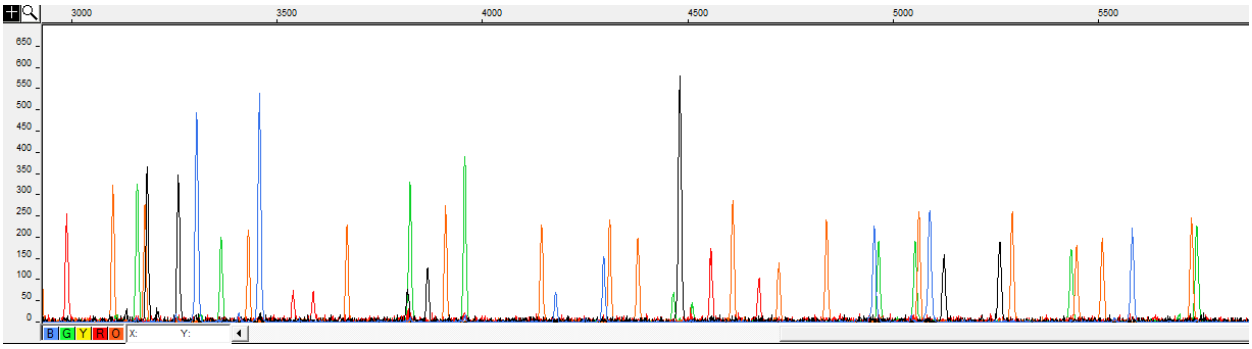

Sample 2-8E:

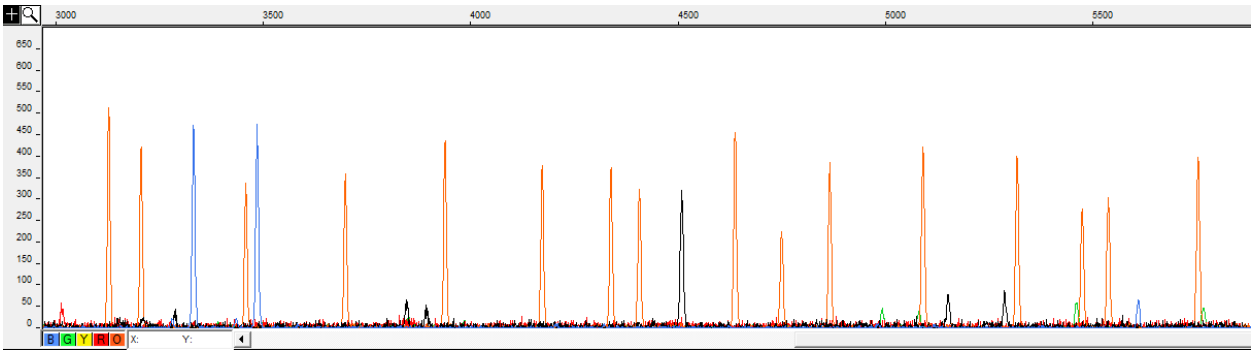

Sample 3-8E:

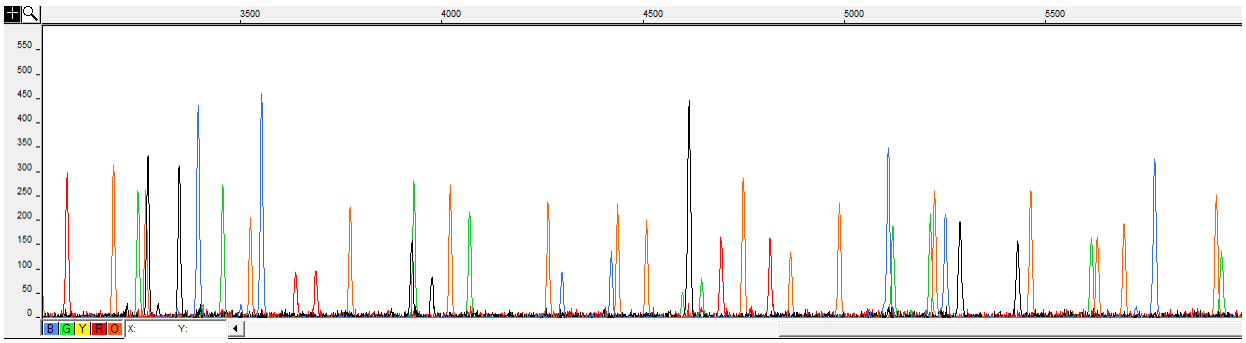

Sample 1-9E:

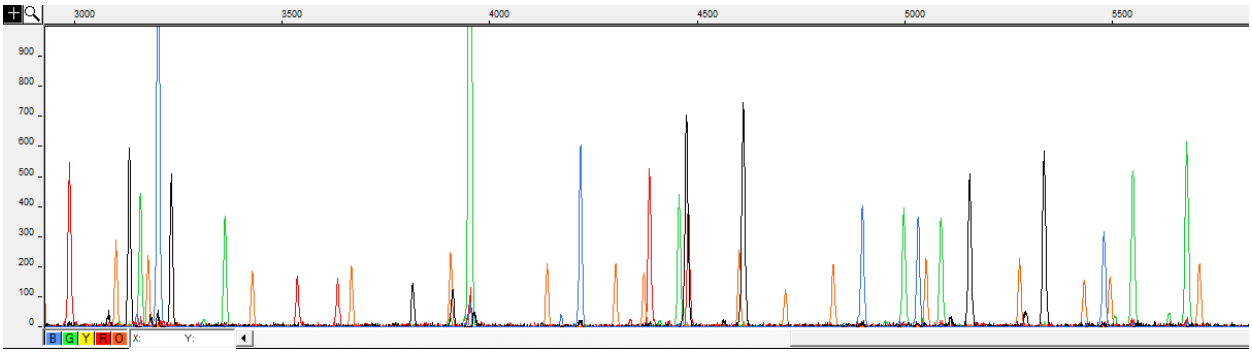

Sample 2-9E:

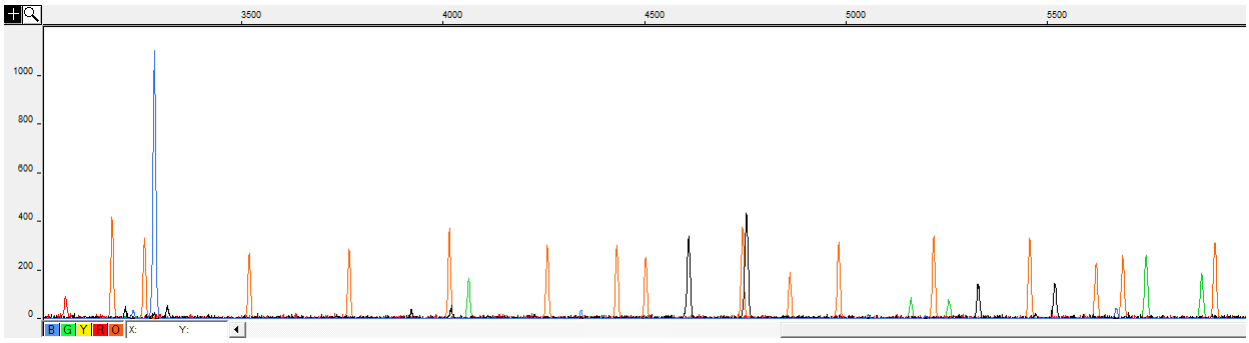

Sample 3-9E:

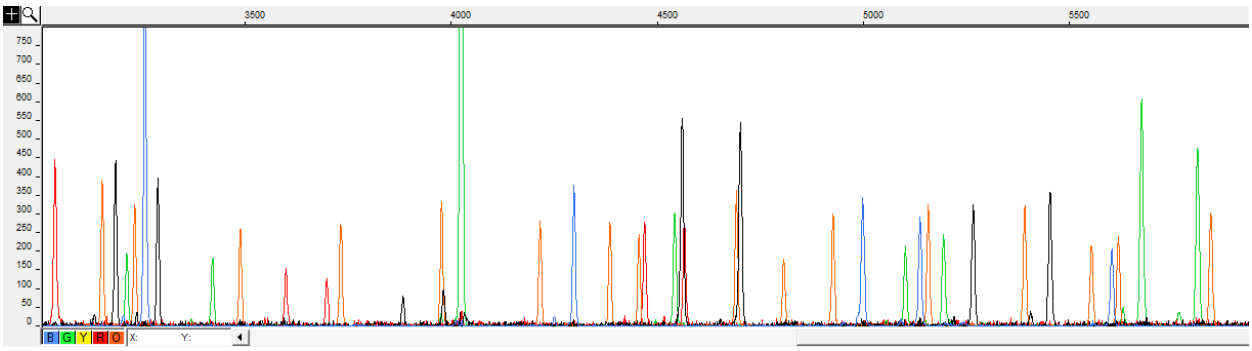

Sample 1-10E:

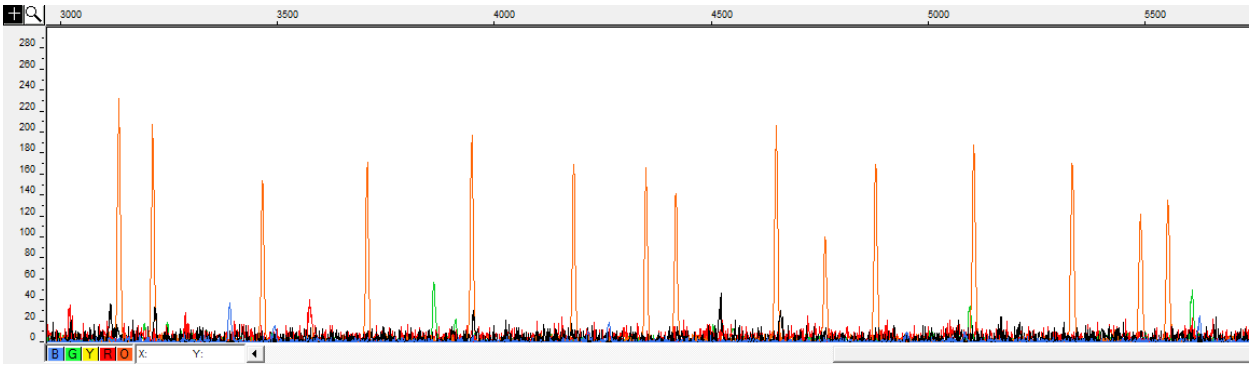

Sample 2-10E:

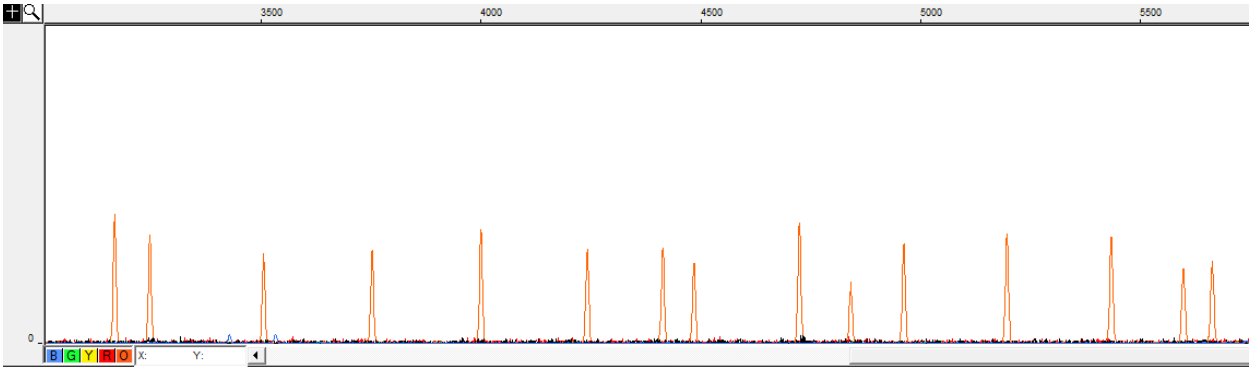

Sample 3-10E:

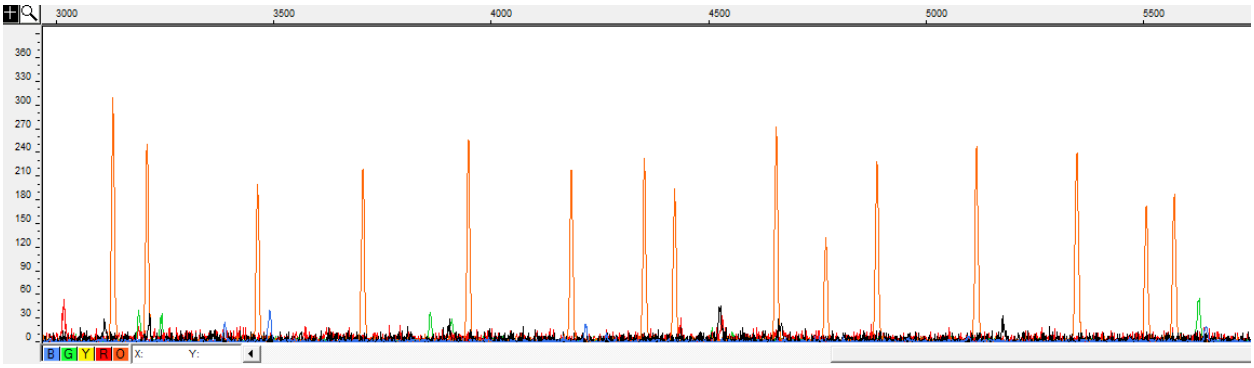

Vita

Erin Knapp was born in Boonton, NJ, to the parents of Robert and Judi Knapp. She is the first of two children and has one brother, Robert II. She attended Sandpiper Elementary, Del Prado Elementary and Loggers Run Middle School in Boca Raton Florida and continued to Reading-Fleming Middle School and Hunterdon Regional High School in Flemington, NJ. After graduation she began undergraduate study at Rowan University in Glassboro, NJ. In her second year, she was introduced to Anthropology and Archaeology and transferred to The Pennsylvania State University to pursue studies in Archaeological Science. Erin completed a summer of field school in Giecz, Poland as part of the Slavia Field School in Mortuary Archaeology. She obtained a Bachelors of Science degree in Archaeological Science and a Bachelors of Arts degree in Classics and Ancient Mediterranean Studies from The Pennsylvania State University in May 2006. She was admitted to the Anthropology Master's program at the University of Tennessee, Knoxville in August of 2007. Erin graduated with a Masters of Arts degree in Anthropology in August 2013. She is continuing her education with a PhD in Anthropology at the University of Tennessee, Knoxville.